Visual Tactile Integration in Rats and Underlying Neuronal Mechanisms

A DISSERTATION PRESENTED
BY
NADER NIKBAKHT NASRABADI
TO
THE COGNITIVE NEUROSCIENCE PHD PROGRAM

IN PARTIAL FULFILLMENT OF THE REQUIREMENTS
FOR THE DEGREE OF
DOCTOR OF PHILOSOPHY
IN THE SUBJECT OF
NEUROSCIENCE

INTERNATIONAL SCHOOL FOR ADVANCED STUDIES
TRIESTE, ITALY
OCTOBER 2015

Thesis advisor: Prof. Mathew E. Diamond Nader Nikbakht Nasrabadi

Visual Tactile Integration in Rats and Underlying Neuronal Mechanisms

Abstract

Our experience of the world depends on integration of cues from multiple senses to form unified percepts. How the brain merges information across sensory modalities has been the object of debate. To measure how rats bring together information across sensory modalities, we devised an orientation categorization task that combines vision and touch. Rats encounter an object–comprised of alternating black and white raised bars–that looks and feels like a grating and can be explored by vision (V), touch (T), or both (VT). The grating is rotated to assume one orientation on each trial, spanning a range of 180 degrees. Rats learn to lick one spout for orientations of 0±45 degrees ("horizontal") and the opposite spout for orientations of 90±45° ("vertical"). Though training was in VT condition, rats could recognize the object and apply the rules of the task on first exposure to V and to T conditions. This suggests that the multimodal percept corresponds to that of the single modalities. Quantifying their performance, we found that rats have good orientation acuity using their whiskers and snout (T condition); however under our default conditions, typically performance is superior by vision (V condition). Illumination could be adjusted to render V and T performance equivalent. Independently of whether V and T performance is made equivalent, performance is always highest in the VT condition, indicating multisensory enhancement. Is the enhancement optimal with respect to the best linear combination? To answer this, we computed the performance expected by optimal integration in the framework of Bayesian decision theory and found that most rats combine visual and tactile information better than predicted

by the standard ideal–observer model. To confirm these results, we interpreted the data in two additional frameworks: Summation of mutual information for each sensory channel and probabilities of independent events. All three analyses agree that rats combine vision and touch better than could be accounted for by a linear interaction. Electrophysiological recordings in the posterior parietal cortex (PPC) of behaving rats revealed that neuronal activity is modulated by decision of the rats as well as by categorical or graded modality-shared representations of the stimulus orientation. Because the population of PPC neurons expresses activity ranging from strongly stimulus-related (e.g. graded in relation to stimulus orientation) to strongly choice-related (e.g. modulated by stimulus category but not by orientation within a category) we suggest that this region is involved in the percept-to-choice transformation.

Contents

Listing of figures

Acknowledgments

There are no proper words to convey my gratitude and respect for my thesis and research advisor, Prof. Mathew E. Diamond. With his genuine intellectual generosity he has allowed me to push my ideas until they hit their limits while supporting me with openness and wisdom. He not only influenced me to do independent research but with critical reasoning helped me understand the complexities of neuroscience experiments.

I would like to express my sincere thanks to Dr. Davide Zoccolan for his continuous intellectual support as the co-advisor of my PhD project. He constantly provided original ideas and insightful comments throughout my PhD project.

I will be always grateful to Prof. John G. Nicholls, an excellent, accomplished and 'real' scientist. He not only taught me fascinating lessons in neurobiology through his marvelous lectures, but also taught me what it really takes to become an enthusiastic genuine scientist.

This work has benefited substantially from the hard work, passion and intellectual power of Azadeh Tafreshiha to whom I am extremely thankful. She actively participated in the development of the behavioral experiments and training sessions while she was doing her Master's degree thesis in the lab. She has been immensely supportive of the work ever since.

I owe my special thanks to Laura Carbonari and Giuseppe Cazzetta for their great help in the behavioral trainings and data collection.

I am grateful to our technical support team—Marco Gigante and Rudi Laco helped in instrumentation and realization of the experimental setup and stimuli. Walter Vanzella developed the core code for video tracking software. Fabrizio Manzino and Fabio Meneghini provided LabView support. Erik Zorzin imple-

mented the electronic circuits. More importantly than that, I benefited greatly from his vast knowledge of electronics and physics. Francesca Pulecchi patiently helped in surgical procedures and performed histologies.

I am grateful to numerous friends and colleagues who influenced and encouraged my thinking: Vinzenz Schönfelder, Romain Brasslet, Neil Rabinowitz, Houman Safaai, Ehsan Arabzadeh and Jacopo Rigosa particularly for their comments on data analysis; Athena Akrami, Arash Fassihi and Vahid Esmaeili for their comments on the experimental design and interpretation of data; Sergey Antopolsky, Sebastian Reinartz for their comments on the thesis and some other members of Diamond lab and Zoccolan lab for their fruitful comments and discussions regarding the experiments.

Finally, I owe my loving gratitude to my family and friends who have been supportive during my graduate studies.

Freedom of thought is best promoted by the gradual illumination of men's minds which follows from the advance of science.

Charles Darwin

1 Introduction

1.1 Overview

Research on sensory systems is perhaps one of the richest endeavours undertaken to understand how brains work. To explain perception, Democritus (430–420 B.C.), said that many small images (eidola) from the external world are received through the senses and are processed and integrated into thinking. He thought this process provided the raw material for sensation, perception, learning and action (Jung, 1984). It is essentially the same question that modern neuroscientists ask: where and how in the brain does a sensory representation transform into perception, memory and action? This ongoing debate highlights the fundamental desire to understand how our experience of the physical world makes us who we are.

Adrian (1928) pioneered the scientific testing of the problem. He recorded from the peripheral fibers innervating skin receptors and saw how

the neuronal impulse rates varied as a function of the stimulus strength applied to the skin. The underlying idea of his approach was that unraveling the neuronal representations of sensory stimuli, from periphery to early stages of cortical processing, was crucial for understanding brain function (Romo and de Lafuente, 2013).

It is not surprising then that much experimental and theoretical focus has traditionally been put on the study of individual senses, one at a time. This has shed light on the fundamental functional properties of each individual sensory modality. These investigations were the ingredients for new questions related to the cognitive processing of sensory stimuli such as: where and how in the brain are the sensory information represented and stored? Where and how in the brain are these representations transformed into perceptual decisions? What components of the neuronal responses evoked by a sensory stimulus are linked to perception and decision making? How are these processes affected by learning? How does the brain create conceptual knowledge?...

My dissertation reports a series of experiments done on rats, inspired by such fascinating and difficult questions. Specifically, these experiments aim at understanding the mechanisms by which the brain integrates cues from multiple senses into a unified percept—where and how does the brain combine information from different sensory channels?

The past few decades have witnessed a surge of interest in multisensory integration. Most research has focused on one of two distinct approaches: one primarily on neurophysiological observations, and the other mainly on mathematical psychology and psychophysics. In the present PhD project we have tried to link these approaches in two steps: (1) assess the integration process with behavioral measures, and (2) probe neuronal processing in behaving animals.

In step 1, we measure the trial-by-trial percept of rats, in response to precisely measured sensory stimuli, as revealed by their behavioral choice. This step will comprise the 'psychophysical' methods by which we measure the relationship between the stimuli and the subjects' percept, and reveal the subject's experience according to a scale along some physical di-

mension. We can then compare the experimental findings with the predictions of computational models and learn about their benefits and possible pitfalls. In chapter 2, we discuss the behavioral methods in detail and in chapter 4, we will discuss the results of the behavioral experiments.

In step 2, we continue by measuring the relationship between neuronal activity and the stimuli, by which we learn about 'neuronal coding'—how the brain converts physical events into the neuronal language of spike trains. Then we measure the relationship between neuronal activity and rats' perceptual decisions by which we learn about 'decoding' and how the neuronal representation of a stimulus is transformed into a behavioral choice. We discuss the neuronal analysis and results in chapters 3 and 5 respectively.

1.2 Multisensory Perception

A significant step in early mammalian evolution was the re-organization and expansion of an area in the roof of the reptile brain, called the dorsal cortex, into the mammalian neocortex (Kaas, 2010; Northcutt and Kaas, 1995). This area progressively changed from a single layer of mixed excitatory and inhibitory cells into the six-layer multi-region brain mantle, with complex internal microcircuitry, the hallmark of all extant species of mammals.

It has been suggested that most early mammals were nocturnal or, more likely, crepuscular. There is evidence they might have been whiskered. The implication is that they combined incomplete sensory signals (e.g. tactile signals under dim light). The challenge of surviving in a hazardous and complex environment, was a driving force behind neocortical evolution, prompting the emergence of cortical maps for multiple sensory modalities, and mechanisms for rapidly integrating across these maps and making rapid yet accurate inferences based on scarce, noisy or ambiguous sensory input (Jerison, 2012).

Each sensory system has evolved to enable animals to act upon signals that can emerge through radically different forms of energy: electromag-

netic radiation (vision), chemical gradients (olfaction), pressure waves (hearing), forces and kinetic energy (haptics), gravity and acceleration (vestibular system), hydrodynamic velocity and pressure field (lateral-line system), etc. Because sensory signals originate with real objects that possess multiple physical attributes, it is reasonable to suppose that sensory systems evolved to function in some intermeshed manner. It would be non-optimal for instance to have one neural circuit dedicated to the control of our gaze towards a source of sound, another one, controlling the eye movements in response to a tactile sensation on the skin, and yet another system to calibrate the eye movement in response to the vestibular input.

Allman (2000) further hypothesized that the evolution of endothermy created a much greater demand for energy in mammals compared to reptiles of similar size. This meant that food foraging had to be much more efficient; thus the neocortex evolved to support a rich multimodal representational capacity that would allow mammals to make better decisions about when, where and how to forage.

The adaptive and survival significance of this capacity is highlighted by the ubiquity of convergence among sensory systems across the existing animal species (Naumer and Kaiser, 2010; van Hemmen et al., 2012). In fact, "there is no animal in which there is known to be a complete segregation of sensory processing" (Stein et al., 1996). It has been postulated that multisensory convergence and integration precedes the evolution of mammals and even the appearance of nervous systems to the extent that these processes are thought to have been present even in unicellular organisms (Stein and Meredith, 1993).

Therefore, in the mammalian nervous system, parallel to single sensory systems, dedicated multimodal circuits have evolved to integrate different modalities to augment the detection of sensory signals by reducing their ambiguity more rapidly and reliably than would be expected from the sum of individual senses. This fusion of information among different senses is termed 'multisensory integration' and the response gain to the cross-modal stimulus compared with the response to the most effective of its component stimuli is termed 'multisensory enhancement' (Stein and

Stanford, 2008).

Another evolutionary ability is the formation of modality-shared or cross-modal representations of percepts. The ability is a natural consequence of the fact that real things are not unimodal, but have attributes that span multiple energy channels. Recognizing things notwithstanding notable variance in the conditions of encountering that thing and in spite of collection of information through different sensory channels was an adaptive advantage of the earliest mammals–e.g. hearing and touch substituting for vision in the dark.

Aside from multisensory enhancement which alters the salience of cross-modal stimuli, and formation of 'amodal'[1] representations, a different aspect of sensory integration concerns creating essentially multisensory perceptual experiences. Our experience of a food taste, for instance, is the result of a combination of olfactory, gustatory, thermal, tactile and even sometimes visual and auditory information[2] (Simon et al., 2006).

As a result, these processes equip the organism with rich experience of the sensory world. This raises non-trivial issues: multisensory integration must not only take into account the inherent properties of each individual sensory modality, but also the fact that each modality has its own particular subjective meaning that should not be disrupted or contradicted by the integration process (Stein and Stanford, 2008).

[1] Also called modality-shared or modality independent or supra-modal

[2] For example, compare the taste of crunchy potato chips with water-soaked softened chips. The modified tactile and auditory components would significantly alter the perceived taste. For related research see: Zampini and Spence (2004).

1.2.1 Multisensory decision-making

We live in a noisy world, full of ambiguities and uncertainties: that is, there is an imperfect match between the world and the signals that it lends to our sensory systems. This uncertainty stems from both the physical nature of stimuli (because they are either thermodynamic or quantum mechanical in nature[3]) and encoding of these stimuli in the brain to messages carried by noisy neurons (Faisal et al., 2008). As a consequence of this uncertainty, it makes sense to believe that the brain must have developed probabilistic inference mechanisms to deal with noisy statistical measurements of the world (Fetsch et al., 2013; Knill and Pouget, 2004)[4].

[3] For example, the stochastic arrival of photons at the retina or all forms of chemical sensing which are affected by thermodynamic noise because molecules arrive at the receptor at random rates due to diffusion.

[4] This follows the statistical tradition of research on perception, starting from Fechner's enunciation of psychophysics in 1860 to the modern view that perception is statistical decision making (Gepshtein, 2010).

Because combining data from multiple measurements is a statistically simple way to reduce uncertainty, forming a *stable* and *unified* perception of the environment depends on our capacity to combine information across different senses. For an adult, this process seems seamless. While listening to someone in a crowd, we look at their lips to better understand speech. While typing, we combine tactile, proprioceptive and visual information to find the relevant keys. When driving we make decisions about when it is safe to over-take based on a combination of visual and vestibular inputs regarding our perceived speed and acceleration. Importantly, we even use knowledge gained from prior experience: "In similar situations in the past, did my automobile provide enough acceleration?".

In addition to reducing uncertainty, multisensory integration can mitigate ambiguities in sensory information. A good example of this process is the detection of linear acceleration of the head using otolith organs in the inner ear. The acceleration could arise from translational motion (for example, running forward) or from tilting the head. This ambiguity can be resolved by combining signals from otolith organs with information about rotational motion from the semicircular canals of the inner ear (Angelaki et al., 2004). Such examples highlight the vital role of multisensory integration.

Notwithstanding their seamless automaticity, it takes several years of development for the brain to compile processes including cue calibration (to improve accuracy), cue integration (to improve precision), causal inference[5], incorporation of prior experience and reference frame transformation[6]. These developmental issues are further complicated because cue combination is implemented by noisy neurons (Seilheimer et al., 2014).

[5] To determine if the sensory cues have a common source (Körding et al., 2007).

[6] To reconcile differences between the reference frames in which each sense is encoded.

1.3 Models of multisensory cue combination

In order to understand the underlying neuronal computations involved in a particular cognitive task, it is helpful to propose biologically plausible mathematical models based on which these computations could be implemented. These models are generally ideal observer or normative

models by which one quantifies optimal performance in a given task, that is, the best possible performance given the noise of the perceptual system and the conditions of the task. Optimality is defined according to a mathematical function (for example, minimizing a cost function) and the term 'ideal' does not mean perfect (error-free) performance (Fetsch et al., 2013). One can then compare the performance of subjects in a psychophysical task with the predictions of such models and infer the underlying neural computations. Indeed much research in cue integration has focused on whether this process is optimal. Optimality requires the experimenter to have a clear idea about the specifications of the task and the stimuli; it forces the experimenter to specify the information available in the task. In addition, as mentioned in section 1.2, it seems plausible that animals have evolved mechanism to combine sensory information optimally (Landy et al., 2011).

Ideal observer models for cue combination were first used to describe problems in the computational vision domain (Jacobs, 1999), and later in other sensory systems to describe within-modality or multimodal cue combination (Alais and Burr, 2004; Ernst and Banks, 2002; Körding and Wolpert, 2006). Here, we first review the general framework for a simple linear model of cue integration and then review one of the best studied "ideal observer" models of cue integration: Bayesian cue combination.

1.3.1 Linear models for maximum reliability

When an animal estimates the environment in order to make a decision or plan an action, it often takes advantage of multiple sources of information or sensory cues—i.e. any signal or piece of information about a particular state of the environment. As discussed earlier, these estimates are noisy and it is reasonable to think that the uncertainty of each of them is proportional to its variance. In the simple case of Gaussian noise, an ideal observer who tries to minimize the uncertainty (maximize the reliability) of the estimate made based on the cues, could perform linear cue integration as an optimal strategy. In this case optimality is defined as an estimate

with the lowest possible degree of uncertainty (i.e. variance) and also one which remains unbiased (i.e. it is correct on average because the mean of the sampling distribution of the estimate can be shown to be equal to the parameter being estimated).

More formally, suppose there are samples, s_i, $i = 1, 2, \ldots n$ of n independent, Gaussian random variables, S_i, with a common mean, μ and variances σ_i^2. The minimum-variance unbiased estimator of μ is a weighted average:

$$\hat{s} = \sum_{i=1}^{n} w_i s_i \tag{1.1}$$

where w_i is the perceptual weight of the ith cue, which is proportional to that cue's relative *reliability*, η_i:

$$w_i = \frac{\eta_i}{\sum_{j=1}^{n} \eta_j} \quad \eta_i = \frac{1}{\sigma_i^2} \tag{1.2}$$

The optimal integrated estimate has a reliability, η_{opt} that is greater than the reliability of the single cue estimates:

$$\eta_{opt} = \sum_{i=1}^{n} \eta_i. \tag{1.3}$$

Therefore, the variance of the integrated estimate will generally be lower than the variance of each individual estimate and never more than the least variable of them. Consequently if the ideal observer in an unbiased estimator of a particular object property, given that these estimates are Gaussian distributed and independent of each other (estimate noise and errors are independent), the minimum-variance estimate is a weighted average of individual estimates from each sensory cue. However, if in different cue estimates, the noise is correlated, the minimum-variance unbiased estimator will not necessarily be a weighted average but could be a nonlinear function of the individual estimates or one that takes into account the covariance of the cues (Fetsch et al., 2013; Landy et al., 2011).

1.3.2 Bayesian Cue Integration

Linear models for maximum reliability have been used extensively in cue-combination literature. However, these models have limitations because in more natural settings they often fail to capture the complexities that observers face. Bayesian decision theory provides a more general computational framework to address these complexities.

Like linear cue-combination models, in the Bayesian framework, a reliability-based weighting scheme is derived by formalizing the problem in terms of Bayesian inference. Here the information provided by sensory information is represented by a posterior probability distribution. According to the Bayes' rule:

$$P(s|d) = \frac{P(d|s)P(s)}{P(d)} \tag{1.4}$$

where, s, is the object property to be estimated and d is the sensory data given to and known by the observer (provided by a noisy sensor). $P(s|d)$, is the probability distribution representing the probabilities of different values of s being true given the observed data (with respect to the actual state of the world). If this distribution is a narrow one it represents reliable data. The probability of obtaining a sensory input (evidence) given each possible value of s is given by $P(d|s)$, the likelihood function of each sensory cue. For example, likelihood could quantify the probability of acquiring a set of firing rates in a population of neurons for each particular value of s. Importantly, because d is given, the likelihood is a function of s and does not behave like a probability distribution and does not need to integrate to one. $P(d)$ is a constant normalizing factor so that the entire expression integrates to one and it is independent of s so can be generally ignored in the estimation process.

According to equation 1.4, one could compute the posterior distribution from prior knowledge of s by knowing $P(s)$—the probability of a particular value of s occurring before any sensory observation.

With the posterior distribution in hand, the Bayesian decision maker can make an optimal decision. An optimal decision maker is one that min-

imizes expected loss (or maximizes the expected gain, $EG(a)$). In this case the loss function is defined as a function of estimation error. This can be calculated from the difference between the chosen (perceived) estimate and the actual value of the environmental property. In many psychophysical tasks, the observer makes a categorical decision which is an estimate of stimulus: $a(d)$. The gain function can be defined as the negative of the loss function: $g(a(d), s)$. Formally:

$$a_{opt} = arg\,max\, EG(a), \tag{1.5}$$

where,

$$EG(a) = \iint g(a(d), s)P(d|s)P(s)\, dd\, ds \tag{1.6}$$

If the prior distribution, $P(s)$ is uniform–i.e. all values of s are equally probable before the observation is made– the equation 1.5 is equivalent to a Maximum likelihood estimation. If the prior distribution is not uniform, a_{opt} is estimated optimally using maximum a posteriori (MAP) estimation.

Assuming that the sensory data associated with each modality are independent we can formalize the likelihood functions as following:

$$P(d_1, ..., d_n|s) = \prod_{i=1}^{n} P(d_i|s) \tag{1.7}$$

From equation 1.4 we we can write:

$$P(s|d_1, ..., d_n) \propto \prod_{i=1}^{n} P(d_i|s) \tag{1.8}$$

Therefore, the goal of the observer is to infer a conditional probability density (the posterior) over the parameter of interest (s), given the sensory input from one (or more) source of information d (the cues). With a prior distribution that is uniform or significantly broader than the Gaussian likelihood functions, the posterior distribution is the product of these individual sensory likelihoods which is another Gaussian with mean corre-

sponding to equation 1.1 and a variance which corresponds to the inverse of equation 1.3 (Angelaki et al., 2009; Fetsch et al., 2013; Knill and Saunders, 2003; Landy et al., 2011).

1.3.3 Application of Bayesian Cue Combination in Multisensory tasks

Various studies have tried to test the optimal cue combination framework in psychophysical discrimination tasks while presenting subjects with stimuli from multiple sensory modalities, separately or simultaneously combined. In these studies, human subjects, non–human primates or rodents, were found to decrease perceptual uncertainty and improve performance by combining multiple cues in a way that approximates a statistically optimal observer (Alais and Burr, 2004; Battaglia et al., 2003; Ernst and Banks, 2002; Fetsch et al., 2009; Gu et al., 2008; Jacobs, 1999; Raposo et al., 2012).

In such experiments the reliability of each sensory cue (its noise or variance) is measured from the psychophysical performance of the subjects in single-modality conditions of the task and then the optimal combined performance is predicted.

Considering a multisensory two-alternative forced-choice task (2AFC) with two modalities, with the simplifying assumption of Gaussian likelihoods, the psychometric data can be fit with cumulative Gaussian functions, yielding two parameters: the point of subjective equality (PSE, mean of the fitted cumulative Gaussian) and the threshold (defined as its standard deviation, σ) [7]. Then thresholds from single-cue conditions are used to estimate the relative reliability of the two cues, which specifies the weights that an optimal observer should apply to each cue (equation 1.1).

[7] This equality is discussed in detail in chapter 7.1.

It is worth stepping through the logic of signal detection theory to understand the basic rationale behind these calculations. When the subject is presented with a cue and has to estimate some feature of that cue (s), its estimate of that feature ($\hat{s}$) is noisy. The simplest and most common assumption is that this internal representation, $\hat{s}$, is Gaussian distributed; if

the representation is unbiased:

$$\hat{s} \sim N(s, \sigma^2). \tag{1.9}$$

If it is a biased representation, then the mean will be non-equal to s. When the subject is asked to compare two cues (or one cue and a fixed reference), it performs a calculation on the $\hat{s}$ values. If we specifically consider comparison between $\hat{s}$ and a fixed reference, r, then the probability that they answer $s > r$, depends on the cumulative distribution of $\hat{s}$. Therefore the psychometric function would take the shape of a Gaussian cumulative distribution function (CDF).

In a 2AFC task, the behavior of subjects can be explained very well by Binary Response Models. The responses on trial i can be described by the binary variable y_i. That is, it can have only two possible outcomes which we will denote as 1 and 0. For example y_i may represent presence or absence of a certain stimulus, or left versus right response in a 2AFC task:

$$y_i = \begin{cases} 1 & \text{with probability } P_i \\ 0 & \text{with probability } 1 - P_i \end{cases}$$

where, P_i is given by Cumulative Distribution Function (CDF) of the standard normal distribution evaluated at $s_i'\beta$. Where, s, is the stimulus parameter, and, β, is a vector of coefficient$([1/\sigma^2, -\mu/(\sigma^2)]^T)$:

$$P(y = 1|s) = \Phi(s'\beta), \tag{1.10}$$

Equation 1.10 implies that the probability that the subject provides one of the two response categories, is the inverse CDF (Φ) evaluated at the subject's internal representation of the quantity. If there are N trials, then we can write the likelihood function:

$$\mathcal{L} = \prod_{i=1}^{N} P_i^{y_i}(1 - P_i)^{1-y_i} \tag{1.11}$$

From equation 1.10 we have:

$$\mathcal{L}(\beta) = \prod_{i=1}^{N} \Phi(s_i'\beta)^{y_i}(1 - \Phi(s_i'\beta))^{1-y_i} \tag{1.12}$$

This gives rise to the log-likelihood expression for the dataset:

$$\ln \mathcal{L}(\beta) = \sum_{i=1}^{N} \left(y_i \ln \Phi(s_i'\beta) + (1 - y_i) \ln(1 - \Phi(s_i'\beta)) \right) \tag{1.13}$$

For multiple cues, from equations 1.7 and 1.8 we know that the joint likelihood is simply the product of the likelihood functions for each individual cue. When the likelihood functions for the cues are Gaussian, the joint likelihood function is Gaussian as well. The mean (μ) of the joint likelihood function is a weighted sum of the means of the individual likelihood functions (Knill and Saunders, 2003).

1.4 Neurophysiology of multisensory integration

At the neurophysiological level, much of the multisensory integration literature is influenced by research on orienting behavior, with primary focus on a midbrain structure primarily involved in orienting the eyes and head towards salient stimuli—the superior colliculus (Wurtz and Albano, 1980). In fact, these neurophysiological investigations started to characterize the "principles" governing multisensory neurons, several years before the theoretical and psychophysical aspects of multisensory cue combination were studied.

The pioneering work of Meredith and Stein (1986), demonstrated that cat SC neurons can combine auditory, tactile and visual cues to elicit multisensory-evoked activity that is often significantly enhanced (and sometimes suppressed) compared to uni-sensory responses. They further showed that these neurons show enhanced responses for multisensory stimuli only when those stimuli occur close in space and time (Meredith et al., 1987; Meredith and Stein, 1996), whereas sufficient separation in

space or time can suppress the multisensory response relative to the best unisensory response. These phenomena were termed the spatial and temporal principles respectively.

Stanford et al. (2005) explained another multisensory principle: inverse effectiveness. According to this principle, multisensory response enhancement is proportionally larger when the same unisensory stimuli presented individually only weakly activate the neuron. Weak unisensory stimuli can cause a substantial fraction of multisensory neurons in the SC to respond greater than the arithmetic sum of unisensory responses–a phenomenon called "superadditivity". Although the inverse effectiveness can be observed regardless of whether superadditivity occurs.[8]

[8] **Subadditivity** is a neuronal computation in which the multisensory response is smaller than the arithmetic sum of the responses to the component stimuli whereas, **Superadditivity** is the neuronal process in which the multisensory response is larger than the *arithmetic* sum of the responses to the component stimuli.

Several behavioral experiments with alert subjects, have reported similarities between the above mentioned multisensory principles (defined in SC neurons) and the performance of subjects in the psychophysical tasks (Frens et al., 1995; Stein et al., 1988). This has urged some investigators to look for the mentioned principles as "signatures" of multisensory integration at different levels. The initial efforts in understanding the cortical integration were based on these principles as well (Sarko et al., 2013).

However, midbrain structures like the superior colliculus lack the unique processing capacities of neocortex (plasticity, adaptation or linkage with memory stores in hippocampus). The multisensory processing of neocortex would be expected to be very different from that of subcortical structures, like the superior colliculus. Recent findings from neurophysiological and neuroimaging studies have challenged the traditional cortical parcellation schemes, by finding that multisensory interactions are common in the cortex and are far more widespread than was thought before. It has been even proposed that the entire neocortex is multisensory (Ghazanfar and Schroeder, 2006).

In an effort to understand how discrete the borders between sensory cortical areas are, Wallace et al. (2004) mapped single-units across the postero-lateral neocortex covering the primary auditory, somatosensory and visual areas (Figure 1.4.1). They found that within each of these unimodal areas there were few neurons that responded to stimuli from an-

other modality, but between these modality specific areas, they found neuronal clusters that not only responded to inputs from more than one modality, but were capable of integrating these multisensory inputs (Ghazanfar and Schroeder, 2006). More recently, Iurilli et al. (2012) found that activation of one sensory cortex causes hyperpolarizing responses in neighboring ones. For example a noise burst activated GABAergic synapses onto layer 2/3 pyramids of the visual cortex. Further they argued that this sound-driven inhibition by salient stimuli degrades potentially distracting sensory processing in the visual cortex by recruiting local, translaminar, inhibitory circuits. Beyond this, numerous other studies have shown that simultaneous activation of a sensory modality is able to modulate local, ongoing, and evoked activity in other early sensory cortices (Bizley et al., 2007; Ghazanfar et al., 2005; Kayser et al., 2008; Lakatos et al., 2007).

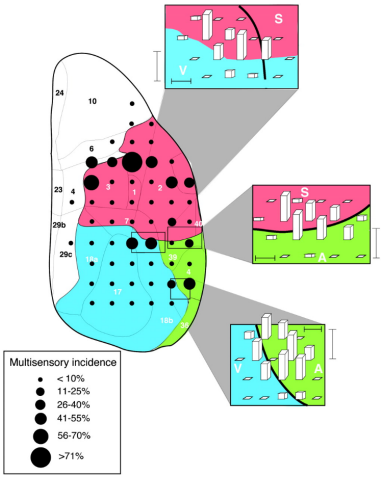

Figure 1.4.1: The widespread distribution of multisensory neurons in rat sensory neocortex. Numbers and solid lines show major cortex subdivisions (parietal, red; temporal, green; occipital, blue). Filled circles are recording sites and bar height indicates the relative incidence of multisensory neurons. Figure adopted from (Wallace et al., 2004).

In the vast majority of electrophysiological studies, recordings have been made from neurons within a single area. The animals were anesthetized or received stimuli passively; making it impossible to look at the animals' capacity to use multiple sensory signals to identify the stimuli. These investigations have led to advances in our understanding of multisensory integration but recording from large neuronal ensembles from multiple brain areas while animals are freely moving during a behavioral task might allow a richer set of experimental findings. The relevance of neurophysiological findings must be combined with and confirmed by precise behavioral measures taken in rigorous psychophysics. Doing so, the investigator will be able to learn how population of neurons interact within and between areas at different time scales to accomplish a task.

In combination with these techniques, the reversible use of light-activated channels and pumps and pharmacogenetic tools provide a way to activate or inactivate certain neuronal populations. In this way the researcher could tease apart the causal role of neural populations in a particular behavior.

1.5 Study of Perception in Rodents

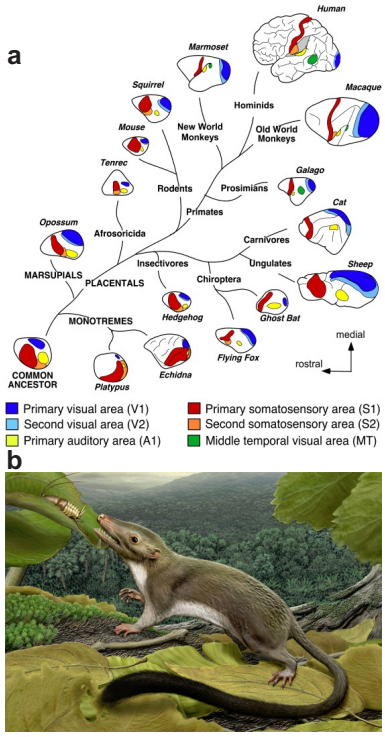

Figure 1.5.1: (a) A phylogenetic tree illustrating the relationship between brain of major mammalian groups. (b) Reconstruction of the phenotype of the hypothetical placental ancestor. (a) Adopted from (Krubitzer, 2007), (b) Illustration by Carl Buell, from (O'Leary et al., 2013).

Much of the classical neuroscience research about higher cognitive functions such as decision-making, learning, attention and working memory have traditionally been carried out on non-human primates. Work on primates, however, has major drawbacks: their maintenance and welfare is expensive and sophisticated and the number of subjects available to each study is usually very limited. Ethical issues abound. Rodents, like rats and mice had long been ideal for research on spatial navigation and the processing of reward and punishment in the brain. But are rodents suitable for the study of perceptual and cognitive mechanisms? Until a few years ago, 'perception' was for the most part attributed to primates but not to rodents. This view has changed and rodents have now become popular for studies of perception and decision making (Carandini and Churchland, 2013; Diamond and Arabzadeh, 2013; Zoccolan, 2015).

Three major factor have contributed to this popularity. First, emerging technologies in rodent research, such as optogenetics, transgenic lines for specific targeting of certain cell types, gene expression and connectivity maps in brain areas[9], two-photon microscopy and possibility for large-scale recording of neuronal ensembles make the rodent system desirable for systems neuroscience research. While it is possible to apply these tools in other species, they are currently far less advanced. Second, increasing evidence for rodent cognitive capacities (Abbott, 2010), such as decision making (Brunton et al., 2013), the ability to weigh sensory evidence (Kepecs et al., 2008), rule learning (Murphy et al., 2008) and working memory (Fassihi et al., 2014). Third, rodents are evolutionary surprisingly close relatives to humans (Dawkins, 2010) and share fundamental similarities in brain organization (Fig. 1.5.1), including a basic common plan for the cortex (Carandini and Churchland, 2013; Krubitzer, 2007).

In this section we will first review the two relevant sensory systems in rats which are in the context of this project: Rats' whisker sensory system as an "expert" active sensory system and then rats' visual system. Finally I will review the study of multisensory integration in rats and mice.

[9] The Allen Brain Atlas, GENSAT and the Mouse Brain Architecture Project provide surveys of gene expression in the mouse brain and maps of connections between brain regions.

1.5.1 Rat tactile sensory system

Transformation of sensory data from the physical world into meaningful "objects" is a fundamental characteristic of the neocortex. After analyzing the behavioral effects of ablations in the auditory system, Whitfield (1979) concluded, that the cortex transforms physical characteristics into the percept of real things that are "out there" in the world. Early investigations on the role of the neocortex asked the question "How does an animal behave after removal of cortex?" These studies showed that although a decorticate animal—like a cat lacking all auditory system above the level of inferior colliculus or a rat without a barrel field—can elicit a variety of simple stereotypical behaviors, only the intact animal can generalize the sensory information about a problem to solve closely related ones (Whitfield, 1979). The decorticate cat, for instance, cannot attach an external objective existence to the stimulus source—like a train of clicks. So in this case, the neocortex transforms the elementary patterns of sensory driven neural activity into objects and concepts. The insightful experiments of Masterton and Diamond (1964), showed that although a decorticate cat can be trained to distinguish two different dichotically presented trains of clicks from one another, the two discriminations have to be learned as separate problems and there is no transfer between them. Neocortex, facilitates the transfer of training by generalization and making sense of the different stimuli by extracting their common signals and attributing them to an 'object in space' (Whitfield, 1979).

Our approach is to some extent motivated and inspired by these classical studies in that we set out to design a behavioral task that involved not abstract, unnatural computer-generated stimuli, but instead a real object that can be seen and felt. We believed that the attribution of sensory properties to a real thing might leverage the key functions of neocortex and thus might bring us to interesting observations on cortical processing.

A productive approach towards understanding cortical transformation of physical characteristics into the meaningful percepts, has been to investigate the so called "expert" cortical processing systems[10].

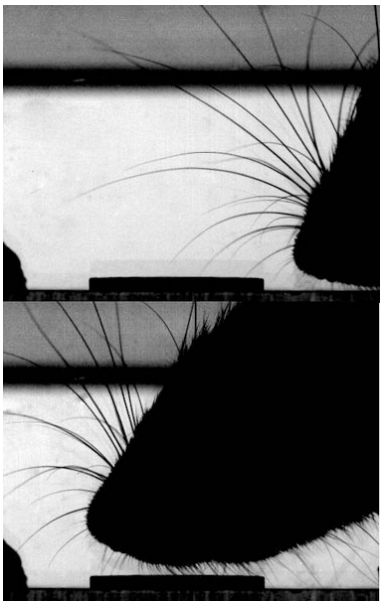

Figure 1.5.2: Macrovibrissae are often used to locate objects that are then investigated further with the shorter, non-actuated microvibrissae on the chin and lips. Pictured are high-speed video frames of a rat locating a coin with its macrovibrissae (top) and next brushes the microvibrissae against the coin surface (bottom). Figure adopted from (Prescott et al., 2011b).

[10] "Expert" cortical processing systems are ones that accomplish complex transformations in a fast and reliable manner (Diamond and Arabzadeh, 2013)

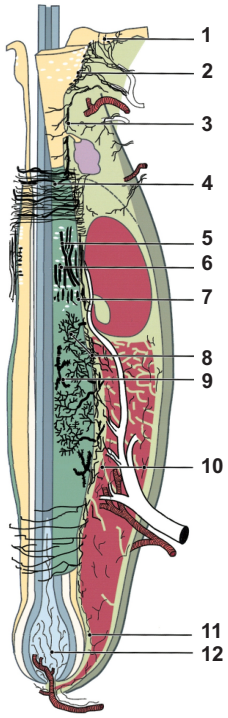

Figure 1.5.3: Schematic view of the rat whisker follicle. 1, Skin innervation. 2, Merkel endings. 3, Innervation of the sebaceous gland. 4, Circumferential fine innervation and lanceolate endings. 5, Merkel endings. 6, Longitudinal lanceolate endings. 7, Club-like endings. 8, Reticular endings. 9, Irregularly branched spiny endings. 10, Fine innervation. 11, Innervation around the follicle bulb. 12, Innervation in the dermal papilla. Adapted from Ebara et al. (2002).

[11] Pronounce: [vai'brisi]; singular: vibrissa; [vai'brisə]

[12] Microvibrissae are short (few mm), densely spaced (87 per cm2) whiskers located on the anterior part of a rats snout. They are not ordered in a regular grid and exhibit little or no whisking motion (Diamond et al., 2008b).

One such system is the primate visual system which is well known for its efficiency in extracting meaning from visual scenes. In mice and rats, perhaps an equally expert system is their whisker-mediated tactile sensation. In nature, rats are active in dim or dark environments and their survival depends on their sense of touch. The classic study of Vincent (1912), showed that a rat's ability to navigate through a raised labyrinth depends on the use of its whiskers. It is believed that whisker touch (along with olfaction) represents a major channel through which rodents collect information from the nearby environment (Diamond et al., 2008b). They use their whiskers to recognize the position and identity of objects, particularly in in the dark.

In this section, we first briefly describe the organization of the whisker sensory system and then describe the process of active sensing.

Organization of the rat whisker sensory system

Whiskers or vibrissae[11] are a type of mammalian hair that are typically characterized by their large size, and a large and well-innervated hair follicle. Vibrissae differ from ordinary (pelagic) hair by being longer and thicker, having large follicles containing blood-filled sinus tissues, by having an elaborate muscle matrix around the base and a corresponding network of motor control centers, and by having an identifiable representation in the somatosensory cortex (Prescott et al., 2011b).

On the rat's snout, whiskers form a grid-like layout of about 35 vibrissae in addition to an array of shorter, non-actuated microvibrissae[12] that can be seen on the chin and lips (Fig. 1.5.2). These two classes of whiskers constitute an array of highly sensitive detectors that project outwards and forwards from the snout to generate and collect tactile information. The relevant sensory pathways pass through the brain stem and thalamus before reaching the primary somatosensory cortex (Diamond and Arabzadeh, 2013).

Whisker motion transmits mechanical energy to the follicle (Birdwell et al., 2007) which is transduced into trains of action potentials by sensory

receptors—the terminals of trigeminal ganglion cells. The whisker follicle is surrounded by receptors (Fig. 1.5.3). Among the most important types are Merkel endings. Other populations include lanceloate endings, which are a form of free nerve ending. The whisker sensory receptor endings are the terminals of the peripheral branch of the trigeminal ganglion (Nicholls et al., 2012).

About 200 ganglion cells innervate each whisker's follicle (Dörfl, 1985), whose nerve endings convert mechanical energy into action potentials. These afferent signals travel past the cell bodies in the trigeminal ganglion and continue along the central branch to form synapses in the trigeminal nuclei of the brainstem (Clarke and Bowsher, 1962; Torvik, 1956). The trigeminal nuclei convey afferent vibrissal information to the thalamus via parallel pathways that then continue to the barrel field of the somatosensory cortex (Deschênes et al., 2005; Diamond et al., 2008b).

Somatosensory cortex[13], consists of a primary field (SI) and a secondary field (SII). In the primary field, macrovibrissae have a distinct representation. Histological and electrophysiological studies have demonstrated a one-to-one correspondence between macrovibrissae and barrels—distinct clusters of neurons in SI. Therefore, the area of SI that received inputs from whiskers is often called barrel cortex (Diamond and Arabzadeh, 2013).[14]

[13] Somatosensory cortex is defined as the area receiving direct input from the ascending somatosensory pathway

[14] The barrel cortex refers to the dark-staining regions of layer four of the somatosensory cortex where somatosensory inputs from the contralateral side of the body come in from the thalamus. Barrels are found in some species of rodents and species of at least two other orders (Woolsey et al., 1975).

Active sensing

Active sensory systems are information-seeking systems which usually involve sensor movement, and involve control of the sensor apparatus, in a manner that suits the task, so as to maximize information gain.[15] Active sensing is perhaps most evident in the modality of touch (Prescott et al., 2011a). The whisker system of rats is a good example of such system. Self-generated whisker motion is critical for wall following (Jenks et al., 2010), distance estimation (Harris et al., 1999), and identifying properties such as texture (Diamond et al., 2008a), shape and size (Brecht et al., 1997; Harvey et al., 2001; Polley et al., 2005).

[15] In the engineering terminology, an active sensor is one that functions by emitting signals and then measuring the effect of the emitted signal on the environment (Nelson and MacIver, 2006). A radar is active while a camera is passive.

It has been argued that whisker-mediated perception can arise through two general modes of operation: (1) generative mode and (2) receptive mode (Diamond and Arabzadeh, 2013). The generative mode involves the process of "whisking" in which rats move their whiskers forward and backward at a frequency of about 10 Hz, to actively seek contact with the objects in the environment.[16] In this manner the rat actively creates the percept by its own movement. For instance the discrimination of textures and localization of objects are performed by active whisking (Diamond, 2010; Diamond et al., 2008a; Zuo et al., 2011). In the receptive mode, rats would immobilize their whiskers to optimize the collection of signals from an object that is moving on its own such as a vibrating surface. Although it is difficult to quantify rodents' use of their whiskers in natural, out-of-laboratory settings, it seems reasonable to assume that some forms of perception rely on blocking motor output to keep the whiskers immobile. For instance, in order to feel the vibration of an object we would place our fingertips on the surface without moving them; rats would perhaps do the same with their whiskers to feel the vibrations emitting by a predator approaching their underground borrow (Fig. 1.5.4). Rats' would use a similar strategy while judging the orientation of a surface or an object feature: they would likely rely mostly on the deformation of their whiskers as they sweep them on the surface of the object using a combination of head and body movements.

[16] The rhythmic sweeping action is called *whisking* and an individual cycle is called a *whisk*. Whisking is the starting point for the perception of texture (Diamond and Arabzadeh, 2013).

1.5.2 Rodent vision

Historically, the common thinking about mice and rats was that they rely on a different combination of senses compared to primates, namely somatosensation, olfaction and hearing. Indeed, rats and mice are equipped with an exquisite olfactory system with nose, as well as vomeronasal organ, and large olfactory bulbs that enables them to make delicate and reliable decisions (Kepecs et al., 2008)[17]. Their "expert" whisker system was discussed in the previous section.

Nevertheless, despite vision being a main research topics in neuro-

[17] There are between 500 to 1,000 types of olfactory receptors, coded for by between 500 and 1,000 genes. That staggering number of genes is about 1% of the rat's DNA and underlines the evolutionary importance of this sense for them.

Figure 1.5.4: The receptive mode of touch. As a predator approaches the rat's hiding place, the vibration signal might be transferred to the whiskers through their contact with the walls and floor of the burrow. Drawing by Marco Gigante.

science, and despite the fact that rats and mice are the most widespread laboratory animal species[18],until very recently, rodents have been largely overlooked by the vision science community, because their brains have been assumed to lack advanced visual processing machinery (Zoccolan, 2015). In general there is an unsubstantiated assumption that rodent behavior is only weakly influence by vision. This assumption is based on several observations—that mice and rats are nocturnal/crepuscular animals (Burn, 2008)[19], they have relatively low visual acuity (e.g., ~1 cycle/deg in pigmented rats (Birch and Jacobs, 1979; Dean, 1981; Keller et al., 2000; Prusky et al., 2002, 2000), compared to 30–60 cycles/deg in human and macaque fovea (Campbell and Gubisch, 1966; Merigan and Katz, 1990). Also, although neurons in rodent primary visual cortex displaying many of the tuning properties found in higher mammalian species, such as orientation tuning (Bonin et al., 2011; Girman et al., 1999; Shaw et al., 1975), they are not arranged into the functional cortical modules, such as the orientation columns (Van Hooser et al., 2005).

On the other hand, there is compelling evidence that vision is a crucial source of information for rodents to locate themselves in the environment during spatial navigation–typically when foraging over large ranges around their nests (Barnett, 2007; Chen et al., 2013). Rats make excellent use of visual cues; when tested in spatial navigation tasks they prefer to rely on visual cues compared to olfactory and auditory cues and path integra-

[18] For example mice and rats account for over 80% of all research animals used in the European Union (Burn, 2008).

[19] Crepuscular animals are those that are active primarily during twilight (dawn and dusk).

tion (Morris, 1981; Suzuki et al., 1980). A hallmark of this dependence is locking of hippocampal place fields to environmental visual cues, and their remapping when these cues are changed (Jezek et al., 2011; Muller and Kubie, 1987; O'Keefe and Speakman, 1987). In addition, several cortical areas in rodents devoted to vision provide possibility of complex visual processing of the scene such as shape-based visual object recognition (Gaffan et al., 2004), transformation-tolerant (invariant) visual object recognition of three-dimantional shape from two-dimensional images (Tafazoli et al., 2012; Zoccolan et al., 2009).

Rats and mice are considered nocturnal animals, however it has been shown that mice are reliably nocturnal only if food is unlimited (in laboratory conditions), whereas when food is scarce they spend parts of the night sleeping in order to lower the body temperature and minimize daily energy expenditure (Hut et al., 2011) and in nature they can become entirely diurnal (Daan et al., 2011). In addition, the eyes of rats and mice lack the reflective tapetum that would be expected in nocturnal animals which contradicts the view that mice and rats are entirely nocturnal (Carandini and Churchland, 2013).

1.5.3 Multisensory Perception in Rats

Cognition in general and multisensory perception and decision making in particular has been studied extensively in humans and non-human primates. From these studies we know that there are multisensory perceptual benefits such as increased accuracy of detection and discrimination and faster reaction times. Appreciation of rodents' cognitive and perceptual abilities, see section 1.5, has created a new wave of interest in the study of perceptual and neuronal mechanisms for multisensory perception in rodents. A question in neuroscience is whether only primates are capable of performing certain multisensory processes such as evidence accumulation in time or from multiple modalities or across space, dynamic weighting of stimulus inputs according to their reliability, or these are widespread mechanisms in mammalian species.

1.6 Posterior Parietal Cortex in Rats

The parietal cortex is covered by the parietal bone. It includes at least two functionally distinct regions: the somatosensory cortex and an area that is considered part of the multimodal association cortex—the Posterior Parietal Cortex (PPC) (Krieg, 1946). This definition is based on several criteria, such as topological relationships among cortical areas, cytoarchitecture, myeloarchitecture, and expression patterns of different neuroactive substances and neurotransmitters. Combined with connectional criteria focusing on thalamocortical and/or corticocortical connectivity, electrophysiological and behavioral comparisons, it is suggested that a PPC can be defined in most species (Whitlock et al., 2008). The PPC lies in between somatosensory cortex anteriorly and visual cortex posteriorly (Krubitzer, 1995). A distinguishing feature which helps to differentiate the PPC from the adjacent somatosensory cortex is that only the somatosensory cortex exhibits strong callosal connections (Akers and Killackey, 1978).

1.6.1 The Organization of Parietal Cortex in rats

In various species, PPC is characterized by its connection with the higher-order associative posterior thalamus. In non-human primates, it is characterized by thalamic input from the posterior domain of the thalamus, in particular, the pulvinar. In other mammals, including the rat, thalamic inputs to PPC arise predominantly from the lateral posterior nucleus and adjacent nuclei, including laterodorsal and posterior nuclei which are considered to be homologous to the primate pulvinar and posterior thalamic domain. Importantly, like primates, thalamic projections from the ventral nuclear complex and lateral geniculate in the rat do not seem to innervate the PPC (Reep et al., 1994). This pattern of thalamic inputs helps in defining borders between PPC, somatosensory cortex, and visual cortex (Wilber et al., 2014).

The PPC, receives input from cortical areas representing all main sensory modalities and communicates back to these domains (Cavada and Goldman-Rakic, 1989; Leichnetz, 2001; Miller and Vogt, 1984). It is also

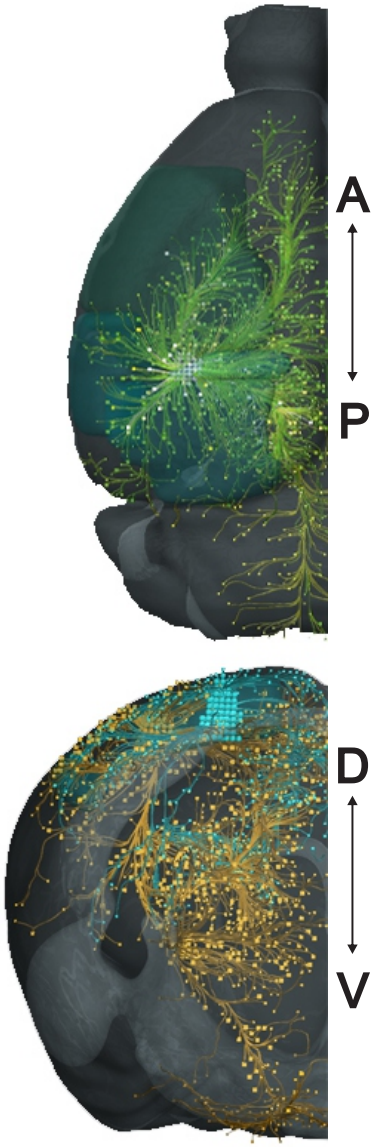

Figure 1.6.1: The projections of mouse PPC. Green, cortex; Cyan PC. Lines denote projections; Green, efferents to PPC; yellow afferents. Image copyright Allen Institute for Brain Science http://mouse.brain-map.org/, using Brain Explorer 2.

reciprocally connected to almost all of the other multimodal association cortices, such as prefrontal, frontal, temporal, and limbic association cortex as well as motor and premotor areas of the cortex (Akers and Killackey, 1978; Reep et al., 1994).

In rats, the parietal cortex (PC) has input-output relationships with motor, sensory, and limbic brain regions. PC in rats can be subdivided into four distinct rostral-caudal and medial-lateral regions, which includes a zone previously characterized as secondary visual cortex[20].

A recent anatomical investigation of cortical connectivity maps by Wilber et al. (2014), revealed anatomically distinct areas in the parietal cortex of the rats (Fig. 1.6.2). They demonstrated that the lateral portions of PC have a connectivity profile that is distinct from the medial zones. Specifically, medial portions were almost exclusively reciprocally connected to dorsal retrosplenial cortex (part of the medial network), and received dense inputs from anterior and lateral associative thalamus. While the lateral portion received inputs from a wider range of cortical and thalamic structures including medial secondary visual and parietal, motor, somatosensory and visual cortices and sensory and motor thalamus (Wilber et al., 2014). One of their surprising findings was a relatively weak primary visual cortex input to the PC, particularly to the medial secondary visual cortical (caudal) zone of PC (according to Paxinos and Watson 2007, V2MM/V2ML).

[20] These four zones are defined on the basis of cytoarchitectural differences: a rostral region which is composed of medial and lateral components (MPta and LPta, respectively; Paxinos and Watson 2007), and a caudal PC also composed of medial and lateral components (V2MM and V2ML, respectively; Paxinos and Watson 2007)

1.6.2 The role of posterior parietal cortex in decision making in rats

Much of our current knowledge about the PPC comes from the primate studies. For instance we know that in primates the PPC is involved in perceptual decision-making and categorization (Gold and Shadlen, 2007; Roitman and Shadlen, 2002; Shadlen and Newsome, 2001), action planning (Andersen and Cui, 2009) and spatial attention (Bisley and Goldberg, 2010). [21]

Recently, several laboratories have chosen to explore the role of this

[21] In primate brain an area of posterior parietal cortex (PPC) that is characterized by multimodal sensory projections to and from the frontal association cortex could be identified. It is known that lesions to this area lead to a clear behavioral syndrome (Kolb and Walkey, 1987). For instance in humans, the most common symptom following unilateral PPC damage is hemispatial neglect.

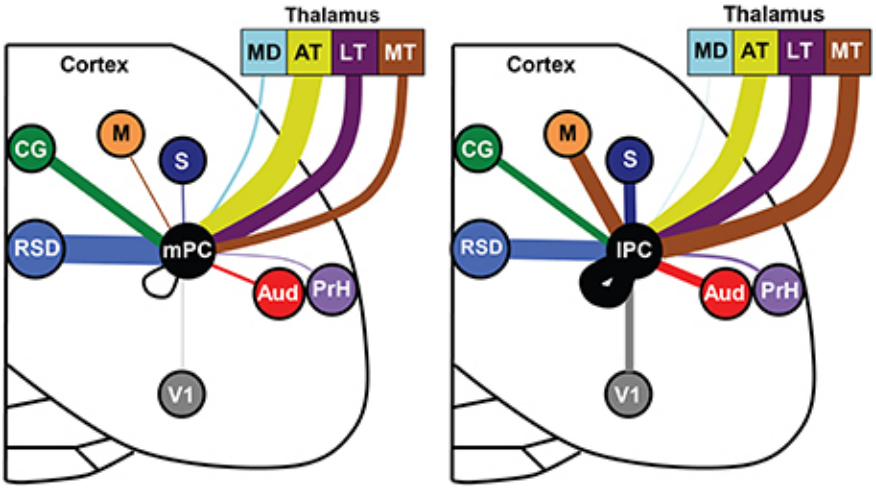

Figure 1.6.2: Distinct input patterns for medial vs. lateral parietal cortex of the rat. Brain regions are depicted by different colors and the connecting line thickness represents the strength of thalamic and cortical projections to the medial PC **(left panel)** and lateral PC **(right panel)**. Here the thalamic data is normalized separately from cortical data. This analysis shows projections to lateral PC (lPC) involve stronger projections from the somatosensory (S), motor (M), visual (V1), auditory cortex (AUD), and motor thalamus (MT). The medial PC (mPC) receives stronger inputs from the dorsal retrosplenial cortex (RSD) and cingulate region (CG). Mediodorsal thalamus (MD), anterior thalamus (AT), lateral thalamus (LT), perirhinal cortex (PrH). Figure adapted from (Wilber et al., 2014).

brain region in the context of complex behavioral tasks in rodents. Several reasons have contributed in this choice. As discussed in the previous section, the posterior parietal cortex is well poised to include essential neural mechanisms for decision making in rodents. Anatomically, it is well-connected to the sensory areas, receiving inputs from auditory, visual and somatosensory areas making it a suitable candidate site for multisensory integration (Kolb and Walkey, 1987; Reep et al., 1994). It has been shown to be involved in navigation and locomotion (Nitz, 2012; Whitlock et al., 2008). It has been shown that neurons in the PPC ramp up their activity during accumulation of sensory evidence (Hanks et al., 2015). Notably it has been shown that mouse PPC, in a navigation-based decision task, is involved in holding a perceptual decision in short time scales and has a causal role in short-term memory for orienting acts (Harvey et al., 2012). The rodent PPC shows a delay activity that is correlated with performance on short-term memory tasks (Harvey et al., 2012; Nakamura, 1999).

In summary, PPC seems to be a fascinating candidate network of rat association cortex which plays important roles in perceptual decision making and multisensory integration. Therefore we have decided to first focus on it in the neuronal investigations of the current thesis project.

Choices are the hinges of destiny.

Pythagoras

2

Behavioral Methods

The general structure of the behavioral experiments presented in this thesis was "two-alternative forced choice (2AFC)" task. A subject in such a task typically is presented with a stimulus and must classify the stimulus as belonging to one of two distinct categories. The subject must then report its decision by choosing between the two possible responses; the "alternatives" refer to the two possible actions. In this general task structure, as compared to many other tasks such as go/no-go, measures of accuracy are less affected by changes in a subject's motivation or willingness to respond: they *must* report a decision on every trial. This also makes it clearer which responses constitute true decisions (Carandini and Churchland, 2013). A 2AFC task lends itself to precise mathematical characterization of subjects' performance through signal detection theory and psychometric analyses.

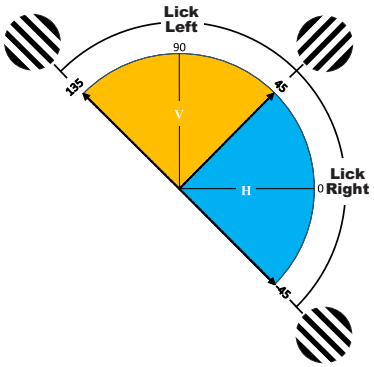

Figure 2.1.2: Schematic orientations of the stimuli and rule of the categorization task. Rats were trained to categorize orientations less than 45 degrees as horizontal and respond by licking right reward spout. Likewise, they must categorize orientations greater than 45 degrees as vertical and respond by licking the left reward spout. For some rats the opposite rule was used to counterbalance possible biases in the behavior arising from asymmetries in the apparatus or left/right biased preference of the rats.

[1] The orientation of stimulus was measured with respect to the horizontal plane of the behavioral apparatus– 0 degrees.

2.1 General Experiment design

To encourage rats to combine information across sensory modalities we designed a visual-tactile orientation categorization task. Figure 2.1.1, illustrates in a schematic manner the sequence of events in the behavioral task.

Each trial started with a head-poke that triggered the stimulus presentation. Stimuli looked and felt like gratings which were rotated across angles that spanned 180 degrees. The stimuli were presented in four conditions: visual-tactile, visual-only, tactile-only and control (neither tactile nor visual access to the stimulus). Rats had to categorize any orientation between 0 ± 45 degrees as horizontal, and any orientation between the range 90 ± 45 as vertical[1]. Therefore orientations 45 and -45 (the same as 135) would mark the boundaries between the categories (Figure 2.1.2).

Rats typically had a 2,000 ms 'window of opportunity' to respond by licking. After licking the trial was terminated. The reward rule was set reversed for some of the rats throughout their training to control for possible biases in the behavior which could arise as a result of asymmetries in the apparatus (e.g. reward pumps) or left/right biased preference of the rats. The boundary angles (45, -45 and 135) were rewarded randomly with probability of 0.5 on left/right. The perceptual difficulty of the trial depended on the angular distance from 0 and 90 degrees. Further details are discussed in the following sections.

As mentioned in the Introduction (chapter 1), one advantage of our behavioral design is that it allows the rat to explore a real object through two sensory channels; vision and touch can be integrated while the animal examines its shape, form and spatial properties. In contrast, many studies use unrelated stimuli in different modalities but train the subject to associate them by some arbitrary (and possibly non-ecological) rule (Sarko et al., 2013).

Our canonical training procedure turned out to be fast. Training duration is an important question in the design of a rodent psychophysics experiment. A quick training phase not only saves time and lowers the cost

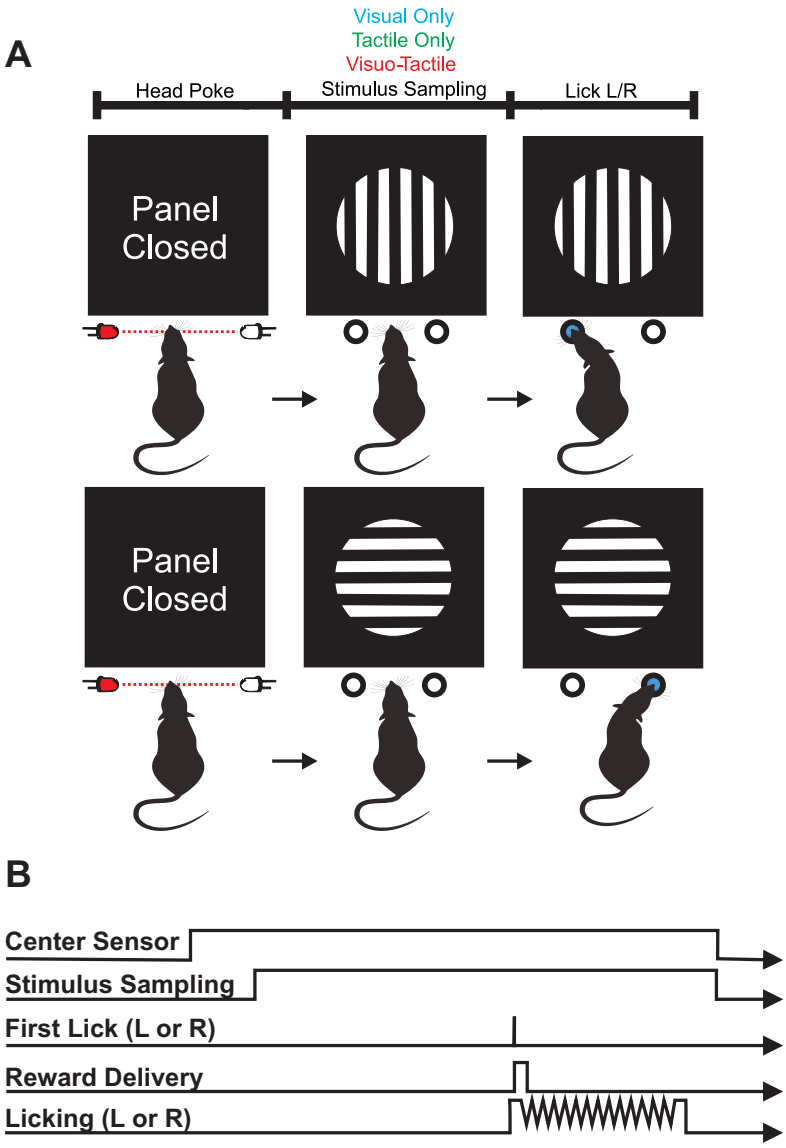

Figure 2.1.1: Schematic outline of the behavioral task and events (A) Each trial started by a head poke that opened an opaque panel that revealed the stimulus. Through the experimenter's precise control of lighting and a transparent panel, rats had the opportunity to categorize the orientation of stimulus as horizontal or vertical under four experimental conditions. They reported their decision about the orientation of the gratings by licking on the left/right spouts (B) Illustrates the events structure of the behavioral task. The signals from these events were digitized and sent synchronized with the neuronal recordings to a digital signal processor (DSP) and stored for offline analysis.

of training and subsequent chronic neurophysiological procedures but also makes neuronal investigations of the learning process more feasible. It is possible that long training schedules would include more unwanted brain plasticity and even alter the brain regions involved in the performance of the task. This could perhaps affect the interpretation of both behavioral and neuronal results.

2.1.1 Subjects

Fifteen male Long–Evans rats (Charles River Laboratories) were used in total. Animals were 8 weeks old upon their arrival to the laboratory and weighed approximately 250 g. They typically grew to over 600 g over the course of the study. Rats had free access to food but were water-deprived during the days they underwent behavioral training after each experimental session, and received a total amount of 17-22 ml of pear juice diluted in water (1 unit juice: 4 units water) as reward during the training. The water restriction schedule allowed access to water *ad libitum* for 1 hour after each training session. Rats were caged in groups of two animals, except for implanted rats who were housed alone in a cage. Rats were maintained on a 12/12 light/dark cycle. Experiments were conducted during the light-phase cycle. Rats were habituated to the researcher (handling procedure) for five days before the behavioral training started.

Rats were examined weekly by a veterinarian. Protocols conformed to the international norms and were approved by the Italian Health Ministry and the Ethics Committee of the International School for Advanced Studies.

2.1.2 Behavioral apparatus

The behavioral apparatus consisted of a custom-built opaque white Plexiglas chamber measuring 25(height) × 25(width) × 37(length) cm (Fig. 2.1.3). A circular hole[2] (diameter = 5 cm) was implemented in the front wall through which the animal could extend its head from the main chamber to see and touch the stimulus and could reach the reward spouts

[2] Termed head-hole. For implanted rats this was changed to a head-slit.

equipped with licking sensors at the stimulus port. An opaque panel prevented seeing/touching the stimulus before the onset of each trial. The stimulus was placed at 3 cm distance (with respect to the tail-to-snout axis of the rat) from the opaque panel and the reward spouts were placed at 2 cm lateral distance from the stimulus. The rat started a trial by interrupting an infrared beam detected by a phototransistor situated in the head-hole. This signal triggered the fast opening of the stepper-motor controlled opaque panel (40 degrees in 75 ms) to permit access to the stimulus and reward spouts. The apparatus was in a Faraday cage, covered with acoustic insulation which also provided complete darkness. An array of 12 high-power infrared emitter ($\lambda = 850$ nm, OSRAM Opto Semiconductors GmbH, Germany) illuminated the stimulus port to permit the investigator to monitor behavior and to execute video recording without interfering with the experiment. An array pair of 6 visible white LEDs illuminated the stimulus; the intensity of these LEDs could be modulated via pulse-width modulation (PWM) allowing the trial-by-trial control over the visual salience of the stimulus (Appendix 7.4).

Two infra-red (IR) sensitive video systems (Point Grey Flea, Edmund optics) registered the rat's actions. The first camera was equipped with a macro lens mounted 30 cm above the stimulus delivery area (distance with respect to the bottom of stimulus) was used to monitor the action of the rat facing the stimulus and reward spouts. The second camera provided a wide angle view (Fujinon TV LENS) of the interior of the setup and was illuminated with adjustable IR LEDs. The second camera collected videos at 30 frames per second. In some sessions, using the first camera high-speed video images were taken at 250 frames per second through a macro lens (Fujinon TV LENS, HF25HA-1B) to monitor head, snout and whisker position and movement during behavior.

The stimuli were presented in three different conditions, the fourth condition being the no-stimulus control trials: (1) Tactile-only, whereby the rat could examine the stimulus with its whiskers in dark; ambient light measured as 0 cd/mm^2 measured by a luminance meter (Konica Minolta LS-100), (2) Visual-only (a stepper-motor actuated transparent panel in

front of the illuminated stimulus prevented tactile contact; ambient light in visual condition was 10.24 cd/mm^2), and (3) Visual-Tactile condition in which rats were able to both see and touch the stimuli. (4) In the control condition rats could neither see nor touch the stimulus (transparent panel in front of the stimulus and white lights off).

The rats' responses were registered by the licking sensors on the right or left spouts. Correct responses were rewarded by a precisely controlled amount of diluted pear juice (0.05 mL per trial in normal conditions). Reward spouts included custom-made infrared diode sensors that rats interrupted with tongue movement while licking. The licking signal triggered the pump motor to extrude juice only if rats licked the correct spout. After this step the trial terminated by the closure of the opaque panel. The 'window of opportunity' for reward collection was set to 2 s, but could be varied by the experimenter in order to influence the behavioral cadence of the rats (e.g. in a slow rat, window of opportunity could be reduced to promote urgency). Before the successive trial began, the motor on which the stimulus was mounted rotated to generate the next orientation (Fig. 2.1.4). To avoid acoustic cues about orientation, an orientation that differed from that of the previous trial by n degrees could be achieved by rotating the stimulus by n or by n plus some integer multiple of 180 degrees (see Controls section 2.4).

The chamber contained left and right reward pumps mounted on vibration-cancellation pedestals. An AVR32 board (National Instruments) and several Arduino motor shields acquired all sensor signals and controlled the motors, LEDs and the liquid syringe pump (NE-500 programmable OEM; New Era Pump Systems) for reward delivery.

The stimulus stepper-motor was controlled through a feedback system with a digital step counter to maintain the exact desired stimulus orientations and prevent possible changes due to the rat's contact with the stimulus, e.g. the rat could not rotate the stimulus with its paws.

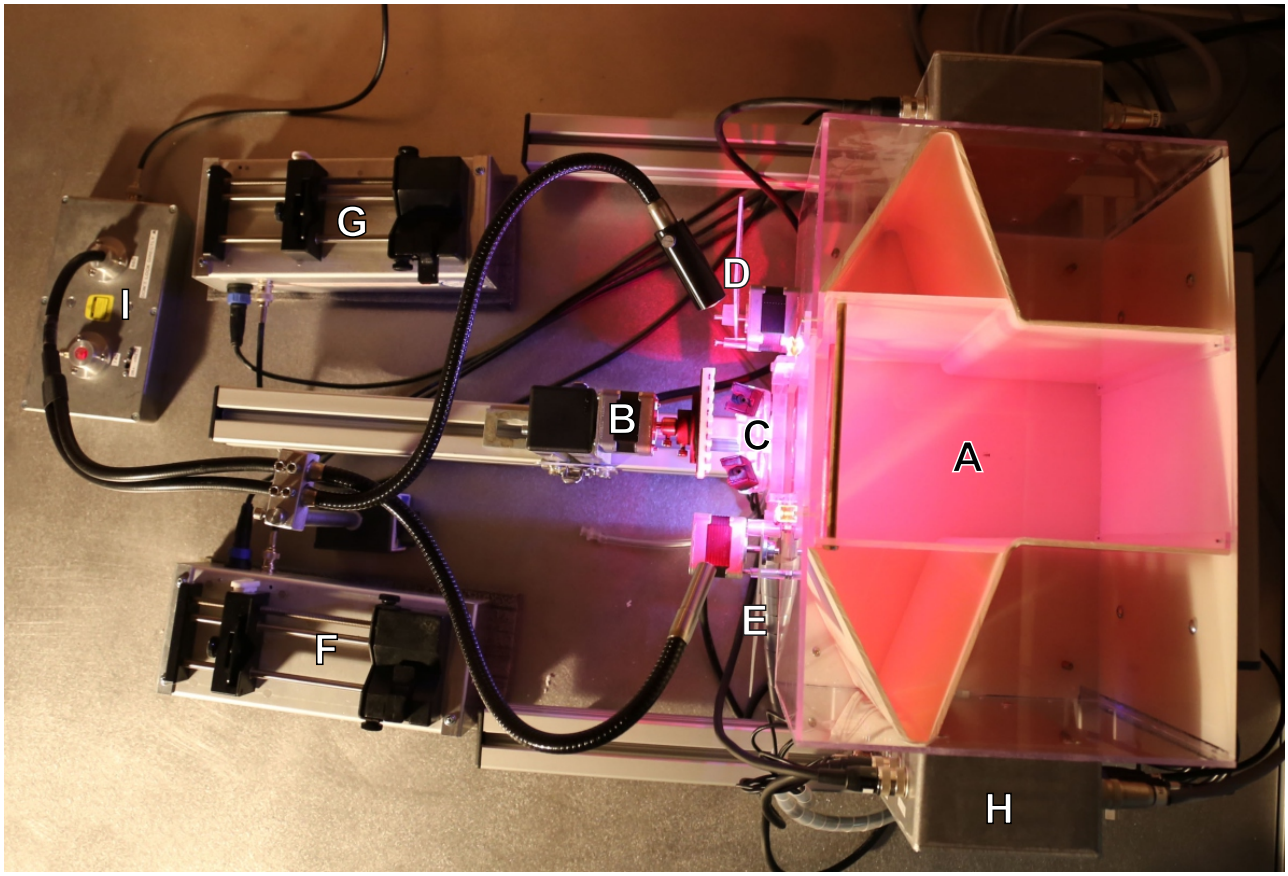

Figure 2.1.3: Behavioral apparatus, view from top. The rat is placed in the main chamber (A). (B) the stimulus and stepper motor controller. (C) the reward delivery area and licking sensors. (D and E) transparent and opaque panels respectively. (F and G) the reward pumps on which syringes will be loaded. (H) the electronic control box, housing the microcontroller-based D/A boards and sensors and lights controllers. (I) the high-power infra-red light source attached to optic fibers.

2.1.3 Software control environment

Custom made software was developed using LabVIEW (National Instruments) to automate all functions of the apparatus. All the sensors, actuators (including motors and pumps) and lights were interfaced with the computer program allowing full control over a wide range of parameters governing the flow of the training and testing. Although fully automatic, the software flexibly allowed the experimenter to modify all the parameters of the task and control the lights, sensors and motors if needed in an on-line fashion.

2.1.4 Stimuli

Main b/w grating object

The main stimuli used in the experiments were black and white square-wave gratings (wave-length, λ=7 mm) built in-house by a 3D printer (3D Touch, BFB Technologies, Fig. 2.1.4). The stimulus was mounted on a stepper-motor that rotated the object in order to generate various orientations that spanned 180 degrees (Fig. 2.1.2). Each stimulus angle was sampled from a uniform distribution and presented in a semi-random fashion (sampling without replacement) with target angles in five degrees steps. The stimulus object was placed at 3 cm distance from the opaque panel (Fig. 2.1.3). Rats easily extended forward across this distance in order to touch the stimulus. This distance would be the optimal compromise for visual and tactile characteristics of the rats (see discussion below).

The depths and widths of the groves were 3.5 mm, designed to be both visually and haptically salient for rats. Visual acuity is measured in *cycles per degree* (cpd), a measurement of the number of lines that can be seen as distinct within a degree of the visual field, which is calculated by the following equation:

$$Acuity = \frac{1}{2 \times tan^{-1}\left(\frac{h}{d}\right)} \quad cpd \tag{2.1}$$

Where, h is the width of each line in the stimulus and d is the dis-

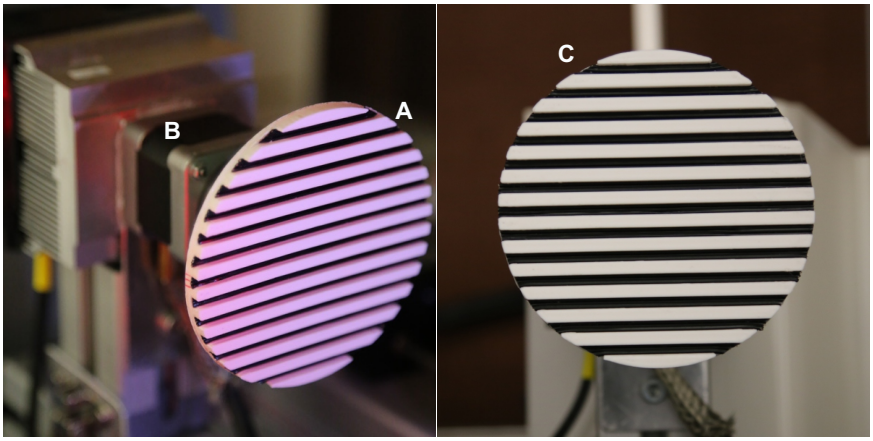

Figure 2.1.4: (A) Main black and white grating object mounted on a micro-stepper motor (B) which presents the orientations in each trial. The stimulus feels and looks like a grating. The stepper-motor was controlled with a feedback system with a digital step counter to maintain the exact presentation of desired stimulus orientations. (C) Stimulus from rat's point of view.

tance from the rat's eye. Each cycle of the stimulus would occupy $2 \times tan^{-1}(3.5/30) = 13.31^{\circ}$ of the visual angle. Consequently, the spatial frequency of the gratings at distance 30 mm can be calculated as $\frac{1}{2 \times tan^{-1}(3.5/30)} = 0.075$ cycles per degree of visual angle. The normal visual acuity of Long–Evans rats is estimated to be ~1 cpd (Prusky et al., 2002). Rats also have a very large depth of focus which is from 7 centimeters to infinity (Powers and Green, 1978). Further, the width of the binocular field directly in front of the rats' nose, which is generally considered the animal's binocular viewing area (Mei et al., 2012), ranges from approximately 40° to 110° depending on head pitch (Wallace et al., 2013). The stimulus was built in shape of a circular disk with diameter of 98 mm, comprising 14 cycles of the gratings that occupies $2 \times tan^{-1}(\frac{98}{2 \times 30}) = 117^{\circ}$ of the visual angle, completely covering the rats' binocular visual field[3].

[3] Depth of focus is the range of distances at which an object is in equivalent focus for an unaccomodated eye. In optics, it is the tolerance of placement of the image plane (the film plane in a camera) in relation to the lens.

Visuo-tactile disparity

This stimulus object was designed in order to allow introduction of disparity between tactile and visual orientations in future studies (Fig. 2.1.5). The gratings were generated with the same spatial frequency and tactile

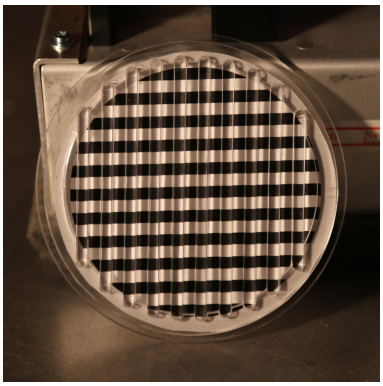

Figure 2.1.5: Visuo-tactile disparity grating object. This stimulus would allow introduction of disparity between tactile and visual orientations. In this picture visual and tactile features are orthogonal to each other.

dimensions as the main b/w stimulus. The stimulus comprised of transparent Plexiglas bars (tactile features) attached to a circular structure that could be rotated with respect to the visual gratings to provide an orientation disparity. The visual gratings were printed on a paper.

Various other types of stimuli

Either for control experiment purposes or further characterization of visual and tactile and bimodal performance we designed different types of gratings.

2.2 Behavioral training protocol

Depending on the question at hand, we developed different training protocols described in the following sections. Typical duration of training to reach stable performance in the complete task was around 4–6 weeks but varied according to the experiment's intended data set and individual differences in rats' rate of learning.

2.2.1 The canonical training scheme

This training protocol was used for the majority of rats (12/15 of subjects) and consisted of 6 stages.

Stage 1: Handling. For half an hour each day, the investigator held and petted the rats and fed them by hand and a dropper pipette. This stage lasted for 5–7 days. From this stage onward, a water restriction schedule was implemented, whereby the rat collected rewards in the apparatus and had free access to water during the week-end.

Stage 2: Training to head-poke and collect the reward. As the first step of this stage, rats learned to perform the head-poke that opened the opaque panel in order to initiate a trial. After that, they were allowed to lick both of the reward spouts, so they could learn the location and the function of the reward spouts. To train them how to use the reward spouts by licking, they were given a drop of juice in the reward spout on the side

contingent to the rule of the task, by the control program. Rats very quickly (<10 trials) learned that reward would be triggered only after licking.

Stage 3: Implementation of the stimulus rule on cardinal angles. In this stage, we trained rats on the bi-modal condition, where they could both touch the object with their whiskers and see it (Fig. 2.1.4). They were rewarded on the spout corresponding to the stimulus orientation and the contingency set for each rat. As described in section 2.1 the orientation/reward side rule was constant for a given rat but varied among rats. This allowed us to control for possible biases in the behavior that might arise as a result of asymmetries in the apparatus (e.g. reward pumps) or left/right biased preference of the rats. Overall, we did not detect any such bias.

Rats in this stage had the chance to explore both spouts. The rats did not receive the reward at the side deemed incorrect on that trial; however, when their first choice was wrong, they were allowed to continue to the opposite (correct) spout, where the reward was dispensed immediately. By this 'error remediation' protocol, rats began to uncover the relationship between stimulus features and reward location. This not only kept them motivated in the task but also gave them further opportunities for stimulus/reward association since they could sample the stimulus during error remediation.

Stage 4: Introducing delay as a graded punishment. In the next step, a short delay (Inter Lick Delay, 0.5–2.5 s) was introduced if rats licked the incorrect spout, after which they had the chance to try again within the same trial. Of course, in each trial the first lick was regarded as the correct/incorrect response for performance measures. When rats showed relatively stable performance, they were rewarded only when they licked the correct spout, and the trial ended with a delay of 1-2 seconds (as punishment) if they licked the incorrect spout. With this gradually-increasing punishment method, the rats were able to learn to distinguish between 0 and 90 degrees as fast as 2 to 7 days (Fig. 2.2.2). Rats completed an average of 200–300 trials in these initial training stages.

Stage 5: Training to discriminate cardinal angles in interleaved

modalities. When rats could perform above 75% correct in the previous stage, they were presented with interleaved trials of vision-only (V), tactile-only (T) and bi-modal (VT) conditions with equal probability in a random format. In vision only trials, a white light illuminated the stimulus and a transparent panel moved in front of the object to prevent the rat from touching the object. The light was turned on immediately after the opaque panel was lifted but the transparent panel was already set tangential to the stimulus before a visual only trial started. In the touch-only trials, all lights were off except an infra-red LED array that was used for monitoring the animal through infra-red sensitive high-speed cameras. Interestingly, in the first session of this stage, rats could recognize with accuracy far above chance the object and apply the rules of the task on first exposure to V (80–90% correct) and T conditions (70–90% correct), suggesting that the multimodal percept corresponds to that of the single modalities. However they improved after further training.

Stage 6: Training to discriminate interleaved modalities with full orientation range. The training so far was limited to the vertical (90°) and horizontal (0°) orientations, which were used as the exemplars of the two categories used (cardinal stimulus angles). In this training stage, all of the orientations were presented within each category (i.e. 0° ± 45° versus 90° ± 45°; Fig. 2.1.2) with minimum of 5° angular distance. At -45, 45 and 135 degrees the reward was given with 50% probability at either spout. Remarkably, rats were able to generalize the categorization rule to the single modality conditions as well as to the the whole range of orientations in the first session of exposure to this stage of their training. Rats received equal number of trials in each orientation and in each modality.

All rats learned the canonical task quite fast (see Fig. 2.2.2) and the performance was consistent between rats and between sessions (Fig. 2.2.1).

2.2.2 Random modality training

This training protocol was similar to the canonical training with the exception that rats were presented with interleaved trials of vision-only (V),

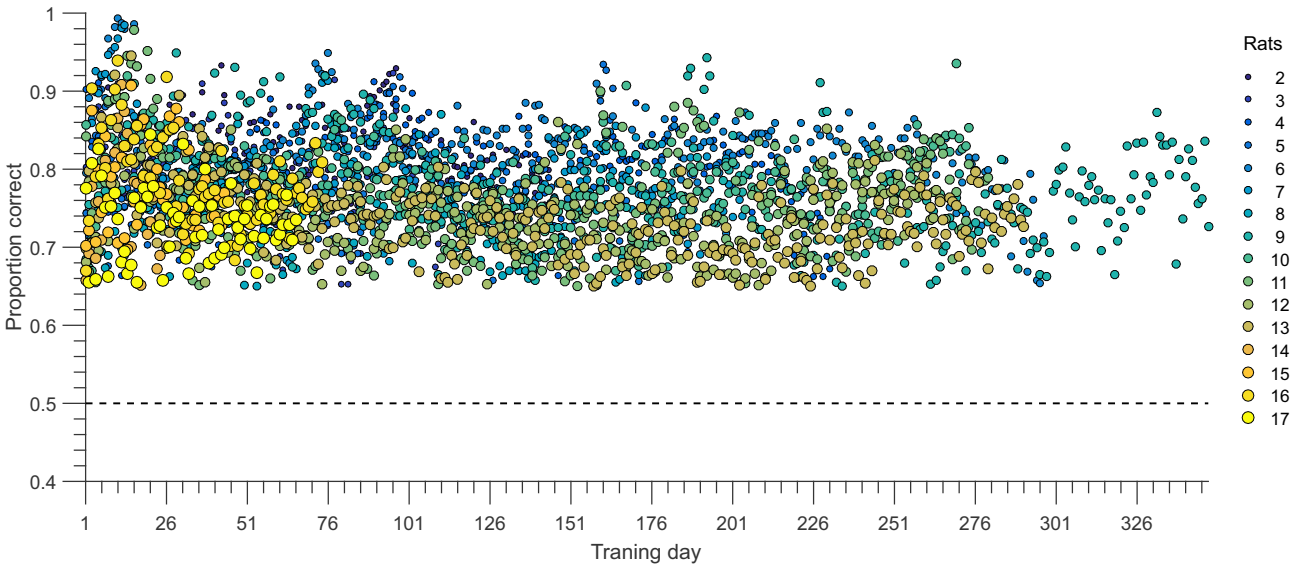

Figure 2.2.1: The performance of all rats in the ask after the completion of training. Each circle shows the average performance of one rat in one session. The performance of the rats was stable between rats and between sessions. Note that not all rats had the same amount of behavioral training days as some arrived earlier or lived longer.

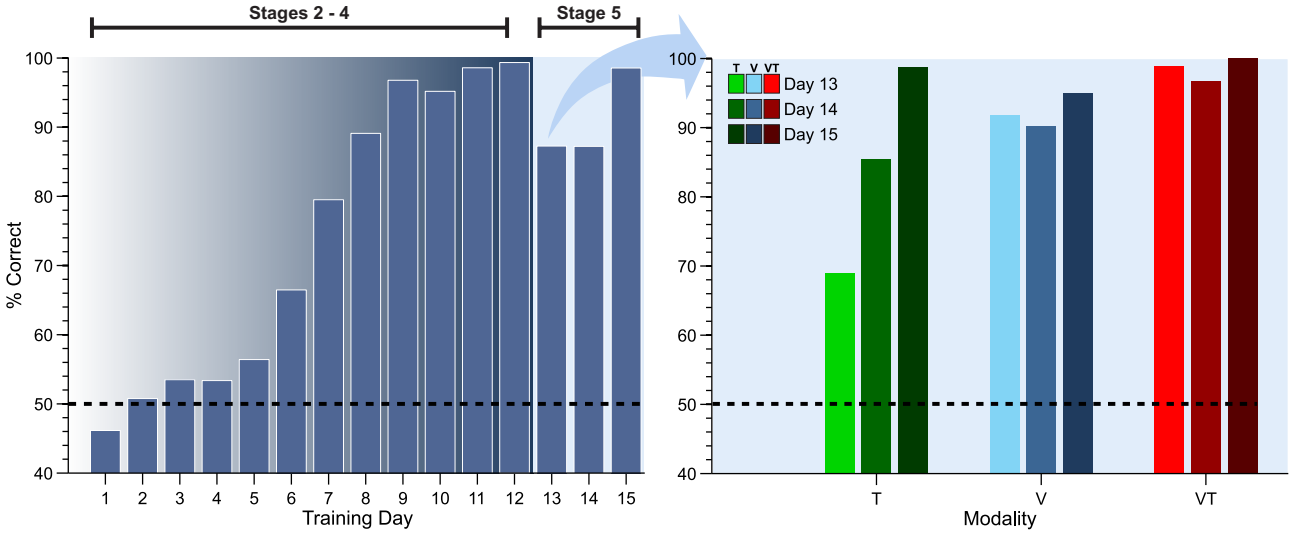

Figure 2.2.2: The progress of a representative rat (no. 6) in the canonical protocol. The figure plots the rat's learning to dissociate 0 and 90 degrees. Stages 2–4 shows the performance of the rat from the first day of training in vision-touch condition (VT) until he could perform the task with about 80% accuracy. The training continued such that the rat had more training in visual-tactile conditions for 5 days until its performance was stable over 95%. In stage 5 we presented the rat with interleaved modalities trials (V,T and VT). They were able to perform the task well in their first session of stage 5 however they improved to over 95% accuracy in 3 days. The plot on the right shows the performance of these 3 days in separate plots for each modality condition.

tactile-only (T) and bi-modal (VT) conditions with equal probability in a random format from the *beginning* of their training—therefore stage 5 of canonical protocol did not constitute a separate stage in this training protocol. We trained rats in this training regime to control the effect of training protocol on multimodal enhancement (discussed in chapter 4).

Four rats were trained using this protocol. Learning stages 2–4 of the task in this protocol was more difficult for rats compared with the canonical protocol and took ~3–5 weeks of training. This probably occurred because discovering the rule of the task and stimulus/reward contingency was more complex. Rats had to learn to exclude stimulus modality (e.g. absence or presence of the light and transparent panel) from the orientation discrimination rule (Fig. 2.2.3).

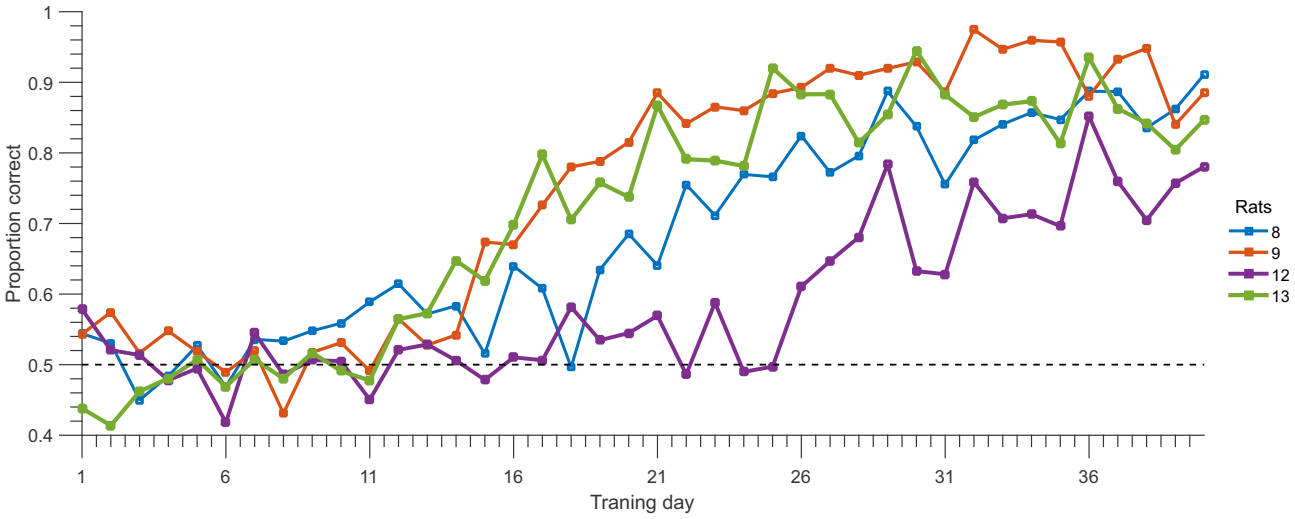

Figure 2.2.3: Learning the task in random modality training was more difficult for the rats compared with the canonical protocol, probably because discovering the rule of the task and stimulus/reward contingency was more complex. Four rats were trained using this protocol. The curve shows the performance in stages 2–4, with the difference that rats were presented with interleaved modalities from the beginning of their training.

2.3 Behavioral protocol for neuronal recordings

In order to collect as much neuronal data per condition as possible, orientation set was reduced to angles between 0 – 90 degrees with minimum of 15° distance between each. Rats usually completed 300–500 trials per

recording session. Similar to the standard task, trials of all modalities were interleaved.

2.4 Control experiments

2.4.1 Catch trials

After initial training, during each session, in 4 percent of trials where rats could not see nor touch the stimulus—the transparent panel was put in front of the stimulus and lights were off. The expected performance on these trials is one that is at chance (50% performance). The main purpose of catch trials was to determine whether rats are using sensory cues irrelevant to the conditions in the task. Most importantly we had to make sure that the tactile-only condition involved complete darkness. These control trials led to the discovery that Long-Evans rats are capable of discriminating a high-contrast black and white visual stimulus under narrow-band (almost monochromatic) red LEDs. This finding, which contradicts to the common belief that laboratory rats cannot see under red light, is discussed later in the appendix (Section 7.3).

In addition rats could perhaps use sensory cues such as possible correlated acoustic and mechanical noise from the stimulus motor, olfactory cues or sequential dependencies of the trials. Catch trials were used to better distinguish between these possibilities.

2.4.2 Exclusion of olfaction

Rats are "experts" of olfaction. They have huge numbers of receptors and correspondingly large olfactory bulbs; they can use their sense of smell to make fine and reliable discriminations(Uchida and Mainen, 2003). Although olfaction has been implicated in experiments involving object recognition (Astur et al., 2002), confounding results originally claimed to be merely based on invariant object recognition (discriminating between *different* objects), it could play an unlikely but possible role in discriminating *object features*, such as grating orientation in the current task. To control

for this possibility five procedures were done.

First, the stimulus object was carefully washed with soap and water before and after each training session. In addition, before each session, stimulus surface and grooves were carefully wiped with a multi-purpose disinfectant solution (Virkon, DuPont). Second, after rats learned the easy conditions (Stage 5 in canonical training protocol), for 3–4 control sessions the experiment was paused every 10 trials, the stimulus was wiped with Virkon solution and put back, letting the rat continue the task. Third, different copies of the stimulus were used in different trials, which would confuse the rat if it were using olfactory cues. Fourth, we made a visual object where tactile features (raised bars) were absent but the stimulus was otherwise exactly similar to the standard stimulus object[4]. With this stimulus, rats could only perform the categorization task above chance level in visual and visuo-tactile trials but not on tactile only condition. Importantly, multisensory enhancement was not observed—the performance in visual trials was similar to that of bimodal, indicating not only a lack of olfactory contribution in this task[5], but also a lack of visual distortion due to the transparent screen put in front of the stimulus for the visual only trials. Finally, on a trial by trial basis, the stimulus was rotated 180° in a random fashion. Doing so would present the same orientation that is intended on each trial but the stimulus and possible olfactory cues on it have been turned on the opposite side.

[4] The visual gratings were 2D printed on the object.

[5] At least as far as odor cues on the surface of the object are concerned.

2.4.3 Exclusion of acoustic and mechanical noise

In order to control for the possible effect of the stimulus motor noise (barely audible to human observer) in solving the task, an algorithm was implemented that generates a series of 2–4 random clock-wise and counter-clock-wise rotations, with variable degrees of rotation and then produces the desired orientation. Only after this step the rats could trigger the opaque panel and sample the stimulus. This way we made sure that rats were not able to perform the orientation discrimination by using the motor noise or mechanical vibration.

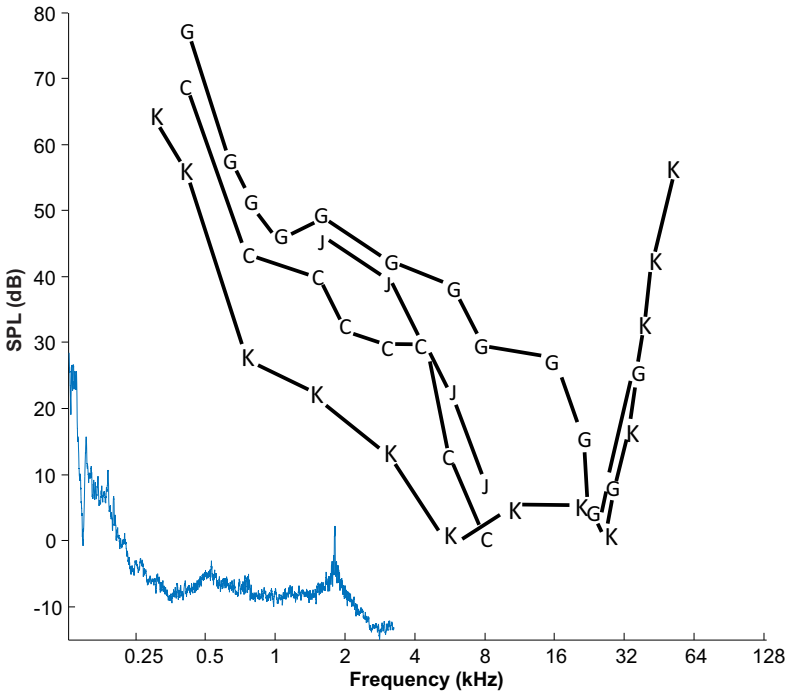

Figure 2.4.1: Comparison of the noise of the stimulus motor with previously reported hearing threshold of rats shows sound cues were below rats' acoustic sensitivity. Black lines, the hearing threshold of rats according to different references. Blue line, frequency content of the stimulus motor noise. K: (Kelly and Masterton, 1977), C: (Cowles and Pennington, 1943), J: (Jamison, 1951), G: Lower frequency range: (Gourevitch, 1965), Higher frequency range: (Gourevitch and Hack, 1966).

In another control experiment we controlled for the noise of motor vibration in solving the task by mounting the stimulus on a similar motor that was powered off while the actual motor worked as usual. The rats only responded to the "dummy" stimulus orientation and not to the motor vibration or noise (Data not shown). Finally, we sought to explore whether rats could hear the sound of the motors at all. We recorded sounds (LAN-XI type 3052; Bruel and Kjaer) during all possible movements of the stimulus motor and examined the frequency spectrum. (Fig. 2.4.1) shows the frequency spectrum of the motor noise we measured in comparison to measured hearing threshold of rats reported previously. The highest acoustic frequencies generated by the motor were below 500 Hz so that rats, which possess the higher-frequency hearing characteristic of mammals (Heffner et al., 1994; Kelly and Masterton, 1977; Masterton and Diamond, 1973; Ölveczky, 2011), would be expected to be insensitive to such sounds.

Figure 2.5.1: Schematic design of the lick sensors shown from different angles. Lick sensor consisted of a fluid delivery cup attached to the reward pumps and an infra-red diode detector pair.

2.5 Recording of Lick Patterns

Using an "optical lickometer" developed in the lab, we sought to monitor the licking behavior of the rats while performing the task (Fig. 2.5.1). The basic idea was to discover meaningful correlations between licking pattern and perceptual decision of rats on each trial. This could be achieved only through a high fidelity licking sensor and licking spout that would not affect the licking pattern of the animal due to the employed drinking configuration (Weijnen, 1998).

The lick sensor consisted of a fluid delivery cup attached to the reward pumps and an infra-red diode detector pair. The placement of the light beam with respect to the fluid cup, and its optical characteristics were adjusted such that it could detect the entire cycle of tongue-protrusion/retraction. Then the analog signals from right and left lick sensors were sent to a digital signal processor unit (RZ2 BioAmp processor, Tucker-Davis Technologies, Alachua, FL), sampled at 20 kHz and then digitized and stored on computer hard disk for offline analysis.

The licking was recorded from 4 well-trained rats. The behavioral paradigm differed with the standard task. After the first lick (response lick) on a given reward spout, a random delay was introduced *before* the reward was extruded by the pump (pre-reward delay). This delay was sampled from a uniform distribution whose min and max were 0 and 3.5 seconds respectively. The probabilistic aspect of the delay is very crucial in preventing rats from forming a predictable, stereotyped behavior. Rodents are known to have a tendency to form stereotyped, inflexible behavioral patterns (Ölveczky, 2011). Further, rats had the possibility of switching to the alternative reward spout in case they had chosen an incorrect side. Therefore all trials were rewarded unless a time-out of 6 seconds passed after which trial was re-started.

The intuition behind the delay and correction possibility was that it would cause the rat to wager during the delay period whether it had made a correct choice–hence he should keep licking on the spout–or the opposite spout might be the correct one. Intuitively, the cost of the pre-reward delay

would cause the rat to continue licking the first spout only if it is confident. A change in the licking pattern *during* the delay period could be correlated with the decision confidence of the animal on that trial.

The results of this study and further analyses are presented and discussed in section 4.4.

2.6 Monitoring of head, snout and whiskers movements

Trial-triggered high speed video recordings (Point Grey Flea, Edmund optics) were analyzed to monitor the movements of the head, snout and whiskers of the rats during behavior. Video recording started with the trial start signal, triggered by the head-poke and stopped by the response lick signal.

2.6.1 Three dimensional tracking of head movements

A three-dimensional tracking pattern was designed and mounted on the head of some implanted rats (Fig. 2.6.1). The pattern consisted of 6 dots using which an image processing algorithm could perform online/offline tracking of the highspeed video recordings. The tracking algorithm allowed precise quantification of the 3D trajectory of the head-movement during a trial.

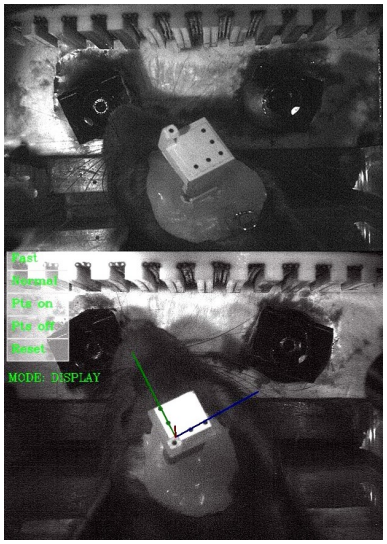

Figure 2.6.1: Two example frames from high-speed video recordings from rats with tracking pattern mounted on the head. The three colored axes (bellow) are computed by the tracking algorithm.

Briefly, the tracking software accomplished the following steps:

1. Perform Difference of Gaussian (DoG) spot detection.
2. Thresholding of the DoG image and Non-Max-Suppression (a simple suppression of the neighbors above the threshold but not representing the local maximum).
3. From the cloud of single points obtained in the previous step the pattern is searched through:

    (a) Detection of all equidistant triples. The distance between the first and last point must be inside a range admitted and precalculated.

(b) Composition of all possible couples of triples that represent the 5-points pattern plane. The common point is the reference point.
(c) After each composition the 6^{th} point is searched over an area around the reference point, and the re-projection error is calculated (every center spot position is calculate with sub-pixel precision). The re-projection error is the distance between the ideal pattern as seen by the camera and the actual one (sum of point to point pixel distance). Of course this means that the internal parameter of the camera are known (in fact the camera must be calibrated before using).
(d) The best composition with the lowest re-projection error is taken.

Then the translation and position values were computed and analysed further in Matlab.

2.7 Behavioral Data Analysis

To quantify behavioral performance we analyzed the behavioral data after rats learned the complete version of the task (after stage 6 training, see section 2.2) and their performance was stable. All of the measured variables in the behavioral task were stored in a data structure that would allow daily analysis of behavioral measures using custom-made algorithms written in Matlab (Mathworks) and LabView (National Instruments).

2.7.1 Psychometric curves

To quantify performance, we fit psychometric curves to the choice data of each rat in each modality. We analyzed the behavioral data from rats that learned the complete version of the task and their performance was stable. Three rats (numbers 8, 14 and 15), were excluded based on this criterion. For each orientation, we calculated the proportion of trials where each rat categorized the stimulus as vertical.

Ideally rats would categorize all the orientations pertaining to angles larger than 45 degree as vertical and all the angles smaller than 45 as horizontal. This ideal performance would resemble a step function which is at 0% from 0 degrees to 45 degrees and steps to 100% from 45 degrees to 90 degrees. However, the task difficulty increases the closer the stimulus gets to 45 degrees, so the performance of the rats (like any tested biological organism) is not perfect. Their real performance is better described by a sigmoid function with an inflection point at the point of subjective equality (PSE), the orientation at which subjects report the stimulus equally horizontal and/or vertical (45°).

For a quantitative modeling of the performance, we fit psychometric functions to the choice data of each rat with a cumulative Gaussian function or a four-parameter logistic function with the general form given in equation 2.2 based on Wichmann and Hill (2001). The parameter estimation was then performed in Matlab using maximum-likelihood estimation.

$$\psi(x; \mu, \sigma, \gamma, \lambda) = \gamma + (1 - \gamma - \lambda)F(x; \mu, \sigma). \tag{2.2}$$

The two-parameter function $F(x; \mu, \sigma)$, will be defined by a logistic:

$$F(x; \mu, \sigma) = \frac{1}{1 + \exp -\frac{x-\mu}{\sigma}} \tag{2.3}$$

or cumulative Gaussian distribution.

$$F(x; \mu, \sigma) = \frac{1}{2}[1 + erf(\frac{x - \mu}{\sigma\sqrt{2}})] \tag{2.4}$$

In these equations, x, is the stimulus angle, γ is the lower-bound of the function ψ, λ is the lapse rate (a reflection of the rate at which observers lapse, responding incorrectly regardless of stimulus value). Often, γ and λ are considered to arise from stimulus-independent mechanisms of guessing and lapsing. μ, is the mean of the probability distribution which determines the displacement along the abscissa of the psychometric function which is a reflection of subject's bias and σ, is the standard deviation of the cumulative Gaussian distribution or the scale parameter proportional

to the standard deviation of the logistic distribution. Therefore, σ, reflects the slope of the psychometric function, a measure of acuity.

To generate the psychometric curves, we utilized the data corresponding to the range of orientations from 0 to 90 degrees and collapsed the data of orientations -45–0 and 90–135 on this range.

2.7.2 Statistical test of significance for the fitted psychometric curves

For performance values in stimulus condition (angle–modality), errors were expressed as 95% binomial proportion confidence interval computed via approximating the distribution of errors about a binomially-distributed observation, $\hat{p}$, with a normal distribution:

$$\hat{p} \pm 1.96\sqrt{\frac{1}{n}\hat{p}(1-\hat{p})} \tag{2.5}$$

where, $\hat{p}$ is the proportion of correct trials (Bernoulli) and n is the number of trials.

For statistical tests of significance, we performed a non-parametric test based on bootstrapping method, as follows. We computed a distribution of the peak slope values from the first derivatives of the fitted functions based on 1,000 resamples of the performance data. We then performed pairwise comparisons between all the slope values generated via bootstrapping from fitted psychometric function of each sensory condition, calculated the overlap between the distributions and computed the p-values.

2.7.3 Modelling data with Bayesian cue combination

As discussed in chapter 1, according to the linear ideal–observer model of cue integration, we can write equation 1.1 as:

$$S_{vt} = w_v S_v + w_t S_t \tag{2.6}$$

where S_{vt} is the combined internal orientation signal, S_v is visual orientation signal and S_t is tactile orientation signal. If each S is considered to

be a Gaussian random variable with mean, μ, and variance, σ^2, then the optimal estimate of $S_v t$, can be computed by setting the weights (w_v, w_t) proportional to the reliability (i.e., inverse variance) of S_v and S_t. The multisensory reliability will then be equal to the sum of the individual cue reliabilities:

$$\frac{1}{\sigma_{vt}^2} = \frac{1}{\sigma_v^2} + \frac{1}{\sigma_t^2}. \tag{2.7}$$

We fitted the psychometric data with a cumulative Gaussian function yielding two parameters: the point of subjective equality (mean of the best fitting cumulative Gaussian function) and the threshold (as its s.d., σ).[6] Solving equation 2.7 for σ_{vt} gives the optimal combined threshold from single sensory estimates.

[6] The equality of psychometric threshold and σ value of the fitted cumulative Gaussian curve is discussed in appendix 7.1.

2.7.4 Information theoretic analysis

To quantify the information extracted by the rat in each sensory modality we performed a mutual information analysis. This analysis allowed us to quantify how informative the rats' behavior was about a particular stimulus orientation in a modality. We assumed that the information extracted by the rat about the stimulus orientation is converted directly into a choice. This allowed us to estimate the signal extracted by the rat according to its behavioral accuracy. The quantity of information that the behavioral response (left or right) conveys about the stimulus category (horizontal or vertical) can be quantified by Shannon's mutual information formula (Cover and Thomas, 2012; Shannon, 1948):

$$I(R;S) = \sum_{r,s} P(s)P(r|s)\log_2 \frac{P(r|s)}{P(r)}. \tag{2.8}$$

where $P(s)$ is the probability of presentation of a given stimulus category (horizontal or vertical), $P(r|s)$ is the conditional probability of the rat's response (right or left choice) given the category of stimulus, and $P(r)$ is the marginal probability of response r (rat's choice to left or right) unconditional on the stimulus category. All of the information values in

equation 2.8 were computed using Information Breakdown Toolbox (Magri et al., 2009).

What I cannot create, I do not understand.

Richard Feynman

3

Neuronal Analysis Methods

After rats reached a stable level of performance in the behavioral task (i.e. >75% correct trials and consistent overall psychophysical performance judged by the slope of psychometric curves, constructed by averaging the trials of the most recent 15 sessions), they underwent a surgical operation for electrode implantation.

3.1 Electrophysiological recordings

3.1.1 Subjects

Seven of the Long-Evans rats trained in the behavioral task were used for neuronal recordings (see chapter 2 for further details). Only rats younger than 1 year-old were selected for surgery due to an increased rate of mortality and anesthesia-related complications in older rats. Two days prior to surgery rats were housed individually to habituate them to the cage condi-

tions and had access to food and water *ad libitum*.

3.2 Chronic Surgical electrode implantation

Animals were anesthetized with Isoflurane (2.5% for induction and craniotomy, 1.5% for maintenance) delivered through a snout mask. Anesthesia was maintained by monitoring respiration as well as foot pinch responses throughout the surgical procedure. The animals were placed in a stereotaxic apparatus (Harvard Apparatus, MA). Ophthalmic ointment (Epigel, Ceva) was applied to keep the eyes moistened throughout surgery. After shaving and sterilizing the scalp with iodine solution, lidocaine topical gel was applied on the scalp to provide local analgesia before performing scalp incisions. Then the skull was cleaned and three to four anchoring screws were fixed in the skull to support the dental cement and the microdrive. One of the screws was advanced deep enough to touch the dura and served as the reference and another one served as the ground (some times reference and ground wires were shorted).

The craniotomy was made above the left PPC (3.8 mm posterior to bregma, 2.5 mm left of midline, ~2 mm anteroposterior; ~3.5 mm mediolateral in size). Although the craniotomy was made as small as possible, in the case of larger craniotomies we performed additional steps to minimize brain dimpling during electrode insertion. First, dura mater was removed using a small hypodermic needle (guage-25) whose tip was bent to form a small hook. Then a drop of sterile Vaseline ointment was put in the middle of the craniotomy and the surgical cyanoacrylate adhesive (Histoacryl, B.Braun) was applied directly to the pial surface bordering the edge of the cranial opening. This procedure fastens the pia mater to the overlying bone edge and the resulting surface tension prevents the brain from depressing under the advancing electrodes. The hydrophobic ointment in the middle of craniotomy prevents the spread of tissue adhesive on the brain.

With the brain anchored to bone, the 16 or 32 channel microwire arrays (Tucker-Davis Technologies) were inserted by slowly advancing a stereotaxic micromanipulator (SM-25C, Narashige). While lowering the arrays

Drug	Dose	Delivery	Usage
Isoflurane	2.5-1.5%	Gas Mask	Anesthesia induction and maintenance
Atropine	1.5 mg/kg	Subcutaneous	Control heartbeat and mucus secretion
Rymadil	5 mg/kg	Intramuscular	Analgesic
Baytril	5 mg/kg	Subcutaneous	Antibiotic after surgery
Baytril	5 mg/kg	Soluble in water	Antibiotic post surgery
Urethane	1.5 mg/kg	Intraperitoneal	Acute anesthetic

Table 3.2.1: Drug concentrations, methods of delivery and use in surgical procedures.

during implantation, the quality of raw signals was monitored and the detected spikes were clustered and sorted online using the OpenEx toolbox (Tucker-Davis Technologies). The array was fixed at a depth of ~1100 μm, where it became possible to distinguish spontaneous firing of action potentials. The depth of the recording site is consistent with an electrode tip position in cortical layer 4. However our analyses and conclusions do not depend on the precise laminar localization of the neurons.

Once at the desired depth, the remaining exposed brain surface was either covered with bio-compatible silicon (KwikSil, World Precision Instruments) or a custom-made antibiotic containing Vaseline based ointment depending on the type of electrode array implanted—fixed or movable microdrive respectively. The fixed array or the body of microdrive was then attached to the skull by dental cement (SEcure Starter Kit, Sun Medical).

In order to keep the heart rate constant and prevent mucus secretion in the airways, animals were injected with atropine (1.5 mg/kg) one hour after the onset of anesthesia. Half of the dose of analgesic (Rymadil, 5 mg/kg) was injected one hour after the onset of anesthesia and the rest of the dose was injected at the end of the surgery before waking the animal. Antibiotic (Baytril, 5 mg/kg) was also injected before waking the rat.

Rats were then given antibiotic enrofloxacin (Baytril; 5 mg/kg delivered through the water bottle) for up to 48 hours after surgery. During the one-week recovery time, rats had unlimited access to water and food. Recording sessions in the behavioral apparatus began thereafter (see table 3.2.1).

3.2.1 Implants for electrophysiology

Depending on the desired duration of the neuronal recordings and intended neuronal data-set rats were implanted either with fixed microwire array electrodes or custom-made movable arrays.

Fixed Microwire arrays

The microwire arrays (ZIF-Clip, Tucker-Davis Technologies) were comprised of 16 or 32 polyimide-insulated tungsten wires of 33μm diameter, 250 μm electrode spacing and 375 μm row spacing (Fig. 3.2.1-B). Each wire was individually laser-cut to the desired length and configuration with a 45 degrees angle of cut at the electrode tip. The impedance of the each wire was 100-300 $k\Omega$, at 1 kHz, measured in saline, and around 150-400 $k\Omega$ when measured in-vivo. Reference and ground wires were connected to the arrays with impedance 20 $k\Omega$. The arrays were designed in a way that wires with two different lengths were interleaved. This resulted in half of the electrodes having 400 μm tip-length difference with the others. Through this configuration we could record simultaneously from two different depths with a single array.

Movable Micro-drives

The students and postdocs of the lab worked with the technical team to develop a custom-made miniaturized movable micro-drive for microwire arrays (Fig. 3.2.1-A), used in the present experiments and in other projects of the laboratory. The 16 or 32 channel microwire array used in these drives had similar build specification and electrical properties as the fixed arrays. However, the electrodes were connected to the implant connector via a flexible printed circuit board (PCB) that allowed the array end to be moved. The arrays were advanced 50-100 μm after each recording session.

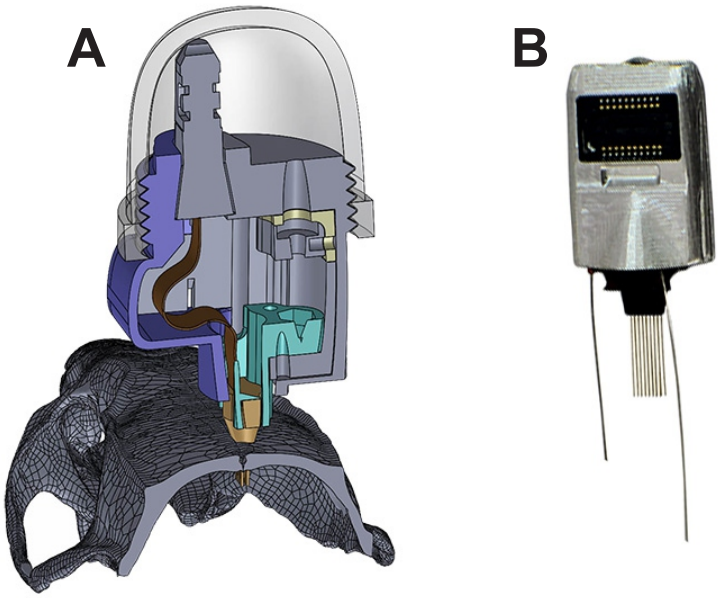

Figure 3.2.1: Two different kind of microwire array configurations used in the electrophysiological investigations. (A) CAD rendering of cross-section of a custom made 3D-printed microdrive for movable microwires. (B) TDT Fixed Microwire arrays (A, courtesy of Marco Gigante, SISSA, B adopted from TDT).

3.2.2 Electrophysiological recordings

After passing through a unity-gain digital headstage using an Intan amplifier chip physiological recordings were digitized at sampling rates up to ~25 kHz directly inside the headstage clip (ZCD-32, Tucker-Davis Technologies). Digitized signals were then routed to a digital commutator (ACO-32, Tucker-Davis Technologies). This active commutator prevented twisting or binding of the headstage cable while reliably tracking rotation on the headstage cable. The signals were passed to a digital headstage manifold (PZ-4, Tucker-Davis Technologies) through a single cable for transfer to a digital signal processor (DSP) base station (RZ-2, Tucker-Davis Technologies) via optical fibers, where they were amplified and stored on a computer.

Together with the neuronal data, all of the event related signals from the sensors, lights and motors in the behavioral apparatus were sent synchronously to the RZ-2 DSP, digitized and stored.

3.3 Histology

At the conclusion of physiological recordings, rats were deeply anesthetized with Urethane (1.5 mg/kg). To mark the final positions of electrode tips, electrolytic microlesions were made by passing ~10 μA current for a through each electrode for ~10 s to achieve optimal charge density necessary for lesioning. The calculation of charge density varied according to the exact geometry of the electrode tip as described in appendix 7.2.

After lesioning, animals were perfused transcardially with 4% paraformaldehyde. Brains were extracted and postfixed in 4% paraformaldehyde for 24–48 hours and then in sucrose solution (15% solution then 30% solution). After postfixing, 30 μm coronal sections of the brains were cut on a microtome (SM2010-R Sliding microtome, Leica). Finally slides were Nissl-stained and analysed under a microscope.

3.4 Neuronal Data Analysis

3.4.1 Signal pre-processing, Spike detection, sorting and clustering

Raw waveforms were analyzed offline using custom written Matlab codes (MathWorks). Rarely there were common artifacts (among different channels) on the multi-channel recordings. To remove these artifacts and improve signal to noise ratio, we performed local referencing on each array. This was achieved by visualizing bandpass filtered (300 Hz–3 kHz) signals of multiple channels and selecting the most "silent" one, which then served as the reference for the other channels on the same array.

For the analysis of neuronal data, spike detection and sorting were performed using automatic clustering algorithms (Wave-Clus, Quiroga et al. (2004)) for Matlab. Spikes were categorized to well separated single units and multiunits with stable waveform and firing rates over the course of a recording session.

In each session, neuronal recordings of a channel were excluded if a por-

tion of the recording had a nonstationary average firing rate over time.

3.4.2 Generation of Spike density functions

Only well separated single units with stable waveform and firing rates were included in the analysis. An initial analysis of neuronal responses included a continuous-time data analysis approach. We first convolved the spike train of each neuron (with 1 ms resolution) with Gaussian kernels ($\sigma = 50ms$) to obtain spike density functions. Kernels were corrected for the edge effect.

The time-dependent spike density functions, which give an estimate of the instantaneous firing rate, were used for the rest of the analysis explained below.

3.4.3 Generation of Peri-event time histograms

Peri-event time histograms (PETHs) were computed for two reference epochs in the trial: stimulus presentation and pre-decision epoch. The spike trains for these epochs were aligned to the stimulus onset (as defined by the opening onset of the opaque panel) or to the first response lick, respectively. The average firing rate was then computed from spike density functions for trials that were grouped together based on the intended analysis.

3.4.4 Information theoretic analysis

In order to evaluate the role of PPC in the multisensory task we sought to characterize the magnitude and statistical significance of the task-related firing rate modulations of neurons at single cell and population level. We hypothesized that PPC neurons carry information about the stimulus orientation, sensory modality, and the decision of the rat, or a combination of these parameters. We computed Shannon's Mutual Information (Shannon, 1948), hereafter referred to simply as information, for this purpose. In this formulation, the amount of information which can be extracted from

the firing rate of a neuron R, about the task-related parameter, S, can be computed as:

$$I(R;S) = \sum_{r,s} P(s)P(r|s)\log_2 \frac{P(r|s)}{P(r)}. \tag{3.1}$$

where $P(s)$ is the probability of presentation of a given task parameter, s, $P(r|s)$ is the conditional probability of observing a neuronal response, r, given the presentation of the task parameter, s, and $P(r)$ is the marginal probability occurrence of neuronal response, r, among all possible responses unconditional on the task parameter. For example when measuring information about stimulus angle, $P(s)$ is the probability of trials where a stimulus with a given angle.

Intuitively, mutual information measures how much knowing the neuronal response reduces an observer's uncertainty (or entropy) about the parameter of interest.

When estimating the information in the neuronal response, we were concerned about spurious information values caused by the inherent correlations between task parameters. This correlation comes from angle values close to cardinal orientations (0 and 90), where a unique stimulus angle will be almost always followed only by one possible decision. So that a neuron encoding (and so having only information about) stimulus angle will necessarily have information about the decision, and vice versa. For instance, a "sensory" neuron that fires at highest rate (and with little cross-trial variability) for the 90-degree orientation and at lowest rate (and with little cross-trial variability) for the 0-degree orientation, would also appear to carry "decision" information because a high firing-rate would well correlate with the rat making the "vertical" choice.

Thus, to determine whether neurons encode the stimulus angle in a graded manner, we computed the stimulus information that could not be explained by other possible parameters (like future action of the animal) and vice versa. For this purpose we computed *conditional* mutual information to disentangle the information about stimulus from the information

about animal's action:

$$I(R; C|\theta) = I(R; C, \theta) - I(R; \theta) \tag{3.2}$$

likewise,

$$I(R; \theta|C) = I(R; C, \theta) - I(R; C) \tag{3.3}$$

Where, θ is the grating orientation, C is the binary action of the animal (left or right), R, is the neuron's firing rate, $I(R; C, \theta)$, is the joint mutual information between firing rate and stimulus angle and rat's choice, $I(R; \theta|C)$ is the information between firing rate of the neuron and stimulus angle, conditioned on animal's decision and $I(R; C|\theta)$ is the information between firing rate and rat's choice, conditioned on stimulus angle. In simple words, we measured information in the response of a neuron about stimulus angle that exceeded the information that could be extracted merely by knowing rat's decision and vice versa. Simply put, for a given value of C, we measured whether there was still statistical dependence between R and θ.

3.4.5 ROC Selectivity Analysis for choice and modality

To quantify selectivity for choice and modality, we used an ideal observer decoding based on ROC analysis (Green and Swets, 1966).

PETHs from the pre-decision epoch were constructed from spike trains by averaging firing rates in 1 ms bins and smoothing with a Gaussian kernel (see section 3.4.3). Trials were grouped according to two different aspects of the trials: animal's response (left or right) and based on the stimulus modality (visual trials versus tactile trials).

The ROC analysis was done on the distribution of the group of trials from the smoothed spike trains (Feierstein et al., 2006; Raposo et al., 2014). Choice and modality preference were calculated from the area under the ROC curve (AUC) and defined for $2 \times (AUC - 0.5)$. This value ranged from -1 to 1 where -1 indicates that the neuron always fired more during trials with leftward choice and 1 means that the neuron always fired more during trials with rightward choice. Similarly a modality preference of -1 indicates that neuron always fired more during tactile trials and a

modality preference of 1 means that the neuron always fired more during visual trials. The modality preference was calculated for leftward and rightward choices separately and was then averaged.

3.4.6 Construction of neurometric functions

The relationship between neuronal coding of the stimulus and the animal's behavior can be described by neurometric functions. To compute the neurometric functions we made a simplifying assumption that the neuronal thresholds could be calculated by comparing two signals: the the preferred grating orientation and the non-preferred one, the null orientation: 45 degrees. Then the ROC curves were computed for the response of neurons to each stimulus angle against the "null" angle of 45. The performance of the ideal observer model is simply the normalized area under the ROC curve (AUC). The neuronal performance scores were then fitted with the same cumulative Gaussian curves used to compute the psychometric curves (see section 2.7.1).

I know that I know nothing.

Socrates

4

Results of the Behavioral Investigation

This chapter presents the main findings in the behavioral investigation of the visual–tactile orientation discrimination task. In this experiment we sought to determine, first of all, whether rats could achieve discrimination and classification of object orientation in the two modalities of interest, touch and vision. Next we sought to explore whether rats are able to combine visual and tactile sensory information about the orientation of gratings. Further, if they do combine these signals, does the combination bring about an enhancement in their perceptual decision making? We expected the integration of sensory evidence to result in better (more precise and more accurate) categorization of orientations compared to categorization in unisensory conditions.

4.1 Training and overall performance

Each rat was first trained until performance surpassed 70% correct for the cardinal orientations (0 and 90 degrees). As detailed in section 2.2, under the canonical training condition rats learned to perform the task in approximately seven successive training sessions (Fig. 2.2.2). They completed 200–350 trials each day in a ~45-minute long session until they were satiated. In the canonical training, termed bimodal training, after ~5–7 additional sessions of stable performance (Fig. 2.2.2) in the bimodal condition, the same 0 and 90 degree orientations were presented to them in the unisensory and multisensory conditions (visual only, tactile only, visual-tactile) in an interleaved manner with equal probability in each trial, in addition to 4% probability of control trials where rats could not see nor touch the stimulus. These trials provided the opportunity to check the performance of the rats when deprived of touch and vision altogether in order to establish that they received no sensory information about the orientation except from touch and/or vision. Using a low probability made it possible to probe rats' strategy without interfering with the normal task strategy or discouraging and confusing the animals.

In random-modality training (section 2.2.2), the rats were presented with interleaved trials of vision-only, tactile-only and bi-modal conditions with equal probability in a random format from the *beginning* of their training. Learning in this protocol was more difficult for rats compared with the bimodal training protocol and required ~3–5 weeks of training (Fig. 2.2.3).

Interleaved presentation of stimuli in unisensory and multisensory conditions in a session prevented subjects from adjusting their strategy to optimize only one stimulus condition. It is noteworthy that after the fully intermixed (bimodal) training period, rats performed the categorization with greater than 70% accuracy even though it was their first unisensory stimulus exposure (Fig. 4.1.1).

Finally, after both bimodal and unimodal training protocols, we introduced intermediate orientations with 5 degrees sampling resolution. Such trials were distributed semi-randomly (sampled without replacement). As

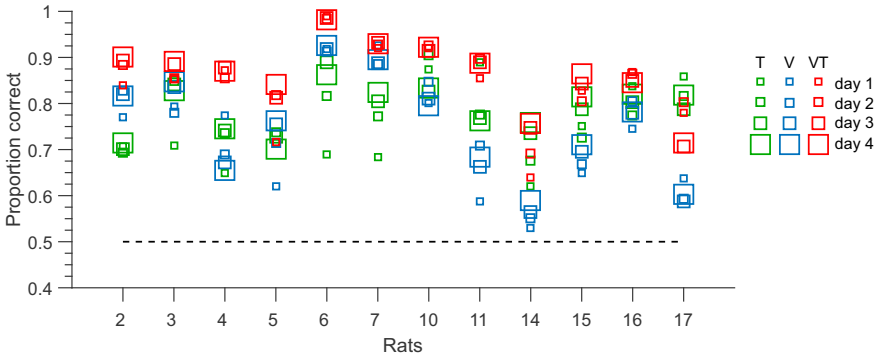

Figure 4.1.1: Cumulative performance of all rats trained with the bimodal training protocol in the first four sessions of presenting single sensory trials. Most rats were able to perform the task on touch-only (T, green) and vision-only (V, blue) trials over 60% in the first session although their performance was best in the bimodal condition (VT, red). Their performance improved with further training. Bigger squares represent training days further into training.

early as the first session containing these intermediate angles, rats performed well with not-yet-encountered angles, and gradually became better at the categorization. This is reflected by the increasing steepness as well as adjustment of the mean (PSE) of the psychometric fits (Fig. 4.1.2).

4.2 Quantitative characterization of performance

To quantify rats' performance in the orientation discrimination task, we fit psychometric curves to the choice data of each rat in each modality as described in section 2.7.1. The psychometric curve is a systematic way to assess performance, since it considers discrimination accuracy and precision in relation to the stimulus.

The steepness of the psychometric curves can be used as a measure of sensory acuity simply by quantifying the slope value of the curve at each point. If the plot represents "percent of trials judged as vertical" perfect performance would yield a step function from 0 to 1 as the stimulus values cross the 45 degree category boundary. Since performance is never perfect, real psychometric functions are not step functions but are rather sloped curves known as sigmoid functions. We fit the psychometric curves with

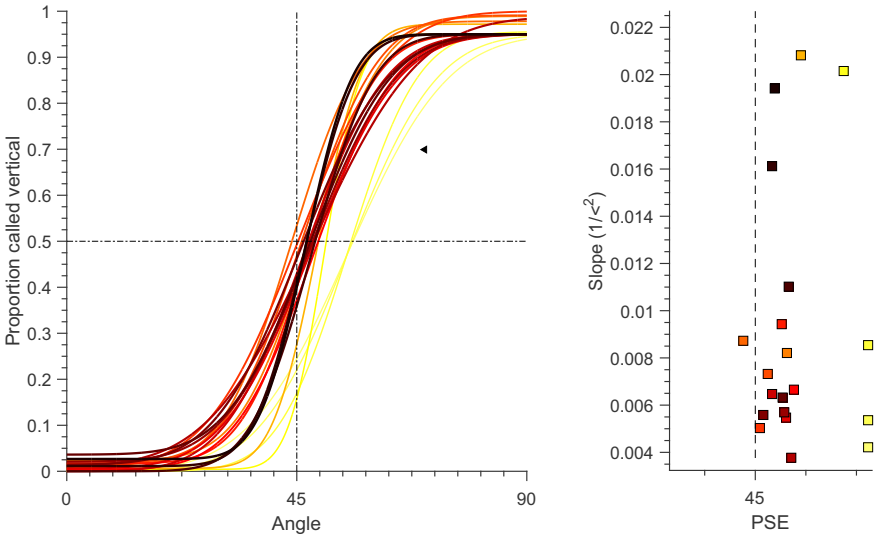

Figure 4.1.2: Left, improvement in a representative rat's performance (rat 7), is evident from a gradual increase in the slope of the psychometric curve (arrow mark) from first sessions (light colored) to later sessions (dark colored) as well as change in the PSE. Each curve is fitted on the data of 3 consecutive days with 1 overlapping day. **Right**, with the progression of training, rats learn to discriminate orientations more precisely (less biased, PSE closer to the category boundary of 45) and more accurately (higher slope of the curves).

cumulative Gaussian functions.

The slope of the psychometric function, a key measure of sensory acuity, is rendered by the first derivative of the sigmoid function and is maximal (by definition) at the inflection point where the second derivative is zero. Slope can be formulated as:

$$Slope = \frac{\partial P(x > 45)}{\partial x} \tag{4.1}$$

Where θ, represents stimulus orientation. For the cumulative Gaussian function we fit the data, the derivative is given by:

$$\frac{\partial}{\partial x}(\gamma + \frac{1}{2}(1 - \gamma - \lambda)(1 + erf(\frac{x - \mu}{\sigma\sqrt{2}}))) = \frac{(-\gamma - \lambda + 1)e^{\frac{-(x-\mu)^2}{2\sigma^2}}}{\sigma\sqrt{2\pi}} \tag{4.2}$$

4.2.1 Rats combine touch and vision and show multisensory enhancement

Figure 4.2.1, shows the psychometric fits for each rat (pale-colored curves) as well as the average performance of all rats (dark-colored curves). Taking the slopes of the curves at their inflection point as a proxy for sensory acuity, we found that rats have good orientation acuity using their whiskers and snout (T condition); however typically their performance is superior by vision (V condition). Regardless of individual differences among rats, performance is always highest in the VT condition, indicating multisensory enhancement.

The enhancement is demonstrated by the red curves in figure 4.2.1 (VT condition) which are steeper than the blue (V-only condition) and the green (T-only condition). In other words, rats made more accurate decisions in multisensory trials. In all rats the VT curves show improvement in terms of slope, lapse rates (lower and upper asymptotes, which are closer to 0 and 1), and the point of subjective equality (PSE), which is closer to the category boundary of 45 degrees—indicating an unbiased application of the decision rule.

Figure 4.2.2 shows the derivatives of the curves shown in figure 4.2.1. The shape of the derivatives of the average psychometric functions depicts the underlying Gaussian distribution of the fits in figure 4.2.1. The small triangles indicate the peak slope which is the inflection point on the psychometric curve and describes the point along the curve that a change in the stimulus value is followed by maximum change in the behavioral performance. Note that the bell–shaped curves in bimodal condition are generally narrower (smaller standard deviation value), symmetrical and centered around the expected value of the mean (45 degrees).

Further characterization of the psychometric curves reveals the linear relationship between the peak slope of the psychometric curve and the cumulative performance of rats (Fig. 4.2.3-a). The two performance measures are correlated, as expected. As a consequence of multisensory enhancement, the point of subjective equality is closer to 45 degrees,

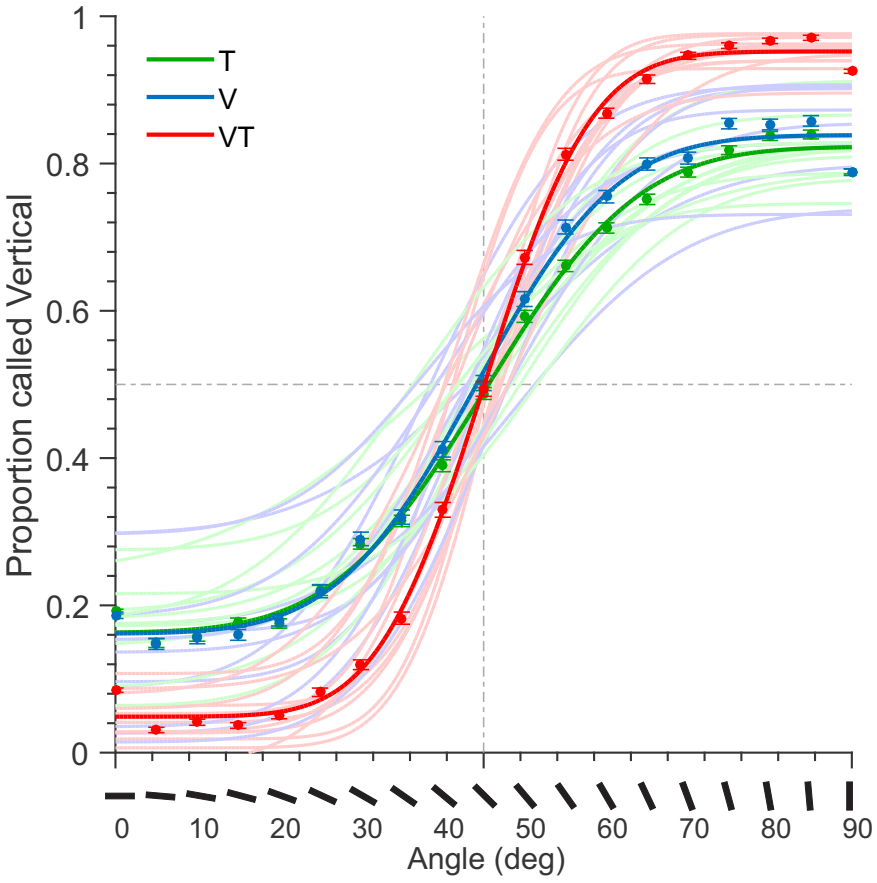

Figure 4.2.1: Fitted psychometric curves of the performance of all rats in all modalities. Pale curves show the performance of each rate in each modality. Dark colored curves show the average over all rats in each modality. Error bars show 95% binomial confidence interval.

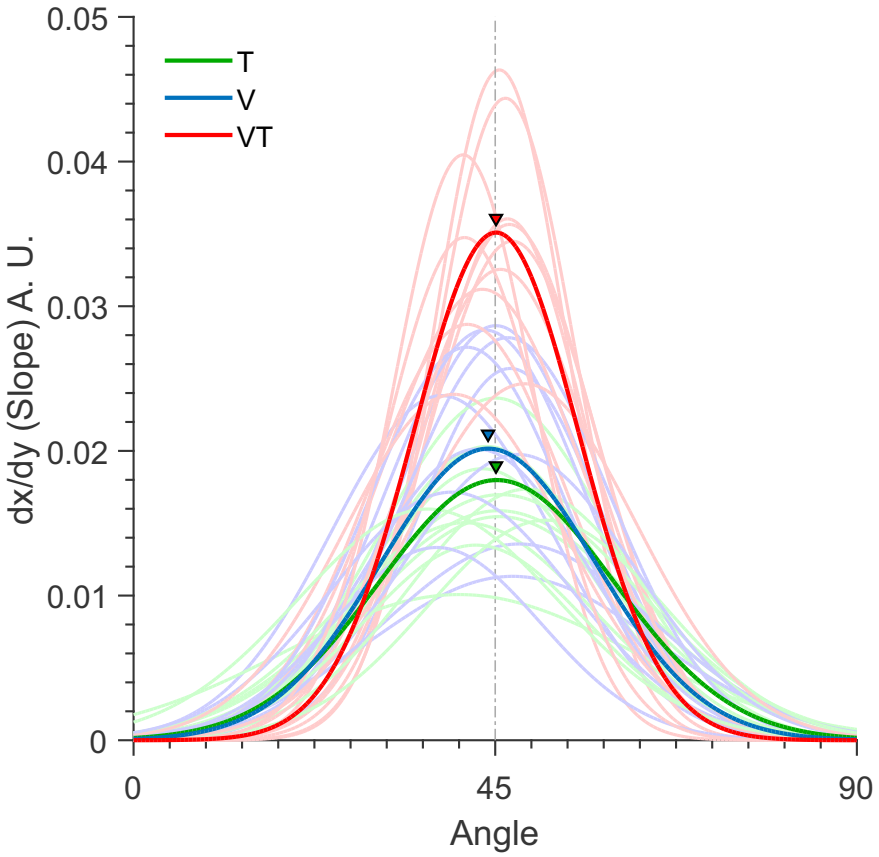

Figure 4.2.2: First derivatives (slopes) of the psychometric functions depict the underlying Gaussian distribution of the fits in figure 4.2.1. Pale curves are slope values for individual rats and dark curves are average among all rats. The small triangles indicate the peak slope which is at the inflection point on the psychometric curve and describes the point along the curve where a change in the stimulus value is followed by maximum change in the behavioral performance.

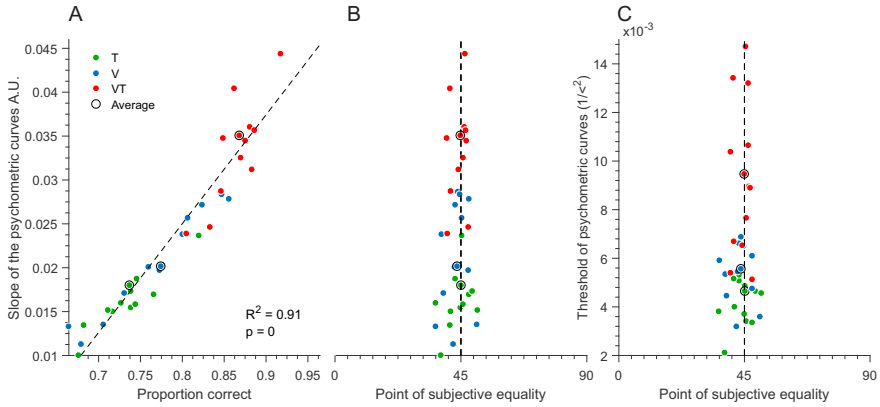

Figure 4.2.3: Psychometric curve parameters for all subjects in different modalities. (A) shows the relationship between two measures of performance: the peak slope of the psychometric curve and overall accuracy of all rats. Dashed lined is linear regression. (B–C) rats are less biased and more accurate (higher peak slope and more reliability as indicated by inverse variance $1/\sigma^2$) in multisensory conditions. Average values are indicated by black circles.

the slope is higher and the subjects have lower psychometric thresholds (Fig. 4.2.3-b–c).

As illustrated in figure 4.2.2, rats have different discrimination capabilities: some are more accurate in touch and some are better in their visual performance but all rats have lower error rates on bi-modal condition.

Statistical tests of significance was performed based on the bootstrapping method described in section 2.7.2 (Fig. 4.2.4). The difference between the peak slope of the uni-modal and multimodal psychometric curves was highly significant for all rats (p = 0.00).

Figure 4.2.5 shows the difference between the absolute performance values of the bimodal condition and each of the unimodal conditions for all rats averaged. For most rats the multisensory enhancement was highest for all orientations in tactile only trials compared to the advantage to visual only condition. The magnitude of multisensory enhancement also correlated with the task difficulty: the highest enhancement values pertain to the orientations between 25–35 and 60–80 degrees whereas multisensory advantage is lowest at 0, 90 and does not exist at the PSE. This observation is consistent with the inverse effectiveness phenomenon as discussed in chapter 1[1]. At 45 degrees, performance in any condition can be, at best, no

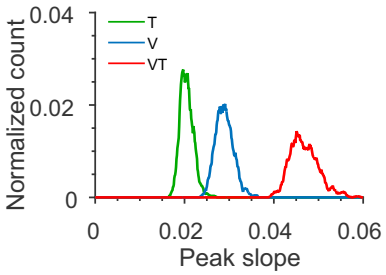

Figure 4.2.4: Bootstrap distribution of slope values at the inflection point based on 1,000 rounds of resampling in each modality for one representative rat. The three distributions are visibly distinct from each other and the slopes of vision-tactile condition are much larger than vision-only or tactile-only. Distributions are normalized.

[1] According to the principle of inverse effectiveness in multisensory integration, as the responsiveness to individual sensory stimuli decreases, the strength of multisensory integration increases.

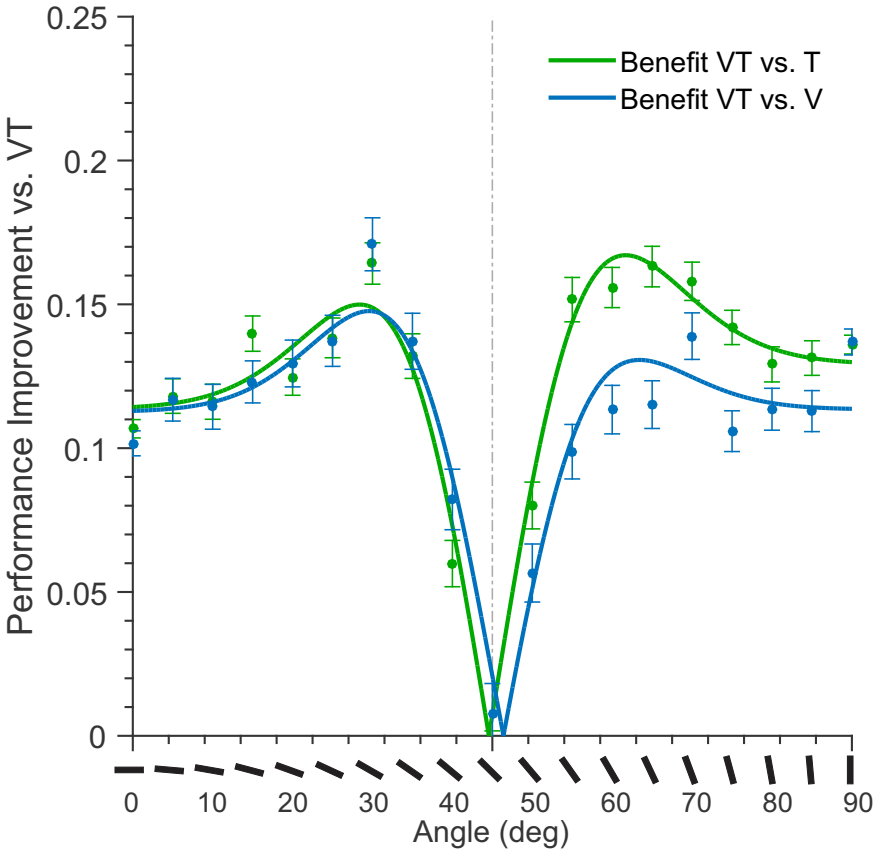

Figure 4.2.5: The difference between the performance of rats in multisensory conditions and each unisensory condition shows the strength of multisensory enhancement. Each data point corresponds to the difference between the performance of rats at each orientation in multisensory condition and touch-only trials (green curve) or vision-only trials (blue curve). Highest gains in sensory enhancement were achieved in comparison to tactile-only conditions. Furthermore, the highest improvement can be seen in orientations close to PSE (25–35 and 60-80 degrees) which were the most ambiguous and the smallest improvement is at PSE (45° category boundary), 0 and 90 degrees (not ambiguous).

better than chance. Thus multisensory integration can provide no benefit. At the cardinal orientations, performance in V and T conditions is high; due to a ceiling effect, multisensory convergence can offer smaller benefit. It is, logically, the intermediate orientations where the rats may gain most by combining information from the two modalities.

4.2.2 Most rats combine touch and vision better than Bayesian optimal prediction

We sought to investigate whether the multisensory enhancement is "optimal" with respect to the best linear combination (see chapter 1). To answer this, we computed the performance expected by optimal integration in the framework of Bayesian decision theory and found that most rats combine visual and tactile information better than predicted by the standard ideal–observer model (maximum likelihood prediction).

We fitted the psychometric data with a cumulative Gaussian function yielding two parameters: the point of subjective equality (mean of the best fitting cumulative Gaussian function) and the threshold (as its s.d., σ). Solving equation 2.7 for σ_{vt} gives the optimal combined threshold from single sensory estimates. White circles in figure 4.2.6-a, shows the comparison of measured versus predicted σ_{vt} values for all subjects. Lower measured σ_{vt} values show close to or better than Bayesian optimal estimates for most subjects.

In a different set of experiments, we tested a group of trained rats (subjects 2–7) on a block design where unimodal and bimodal trials were *not* interleaved. We collected data from blocks of seven subsequent sessions of unimodal trials followed by seven sessions of bimodal trials separately (i.e. 3 blocks of 7 session length for each of the conditions). Our hypothesis was that this could minimize the motivational effects as it forces the rats to their uni-modal or bimodal perceptual limits in each block (see Discussion, section 6.2). Then the psychophysical thresholds were computed as before and compared to the prediction of Bayesian model. Lower measured σ_{vt} values revealed close to or better than Bayesian optimal estimates for the six subjects tested in block design (Fig. 4.2.6-c).

4.2.3 Alternative computational approaches to the Bayesian cue combination model

To delve further into the observed deviation from Bayesian predictions, we interpreted the data in two additional frameworks: probabilities of independent events and summation of mutual information for each sensory channel.

Probability summation of independent events

First, we calculated the performance data on bimodal condition based on probability summation of guess corrected performances. The basic assumption of this framework is that on each trial, the subjects are either guessing or are sure about the choice. The decision maker is required to

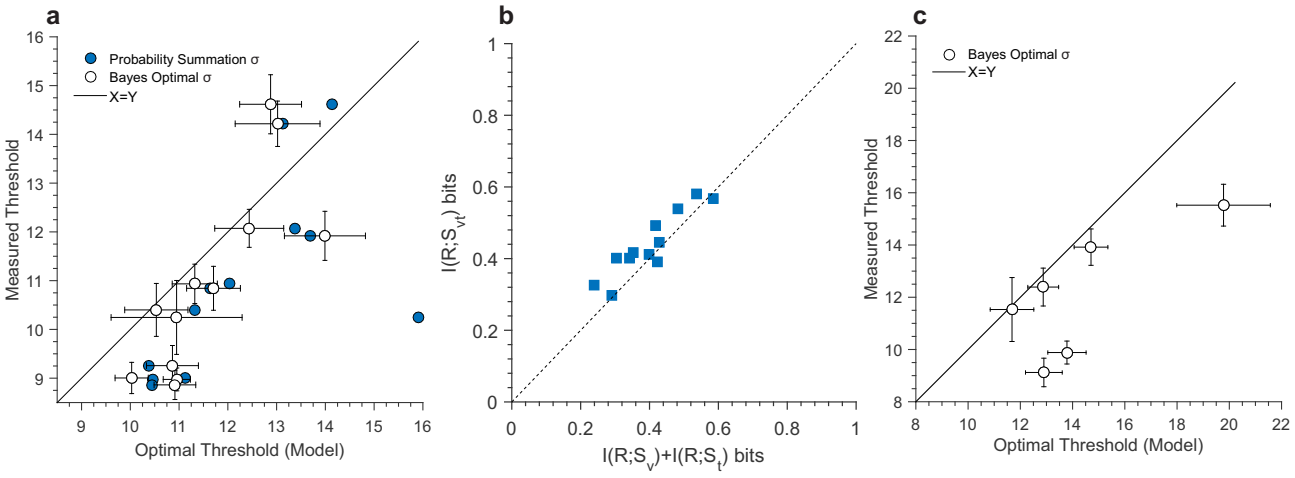

Figure 4.2.6: (a) Comparison of measured versus predicted σ_{vt} values for all subjects based on Bayesian and probability summation predictions. Lower measured σ_{vt} values show close to or better than optimal estimates for most subjects, indicating that performance is better than optimal prediction with combined sensory channels. (b) Comparison of mutual information between behavioral choice and stimulus category in bimodal condition with the sum of mutual information for two single modalities. Most rats show lower value for the sum of the information in two channels compared to the bimodal choice information. (c) Same as (a) for the Bayesian prediction in the block design experiments.

summate probabilities by means of performing a logical inclusive "OR" operation. If at least one of the two modalities (vision or touch) has information about the category of stimulus, the decision maker will commit to it ($0 \vee 1 = 1, 1 \vee 1 = 1$), otherwise it will make a guess ($0 \vee 0 = 0$). One criticism is that the model implies meta-knowledge: when the rat has adequate information ("it knows"), it knows that it knows. Thus the decision maker commits to the choice that is supported by information, but making the commitment requires higher-order knowledge[2]. In spite of such criticism, we thought the approach worthwhile because other lines of research have provided evidence that rats are aware of their own certainty (Kepecs et al., 2008; Lak et al., 2014; Meyniel et al., 2015) and the current work also suggests that they have such meta-knowledge (see section 4.4).

One can convert the "apparent" proportion correct, to the "actual" proportion correct based on this framework. Applied to a two-alternative forced choice task, the intuition is that if the subjects choose option A 50% of the time, then they are not definitively 50% correct. At an upper limit,

[2] According to the metacognitive view, confidence reports as an example of metagognitive processes, are generated by a second-order monitoring process based on the quality of internal representations about beliefs.

they are correct 0% of the time and guessing 100% of the time. Similarly, if subjects correctly choose option A 60% of the time, at the upper limit, they might be guessing on 80% of trials, and correct on 20% of the trials: $(60 = 0.5 \times 80 + 1 \times 20)$, and so on. We can formulate this simple idea as the following:

$$\begin{aligned} p_o &= 0.5 \times p_{Guess} + 1 \times (1 - p_{Guess}) \rightarrow p_{Guess} = 1 - p_{Corr} \\ &= 0.5 \times (1 - p_{Corr}) + p_{Corr} \\ p_{Corr} &= 2 \times (p_o - 0.5) \end{aligned} \tag{4.3}$$

then according to probability summation, for two modalities we have:

$$\begin{aligned} p_{Corr_{V,T}} &= 1 - (1 - p_{Corr_T}) \times (1 - p_{Corr_V}). \\ p_{PScorr} &= (p_{Corr_{V,T}}/2) + 0.5. \end{aligned} \tag{4.4}$$

In equations 4.3and 4.4, p_o is the observed performance for each stimulus angle in a given modality, p_{Guess} is the probability of guessing, p_{Corr} is the probability of subject being correct. p_{Corr_T} and p_{Corr_V} are the computed p_{Corr} values for each modality, $p_{Corr_{V,T}}$ is the upper limit probability of correct answer and finally p_{PScorr} is the bimodal choice probability based on the probability summation of two independent sensory modalities.

Then the cumulative Gaussian curves were fit to the p_{PScorr}, and the resulting threshold value was compared against the observed bimodal thresholds (σ_{vt}). Blue circles in figure 4.2.6-a, shows the comparison of measured versus predicted σ_{vt} values for all subjects.

Summation of mutual information for sensory channels

In a multisensory task several sensory modalities potentially provide information about the stimulus. We sought to determine how the animal combines these sources of information in order to make a decision. The current experiment allowed us to measure the information extracted by the rat when tactile and visual signals were provided in isolation or together

combined (visual-tactile trials). These sensory signals could be redundant, synergistic, or independent of each other.

To test between these possibilities we used a simple model whereby we assume that the information extracted by the rat about the stimulus orientation is converted directly into a choice. This allowed us to estimate the signal extracted by the rat according to its behavioral accuracy. We assume that all of the available information to the rat is used to make a two-alternative forced choice (e.g. 1.0 bit gives 100% accuracy, 0 bits gives 50% accuracy, intermediate quantities of info give intermediate performance etc). Therefore, we computed the mutual information (see chapter 2) between the stimulus category (horizontal or vertical) and the rat's behavioral choice (response left or right) in each modality separately as well as in the combined condition. Then we asked, if rats can combine (summate) signals from the two channels optimally, how much information would they have available and compared this quantity to the mutual information computed from the bimodal condition. If the summated quantity of information is equal to or larger than 1 bit, the rat has more information available than it can express.

Figure 4.2.6-b, shows that for most subjects the summated information from two sensory channels yield a smaller quantity when compared to the information in the visual–tactile condition. These results suggest that information from the two sensory channels are not encoded independently but are combined in a synergistic manner.

4.3 Analysis of Response times

The response times were calculated as the time from opening onset of the opaque panel until the first lick. On average (among all sensory conditions and stimulus orientations) rats performed the task in each trial in ~400-700 ms. Analysis of average reaction times of rats to each stimulus orientation revealed a correlation between perceptual difficulty of the trial and response time (Fig. 4.3.1-a). Highest response times correspond to the most difficult choices (orientations close to the boundaries).

Figure 4.3.1-c shows the distribution of all response times lower than 2200 ms of correct trials in unisensory as well as multisensory trials in all orientations presented to a rat. Figure 4.3.1-b shows the raster plot of response times for a rat in 5 sessions (mean response time=515.4 ms, median=483.2 ms).

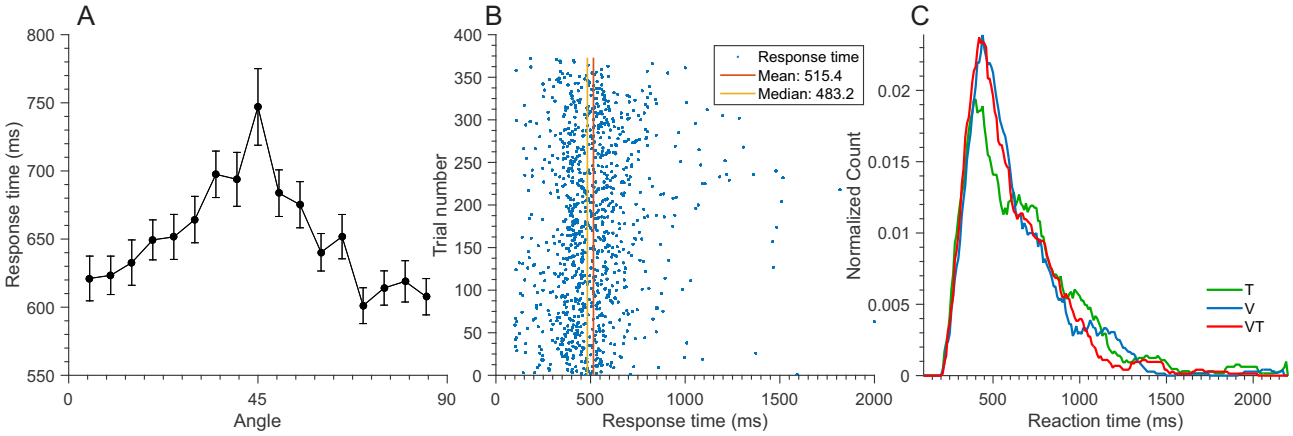

Figure 4.3.1: Analysis of Response times. (a) Average response times of rats at each orientation. The highest reaction times pertain to the most ambiguous orientations of the stimulus (close to 45 degrees). (b) a raster plot of reaction times for one representative rat. Most data points were clustered between 400–600 ms. (c) distribution of all reaction times of the same rat in (b) in each modality condition. Error bars in (a) indicate standard errors.

4.4 Analysis of licking behavior

Rats seem to express their degree of certainty in their perceptual decisions. In some sessions we introduced a random delay before the reward and measured how the rats lick while attending the outcome of their decision (see Behavioral Methods, section 2.5).

Analysis of the lick events during the delay reveals a correlation between trial difficulty and the frequency of the licking: on easier trials rats lick at 7.5 to 8.5 Hz regardless of the modality. On more difficult trials they lick at 6.5 to 7 Hz (Fig. 4.4.2).

Figure 4.4.1-a, demonstrates an example lick recording session of a rat. Black dots are lick events taken into consideration for the lick frequency analysis. Gray dots in figure 4.4.1a demonstrate lick events after the delay

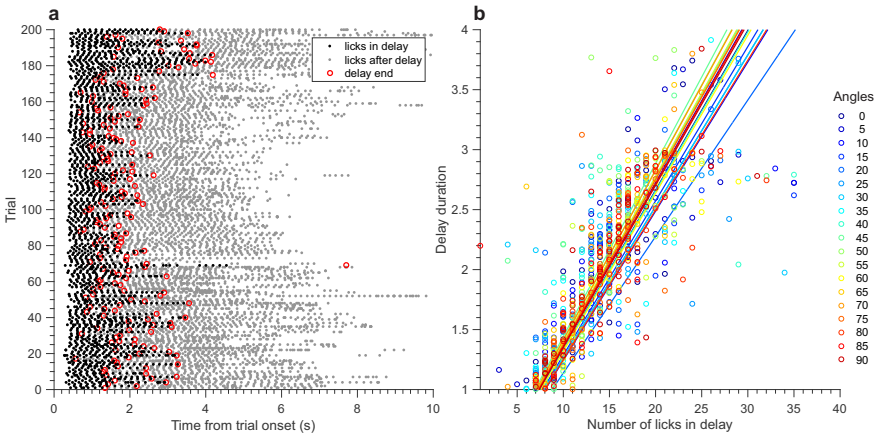

Figure 4.4.1: Analysis of licking patterns. (a) A lick raster plot for 200 trials in a recording session of one rat. Black dots are lick events taken into further analysis. Gray dots demonstrate lick events after the delay period which are marked by red circles. (b) Correlation between lick count during the delay period for each stimulus angle and delay duration. The slope of the fitted curves is inversely correlated with the licking frequency. Color code shows trials belonging to each angle in the range 0–90 degrees.

periods which are marked by red circles. Figure 4.4.1-b, shows the number of licks in a given delay period. Each circle in figure 4.4.1-b is a lick count (vertical axis) during the delay period (horizontal axis) of a trial. The slope of the fitted curves is inversely correlated with the licking frequency shown in Figure 4.4.2.

Figure 4.4.3-a shows the mean licking frequency per stimulus angle averaged across all stimulus modalities of two rats included in the analysis. Figure 4.4.3-b shows the correlation between the performance of rats in a given angle and average licking frequency. Lower performance values are paired with lower lick frequency. Figure 4.4.3-c, is the histogram of inter-lick intervals (ILI) for different angles. Note that the mean of the distribution is moved towards larger ILI values for more difficult orientations. This implies that the lowered licking frequency in difficult trials is due to a general increase in the ILI and not burst-like licking pattern where the lick burst frequency remains constant among different conditions.

These results suggest that licking behavior in rats might be a marker of their internal state as it might reveal their perceptual "confidence".

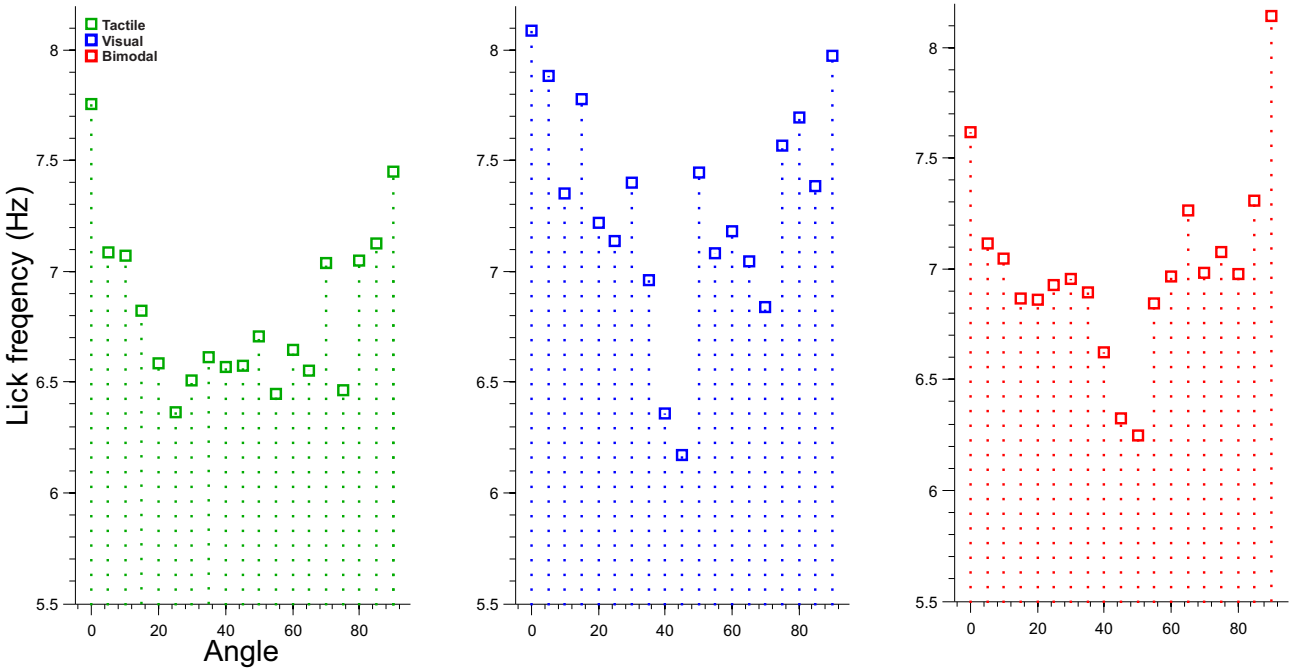

Figure 4.4.2: Analysis of the lick events for one subject during the delay in different modality conditions reveals a correlation between trial difficulty and the frequency of the licking: on easier trials rats lick at 7.5 to 8.5 Hz regardless of the modality. On more difficult trials they lick at 6.5 to 7 Hz.

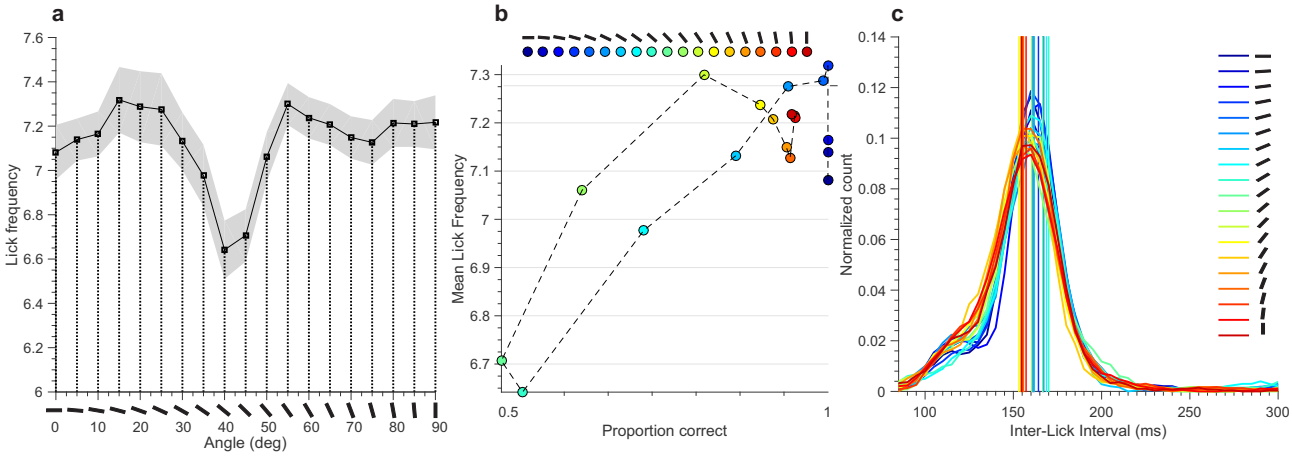

Figure 4.4.3: (a) Mean licking frequency per stimulus angle averaged across all stimulus modalities of two rats. Shading shows S.E. (b) Correlation between the average performance of rats in a given angle and average licking frequency. (c) Histogram of inter-lick intervals (ILI) for different angles. Vertical colored bars indicate mean of the ILI distribution. Note that the mean of the distribution is moved towards larger ILI values for more difficult orientations (green/cyan).

5

Results of the Neuronal Investigation

We recorded the neuronal activity in the left posterior parietal cortex of trained rats after they reached a stable level of performance in the behavioral task. The selection criterion was >75% correct and consistent overall psychophysical performance judged by the slope of psychometric curves, constructed by averaging the trials of the most recent 15 sessions. For most recording sessions the stimulus orientation set was reduced to angles between 0–90 degrees with 15° distance between each (hence 7 orientations in 3 modalities) to allow a greater number of trials (and therefore neuronal samples) per orientation and modality condition. Rats usually completed 300–500 trials per recording session. Similar to the behavioral task during training, trials of all modalities were interleaved (detailed in chapter 3).

The events structure of the recording sessions was similar to that of the behavioral training (see chapter 2, and figure 2.1.1).

To visualize the response characteristics of neurons we first illustrated

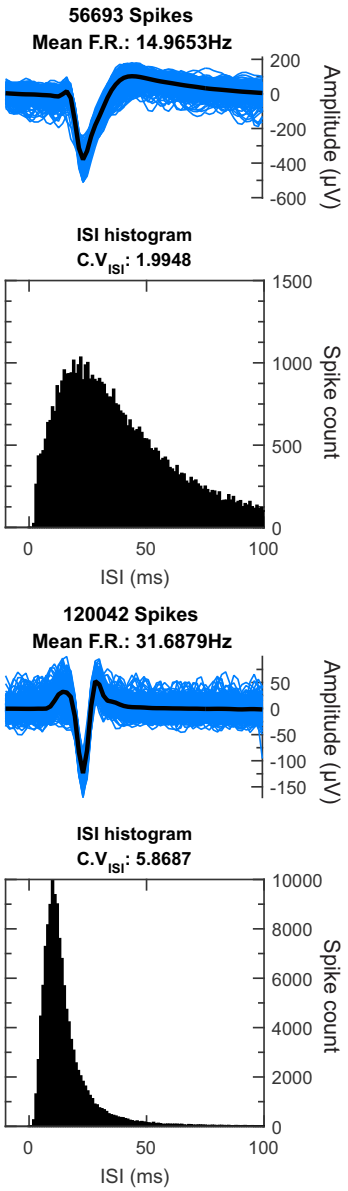

Figure 5.0.1: Spike wave-form (blue, individual spikes, black, average wave-form) and inter-spike interval histograms for two example neurons recorded in PPC. Top neuron is the one illustrated in Fig. 5.1.1-d and the bottom one is illustrated in Figure 5.1.1-a. Mean firing rate value are computed in whole session.

the activity of each neuron as a raster plot and time-dependent firing rate. Mean firing rates were computed from the set of density functions (spike trains convolved with Gaussian kernels) for trials belonging to each stimulus condition. Then we quantified the correlation between the firing rate of neurons and task parameters in each time bin using receiver operating characteristic (ROC) analysis and linear regression. We further computed the mutual information between the firing rate of each neuron and the parameter of interest.

The neuronal data from five out of seven recorded rats are presented in this chapter. The selection of sessions for inclusion in the neuronal analysis was based on a few parameters, such as number of trials in the recording session, stable performance of the rat over the course of the session and quality of the electrophysiological signals in that session. Two rats are not included because they did not meet some of these criteria.

The criteria for including neurons in the analysis included:

1. spike waveform quality (i.e. action potential shape and signal to noise ratio),
2. possible cluster contamination by examining the inter-spike interval (ISI) histograms,
3. average firing rate of at least 1 Hz during trials,
4. stable firing rate over the course of a session (Fig. 5.0.1).

In total we included 622 neurons recorded in the posterior parietal cortex in the following analyses.

5.1 PPC is modulated by categorical as well as graded representations of the stimulus orientation

We examined the encoding of the stimulus as well as the representation of the stimulus category by grouping trials with the same grating orientation together. Figure 5.1.1, shows raster plots as well as peri-event time histograms (PETHs) of four example PPC recordings from two rats in all

stimulus modalities. The neuronal data are aligned to the trial onset (onset of the opening of opaque panel, see Neuronal Methods chapter 3). Error trials were excluded in these plots except for 45-degree orientation where all trials were grouped; error trials will be examined in later sections. The panels on the left column represent two neurons that showed a coding of the stimulus in a graded manner (Fig. 5.1.1-a–b). The firing rate of these neurons was modulated by the stimulus angle and was either negatively or positively correlated with the stimulus angle (0–90 degrees).

The panels on the right side of figure 5.1.1-c–d, demonstrate two example neurons that carried a significant signal about object category in their discharge rate. These neurons exhibited average firing rates that were initially constant in time and then ramped upwards or downwards according to whether the preferred stimulus category was presented. The firing of such neurons did not seem to be modulated by the specific stimulus angle but by the category (horizontal/vertical) to which the stimulus belonged or else the action of the animal in response to these categories (stimulus category and action are not distinguishable on trials with correct response).

Figure 5.1.2, shows tuning curves generated from average firing rates in trials with a given angle for neurons in figure 5.1.1, from a window of neuronal activity 400 ms preceding the response lick. Note the shallow slope of panels a–b compared to steep curves in c–d. The maximum slope of the tuning curves indicates whether the neuronal responses change smoothly between different orientations or they change sharply.

Figure 5.1.3, illustrates the same physiological data recorded from neurons in figures 5.1.1 and 5.1.2. We considered the neurons' response on each trial to be the average firing rate in a 400 ms window prior to the response lick. The histograms in figure 5.1.3-f, show the average firing rate of the neuron in that 400 ms window for each orientation in the bimodal condition. An ROC analysis, similar to Britten et al. (1992) was employed to compute a "neurometric function" for each neuron.

The neurometric functions describe the probability that an ideal observer could accurately categorize the orientation of the stimulus by ex-

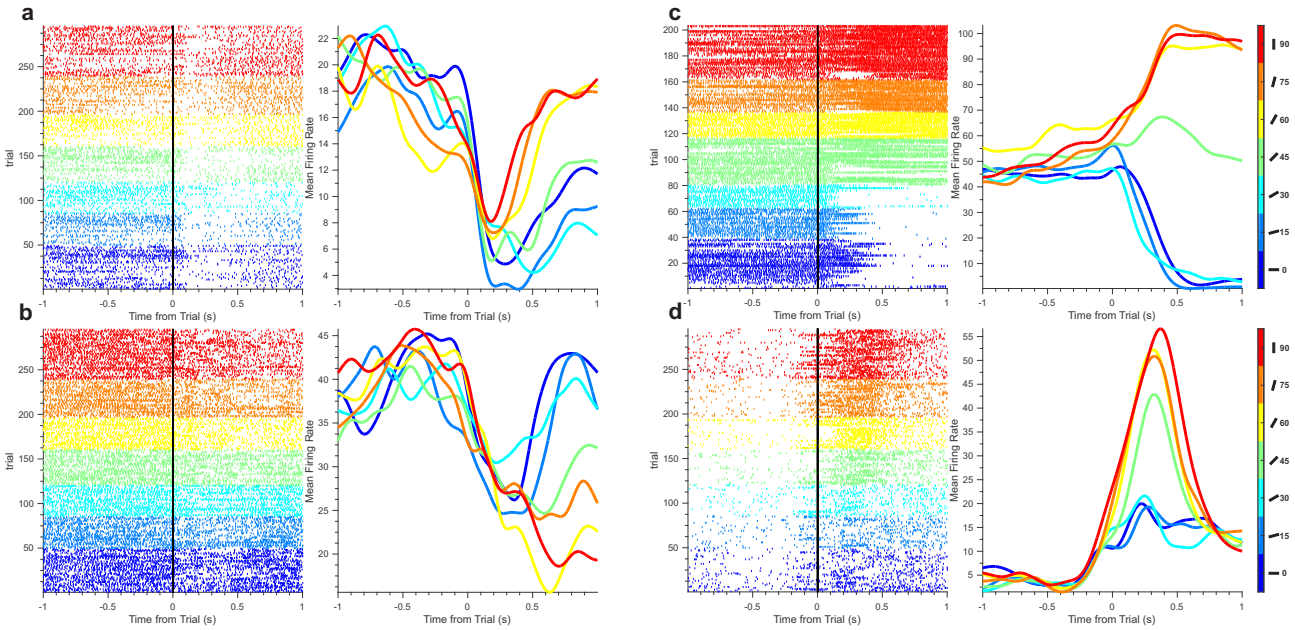

Figure 5.1.1: Neurons in PPC carry information about stimulus angle as well as stimulus category. (a–d) raster plots and peri-event time histograms (PETHs) of four example PPC recordings from two rats in all modalities, smoothed with a Gaussian kernel ($\sigma = 50$ ms). Trials were grouped by stimulus angle (colors). Error trials were excluded (Except for boundary angle, 45-degree, where an error trial is undefined). Responses are aligned to the trial start (t = 0). (a–b) two neurons that showed a coding of the stimulus in a graded manner. (c–d) two example neurons that carried a significant signal about object category.

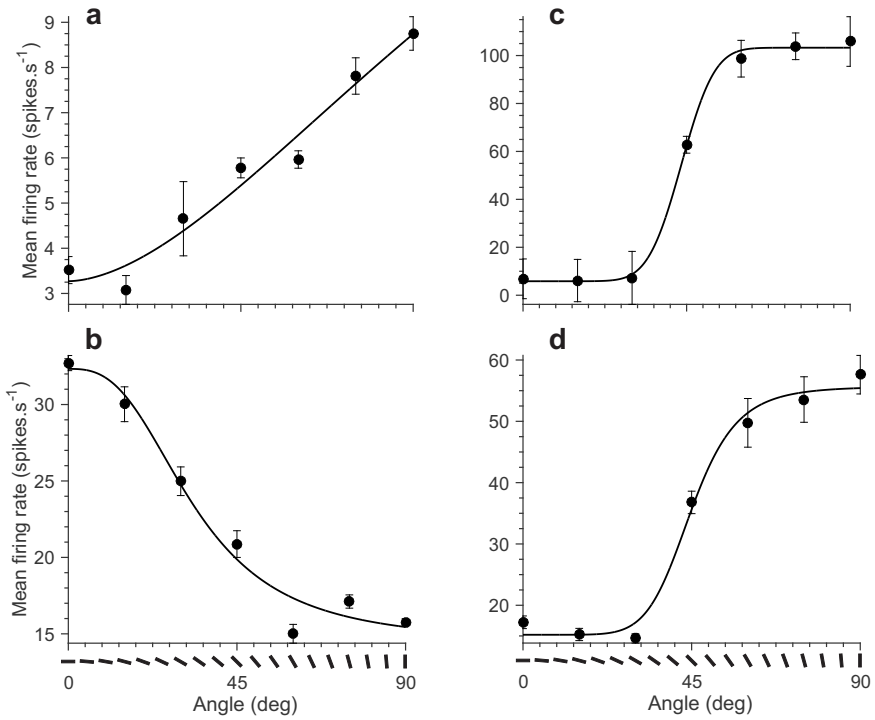

Figure 5.1.2: Tuning curves of neurons demonstrated in figure 5.1.1. These curves show average firing rate for trials grouped with the same stimulus orientation in a 400 ms window preceding the response lick. Data points show the average firing rate per angle. The curves are four parameter logistic fit (equation 2.2). Note the graded slope of panels a–b compared to steep curves in c–d.

ercising a precise decision rule and operating that rule using neuronal responses such as those shown in figure 5.1.3-f. The observer's accuracy increases from chance at stimulus boundary (45-degree) to higher levels at 0 and 90 degrees. An advantage of this simplistic signal detection based method is that it does not require any assumption about the shape of neuronal response distributions (Fig. 5.1.3-f). In this figure, the horizontal axis shows the average firing rate of the neuron in a 400 ms window preceding the response lick and the vertical axis shows the normalized trial count in which a particular neuronal response was obtained. Different colors depict stimulus angles.

In order to compute the neurometric functions we assumed that the sensitivity of neurons could be computed by comparing the responses of neurons at a given orientation to the responses to "null orientation" of decision boundary (45-degree) in each modality condition. On any given trial the decision is made in favor of the responses being larger (call vertical) or smaller (call horizontal) than the responses to the null orientation. The data points in fig. 5.1.3-a–d are the proportion of choices that the model

made in relation to stimulus angle. This probability was computed as the normalized area under the ROC curves such as the one illustrated in figure 5.1.3-e. The curves are fit with the same cumulative Gaussian function used in describing the behavioral data (equation 2.2).

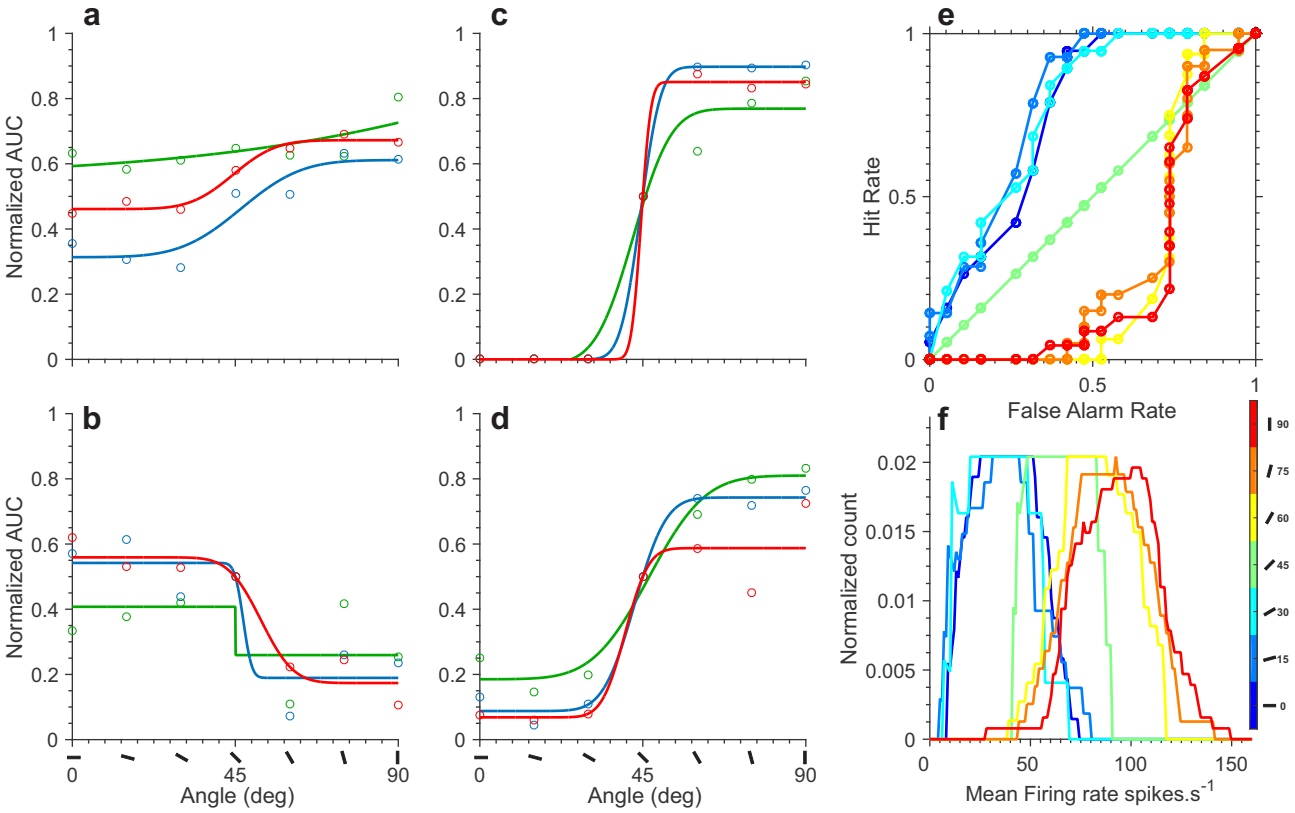

Figure 5.1.3: Neurometric curves of neurons demonstrated in figures 5.1.1 and 5.1.2. (a–d) The data points represent the proportion of correct choices that the model made against the stimulus angle, given by the normalized area under the ROC curves such as (e). The ROC analysis was done on the frequency histograms such as the one demonstrated in (f). Colors in (a–d) depict modalities, green (T), blue (V) and red (VT). The curves cumulative Gaussian fits used in describing the behavioral data (equation 2.2). (f) The horizontal axis shows the average firing rate of the neuron in 400 ms window preceding the response lick and the vertical axis shows the normalized trial count in which a particular neuronal response was obtained. Colors in (e–f) depict stimulus angles.

In addition we computed Spearman's correlation coefficient (Spearman's ρ) for shifting windows of 200 ms of neuronal activity and stimulus angle (Fig. 5.1.4-c). Significant correlation coefficients emerged between the neuronal firing and stimulus angle during the sampling and decision formation window ~500 ms prior to the response lick ($p<0.01$, permuta-

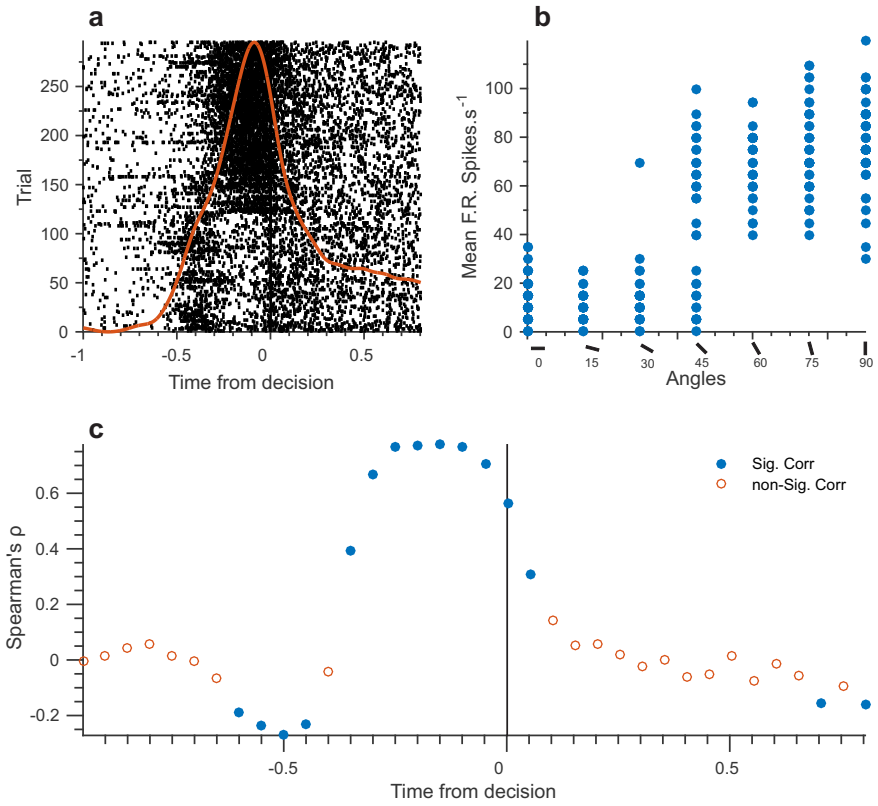

Figure 5.1.4: Neuronal activity in PPC is correlated with the stimulus angle. (a) Raster plot, black dots, and scaled histogram of average firing rate, orange curve, of an example neuron recorded in PPC (shown in Fig. 5.1.1-d). Spikes were aligned to the response lick (decision) and trials were sorted according to the stimulus orientation (b) Average firing rate in all trials corresponding to a given stimulus angle. (c) Spearman's rank correlation coefficient or Spearman's ρ, computed for shifting windows of 200 ms of neuronal activity and stimulus angle. Blue circles, significant correlation value ($p<0.01$), open orange circles, not significant.

tion test).

5.2 PPC encodes animal's decision

We sought to examine the effect of the animal's choice and stimulus modality on the neuronal responses during the task by computing a measure called selectivity (Feierstein et al., 2006). In order to quantify selectivity, we used receiver operator characteristic (ROC) analysis to define a measure of how well the firing rate of a given neuron can be used to classify the choice of the animal (left vs. right) or modality of the stimulus (visual vs. tactile). This metric is proportional to the area under the ROC curve which is scaled from -1 to 1, with 0 being nonselective.

Figure 5.2.1, shows histograms of choice (a) and modality (b) selectivity indices for a population of 622 PPC neurons. Positive selectivity values correspond to higher firing rates for leftward choices or visual trials

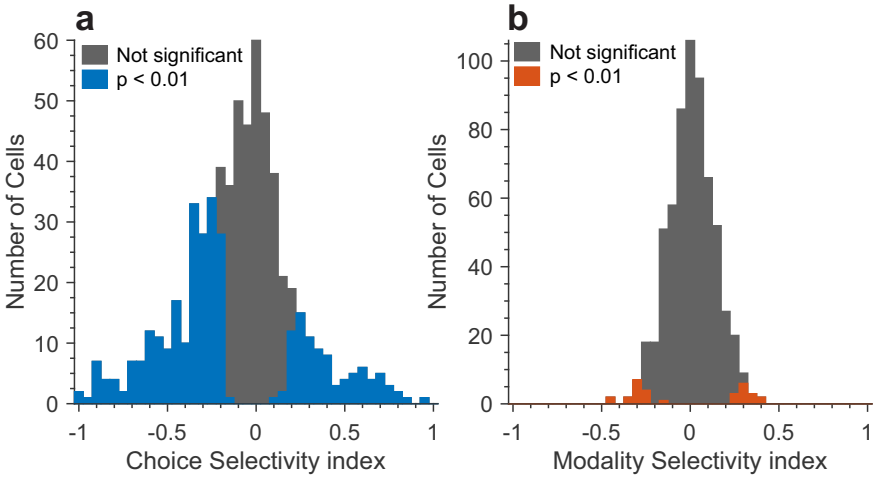

Figure 5.2.1: Choice (a) and modality (b) selectivity for a population of 622 PPC neurons. Selectivity index was calculated using ROC analysis (section 3.4.5 neuronal methods). Positive values correspond to higher firing rate for leftward choices in (a) and visual trials in (b); negative values correspond to cells with higher firing for rightward choices in (a) and tactile trials in (b); 0 is nonselective. Color bars are significant selectivity with $p < 0.01$ based on 1,000 rounds of permutation procedure; blue, cells selective for choice; orange, cells selective for modality. Gray bars, not significant.

while negative values correspond to neurons with higher firing for rightward choices or tactile trials. Very few neurons (Fig. 5.2.1-b, 30/622 neurons; 4.8%, p<0.01 based on 1,000 rounds of permutation procedure) were selective for stimulus modality while a large proportion of neurons where found to be significantly selective for the choice of animal (Fig. 5.2.1-a, 309/622 neurons; 49.7%, p<0.01 permutation procedure). More neurons seem to be selective for turns to the right, suggesting laterality in PPC.

In addition to the selectivity analysis, we did an information theoretic analysis to compute the mutual information available in the neuronal responses about rats' action and modality of the stimulus. Figure 5.2.2-a, shows data from 622 PPC neurons. Most neurons carried significantly larger quantities of mutual information about the choice of the rat than about modality. From 622 neuron included in the analysis, 518 neurons had significant information about choice (95% confidence interval calculated based on 1,000 rounds of bootstrapping), 448 of these neurons had more information about choice than for modality (Blue circles above the dashed line in Fig. 5.2.2-a).

In further analyses we measured the average firing rate of neurons in a 500 ms window preceding the response lick in tactile and visual trials sep-

arately. Clustering of most points on the diagonal of the scatter plot in figure 5.2.2-b, illustrates similarity between average activity of neurons in tactile and visual modalities.[1]

[1] Bimodal trials yield similar results.

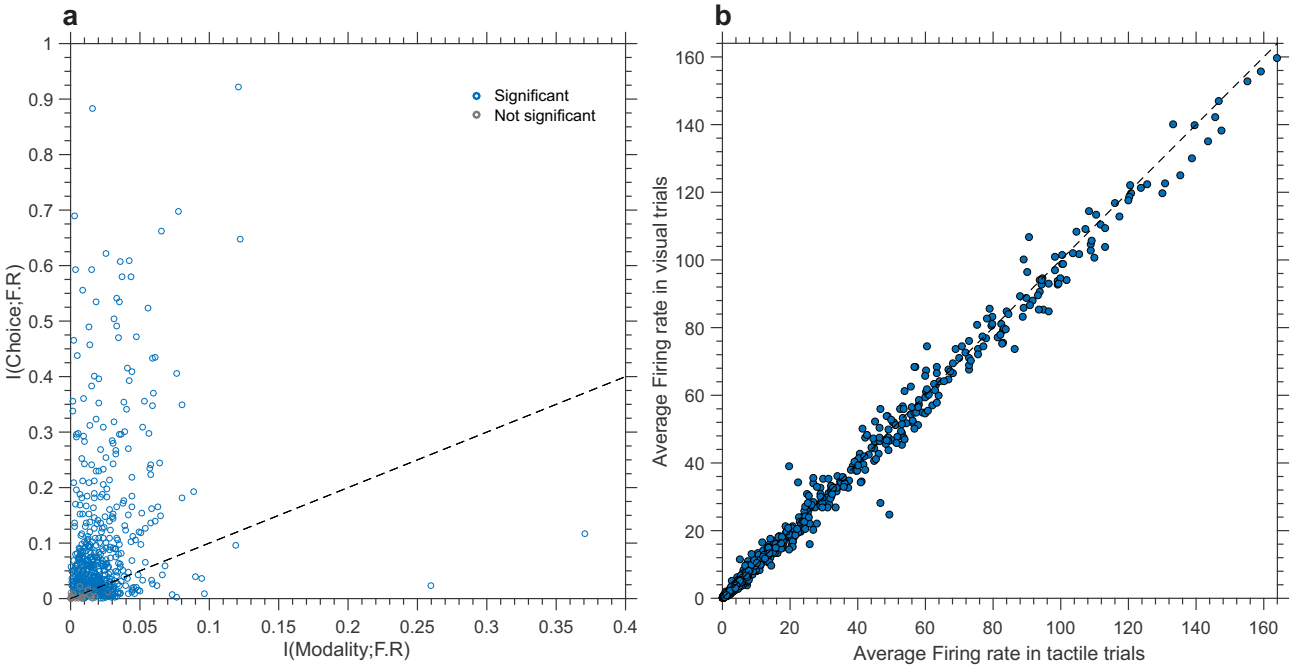

Figure 5.2.2: (a) Circles are the data from 622 PPC neurons. The horizontal axis is the maximum mutual information available between firing rate of the neurons and stimulus modality in the pre-decision epoch. Vertical axis is the maximum value of mutual information between the firing rate of each neuron and choice of the rat. Information analysis was performed on a 250 ms moving window of neuronal activity from start of the trial to the response lick. Blue, significant information values; gray, not significant, dashed line: $x = y$. (b) Each point is the average firing rate of a neuron in 500 ms window preceding the response lick in visual (vertical axis) and tactile (horizontal axis) trials.

In addition we computed the mutual information between the firing of neurons in sliding windows of 200 ms. Figure 5.2.3-a–d shows the quantity of mutual information computed in 200 ms windows of neuronal activity with 50 ms sliding. This quantity of mutual information is calculated between animals' choice (solid lines) or angle (dashed lines) in the same example neurons illustrated in Fig. 5.1.1.

We next performed an information theoretic analysis to calculate the information available in the neuronal responses about animal's action and stimulus angle. In this analysis we excluded the spurious information val-

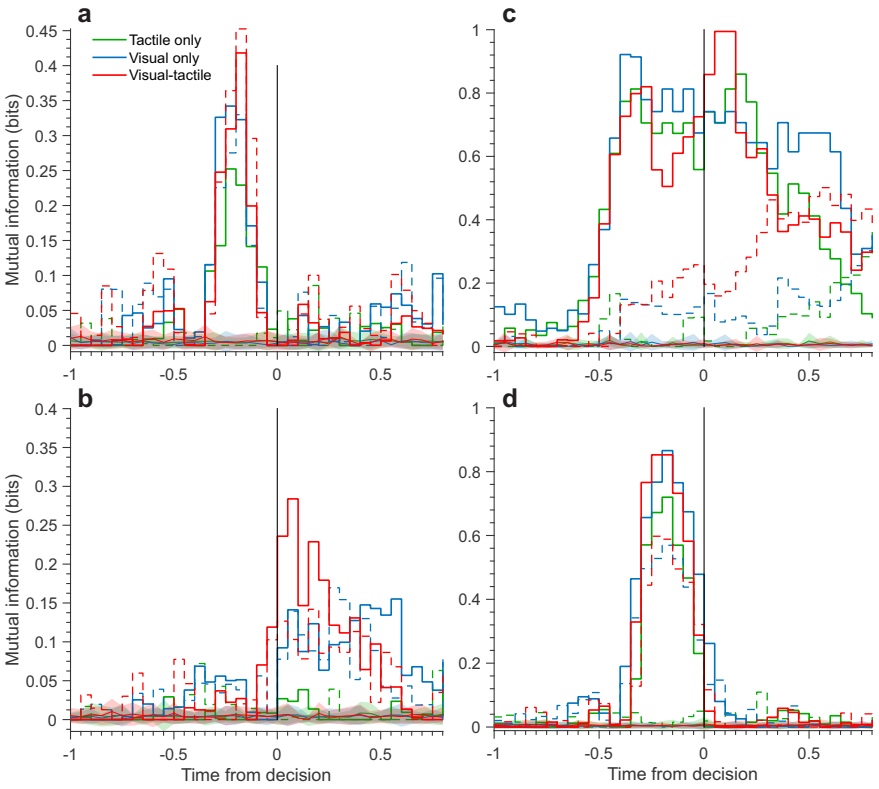

Figure 5.2.3: Mutual information computed in 200 ms windows of neuronal activity with 50 ms sliding windows between animals' choice (solid lines) or angle (dashed lines) in different modalities (shown in different colors). Neurons a–d, same as Fig. 5.1.1. Shaded area shows 95% confidence intervals computed from 1,000 bootstraps. Neuronal activity aligned to the response lick.

ues caused by the inherent correlations between task parameters since angle values close to cardinal orientations (0 and 90) were each followed by one possible decision (left or right). So that a neuron encoding (and so having only information about) stimulus angle will necessarily have information about the decision, and vice versa.

To determine whether neurons encode the stimulus angle in a graded or categorical manner, we computed the quantity of information that neurons carry about the stimulus that could not be explained by other possible parameters (like future action of the animal) and vice versa. For this purpose we computed conditional mutual information to disentangle the information about stimulus from the information about animal's action (see neuronal methods in chapter 3). The mutual information was computed from start of the trial to the response lick and the maximum information value was selected in each condition.

The scatter plot in figure 5.2.4, demonstrates the maximum quantity of

conditional mutual information between firing rate of 622 PPC neurons about stimulus angle given the choice of animals against the information about the choice given the stimulus angle in different modalities.

We next computed the absolute value of the ROC-based selectivity index for choice and modality in 50 ms sliding windows of 200 ms bins of neuronal activity. The choice selectivity was computed in each bin for different modalities. Similarly modality selectivity for visual and tactile trials was computed for left and right responses separately and then averaged (Fig. 5.2.5 and Fig. 5.2.6. Figure 5.2.7-a–b, shows the result of a similar analysis on all neurons. Figure 5.2.7-c, shows the dynamics of the proportion of neurons that manifest significant choice (black) or modality (red) selectivity from 1 second preceding the response lick.

Raster plots in figure 5.2.8, summarize the temporal dynamics of choice and modality selectivity from the start of the trial.

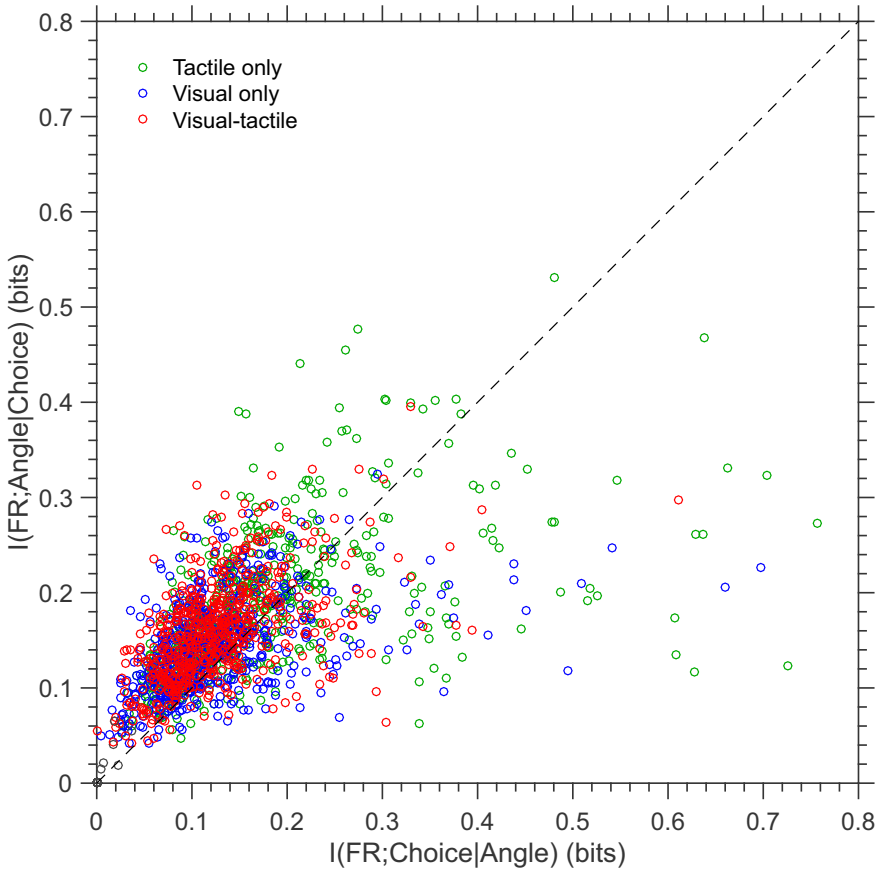

Figure 5.2.4: Circles show maximum value of conditional mutual information computed in 200 ms windows of neuronal activity with 50 ms sliding windows in the pre-decision epoch. Information was measured between firing rate of neurons and stimulus angle given the choice of the animals or the conditional information about the choice given the stimulus angle in each modality. Dashed line: $x = y$. Colors are different modalities.

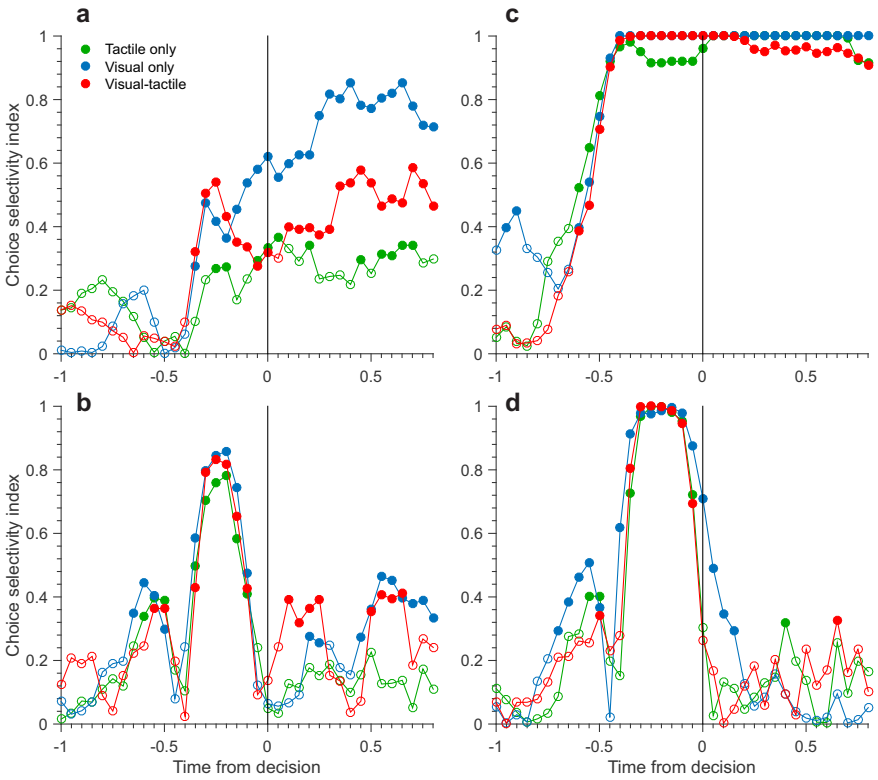

Figure 5.2.5: Absolute value of choice selectivity computed in 200 ms windows of neuronal activity with 50 ms sliding windows in different modalities (shown in different colors). Neurons a–d, same as Fig. 5.1.1. Filled circles significant selectivity index ($p<0.01$, 1000 rounds permutation test). Neuronal data aligned to response lick.

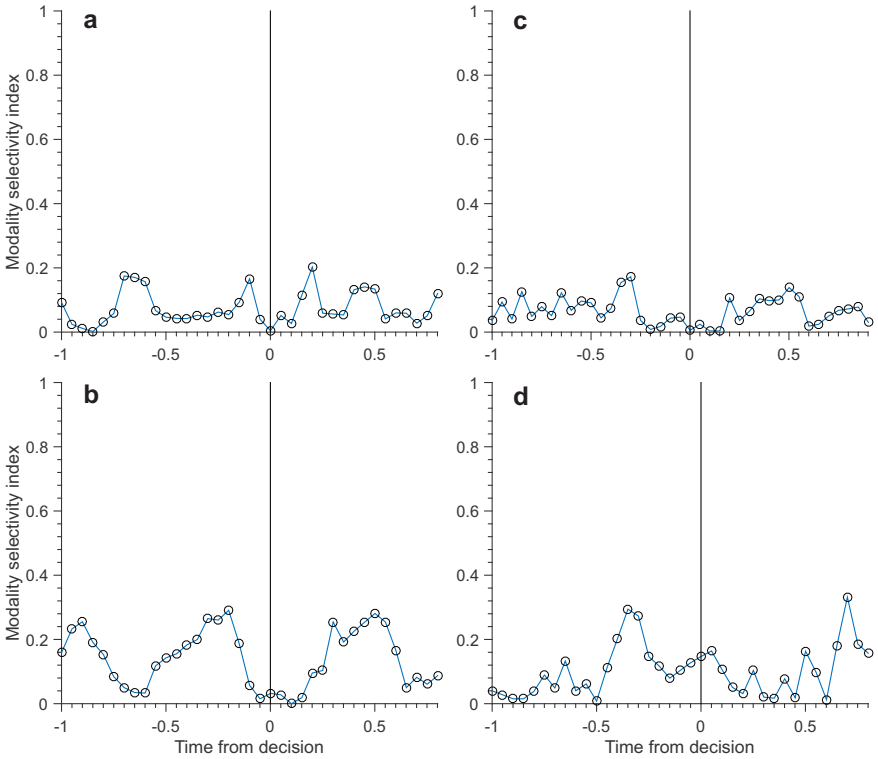

Figure 5.2.6: Absolute value of modality selectivity computed in 200 ms windows of neuronal activity with 50 ms sliding windows for a given choice (left and right choice separately then averaged). Neurons a–d, same as Fig. 5.1.1. Open circles are insignificant selectivity indices ($p<0.01$, 1000 rounds permutation procedure). Neuronal data aligned to the response lick.

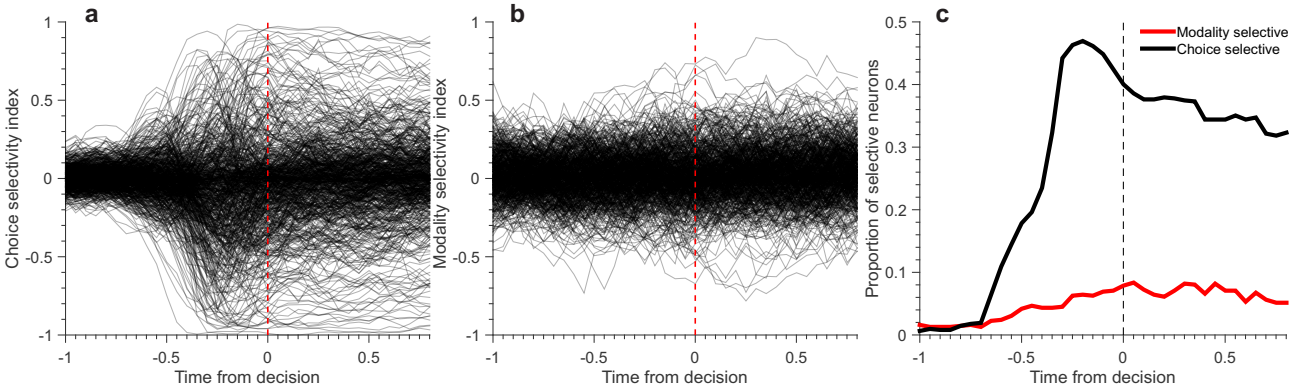

Figure 5.2.7: Selectivity analysis on a population of 622 PPC neurons. (a) Time course of dynamics of choice selectivity index measured for each neuron (black lines) from a window of 200 ms neuronal activity with shifting window of 50 ms. (b) Same analysis as in (a) for modality selectivity. (c) Time course of proportion of neurons that show significant ($p<0.005$, permutation test) choice (black) or modality (red) selectivity.

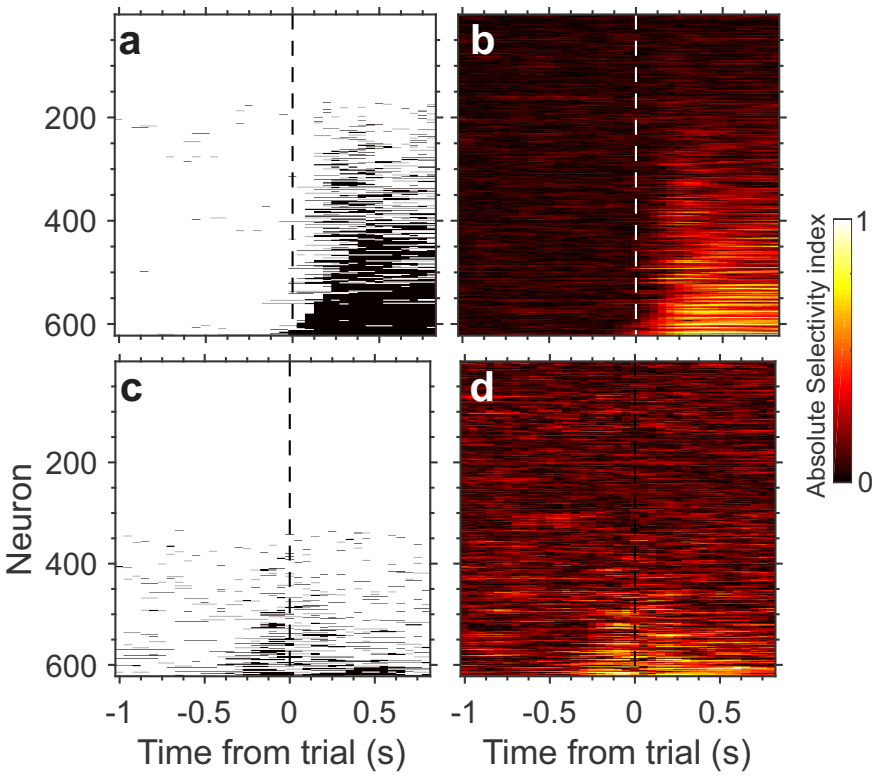

Figure 5.2.8: Choice selectivity (a–b) and modality selectivity (c–d) for neuronal activity aligned to the start of trial (dashed lines). (a, c) Black marks are significant selectivity index ($p<0.005$) bins for each neuron (vertical axis) sorted by the total number of significant bins in the whole duration. (b, d) Absolute value of selectivity index of all neurons sorted similar to (a,c).

6

Discussion and Conclusions

6.1 General discussion

We have devised a robust and largely automatic paradigm for training rats on an orientation categorization task using vision and touch. We presented rats with black and white gratings (raised bars) that could be explored by vision, by touch, or both. The grating was rotated to assume one orientation on each trial, spanning a range of 180 degrees. Rats learned to lick one reward spout for orientations of 0±45 degrees (termed "horizontal") and the opposite spout for orientations of 90±45 degrees (termed "vertical"). We asked whether they are able to achieve discrimination and classification of object orientation in touch and vision. Next we sought to explore whether they are able to combine visual and tactile sensory information about the orientation of gratings: if they do combine these signals, does the combination bring about an enhancement in their perceptual decision making? Finally, what are the neuronal underpinnings

of these unimodal and multimodal decisions?

In order to perform the task, rats had to establish multimodal perceptual boundaries (one about 45-degree and another about 135-degree) and according to these boundaries categorize the presented orientation. Rats learn to recognize the critical feature of a simple object (its orientation) and they must form knowledge about how the properties of the object predict reward location and must do so irrespective of sensory modality.

In this behavioral design, the two sensory systems explore the visual and/or tactile aspects of a single object, rendering the stimulus more ethologically relevant. Importantly, our task involved not abstract, unnatural computer-generated stimuli, but instead a real object that could be seen and felt. We believed that the attribution of sensory properties to a real thing might leverage the key functions of neocortex and thus might bring us to interesting observations on cortical processing (Introduction, section 1.5).

Vision and touch likely could be effortlessly integrated since both modalities have *evolved* and *developed* to explore the shape, form and spatial properties of the environment. In other words, the statistics of the stimuli that are processed by both systems are similar. In both modalities, information about stimulus is extracted from a spatiotemporal pattern of activation across a sensory sheet (the retina and the skin or whiskers). Such natural coherence across modalities stands apart from other cases; for instance the visual shape of an object provides no prediction about its odor. Sensory information extracted from touch and vision might be represented in a common language that allows the two sensory modalities to be integrated and mutually re-calibrated (Pack and Bensmaia, 2015).

Nevertheless, a caveat of such "naturalistic" stimuli is the difficulty in controlling the subjects' interaction with the stimuli. This makes quantification of neuronal responses to the stimuli, particularly in the primary sensory areas, challenging. The neurophysiological investigation in the current project is not aimed at characterizing the neuronal coding of the stimuli at the level of primary sensory cortices (i.e. primary visual cortex and primary somatosensory cortex). However, future experiments with

detailed head, eye and whisker kinematic tracking could be designed to attain this goal.

When interpreting the relevant functional role of visual-somatosensory integration in rats, it is also important to note that vision and touch typically have different time scales (Lippert et al., 2013). While visual information is informative of global information about the environment (Meaney and Stewart, 1981) whisker-related information relates to object contact in the immediate surrounding and changes on a very fast time scale (Montemurro et al., 2007). Therefore, in the rat, visual information can potentially provide a "context" within which whisker-related information is interpreted (Lippert et al., 2013).[1] Signals reach the barrel cortex as early as 5 ms after whisker deflection, whereas visual signal reach the cortex some 40 ms after photoreceptor excitation.

[1] Different timescales are not only due to the difference in sampling frequency of each of these "active" sensory systems but also the presumably slower visual processing compared with faster tactile stimulus processing.

While the primary focus of the study was multimodal integration in behavior and in neuronal coding, the experiments unexpectedly opened up a related area of interest based upon a novel measure of the rat's behavioral output—it's licking frequency. We found that licking may be a window through which to view the rat's certainty in collecting a delayed reward (Behavioral results, section 4.4).

6.1.1 Learning the categorization task and effects of training

In our experiment, training the rats first on the multisensory condition (in the canonical training scheme, detailed in section 2.2.1) allowed them to form a multimodal percept of the stimulus with cardinal orientations (0 and 90 degrees) as exemplars of the two categories (horizontal vs. vertical). This initial multimodal training resembles natural stimulus learning, which might explain the fast training with superior performance[2]. After a short initial multimodal training (2–5 sessions, variable between subjects), when rats encountered unimodal trials, the number of trials in all three modalities were equated. Most importantly, rats could recognize the object and apply the rules of the task on *first* exposure to visual and tactile

[2] In contrast to the random modality training which could take about three to five weeks.

conditions, suggesting that the multimodal percept corresponds to that of the single modalities.

Horizontal and vertical might be innately salient categories with functional significant in the rats' experience. Their cage bars and lids are vertical and horizontal. An interesting question for future investigation is whether learning and performance would be comparable in case of a truly arbitrary boundary, e.g. 60 degrees.

In addition, since in the initial stages of training (stages 2–5), rats were exposed only to the cardinal orientations, their performance on the full range of orientations could not result directly from the training they received; rather they were able to generalize the category rule to the whole range of orientations in all the modalities instantaneously[3]. Of course, rats gradually improved in the categorization, as reflected by the increasing steepness as well as the disappearance of any bias in the mean (PSE) of the psychometric curves (Fig. 4.1.2)[4].

Is the observed multisensory enhancement affected by the training protocol? In order to investigate this, we trained a set of four rats with a different protocol (section 2.2.2): we presented them with randomly interleaved trials of unimodal and bimodal conditions with equal probability from the *beginning* of their training. Although learning to categorize the cardinal orientations in this protocol was more difficult for the rats compared with the canonical protocol and took ~3–5 weeks of training,[5] there were no significant differences observed between the magnitude of multisensory enhancement or discrimination capability of these rats compared to the ones trained on the canonical protocol.

6.1.2 Whisker-mediated orientation discrimination in rats

Our behavioral data demonstrate that rats are systematically able to perform orientation discrimination using their whiskers. Previously, Polley et al. (2005) reported whisker-dependent orientation discrimination using a rapid learning procedure based on fear conditioning in a Y-maze task. In their experiment, unlike ours, it was not possible to characterize the

[3] Although it is possible that rats initially develop a particular strategy to solve the task, preferring one modality and giving more weight to its signal, similarity of performance on bimodal trials seems to suggest they eventually converge to a similar strategy in solving the task after training.

[4] In addition it should be noted that the initial training comprised just ~600–2100 trials, a negligible number compared to the rest of the training over many months giving rise to a data set of ~70,000 trials for each rat.

[5] This was probably because discovering the rule of the task and stimulus/reward contingencies was more complex. Rats had to learn to exclude stimulus modality (e.g. absence or presence of the light and transparent panel) from the orientation discrimination rule (Fig. 2.2.3).

rat's ability by psychophysical measures. The stimulus set was limited to 0 and 90 degrees orientations and the trial count was 1. (Rats learned to escape from the Y-maze arm whose walls were covered with pegs of a given orientation.) How rats achieve object orientation discrimination is beyond the scope of the current project. However, a preliminary analysis of accelerometer data as well as 3D tracking of head movements (data not shown) and careful examination of high-speed video recordings, seem to suggest that they begin the trial with a fast, stereotypical head trajectory towards the stimulus,[6] once they reach the stimulus they feel the gratings with protracted macro vibrissae, without cyclical whisking, while moving their head to the side. Through a "slide-or-collide" tactile strategy, they seem to solve the tactile task by feeling a high degree of resistance when generating later motion against vertically oriented bars (collide), a low degree of resistance when generating later motion against horizontally oriented (slide), and some intermediate degree of resistance for diagonal. This suggests a simple firing-rate based code in the barrel cortex for object orientation. Of course it is simplistic to think that only tactile and/or visual signals contribute in this task. With careful exclusion of olfaction (see section 2.4), rats probably combined vestibular and proprioceptive signals to calibrate their whisker/head centered coordination and resolve reference-frame transformations.

[6] This stereotypical head movement resembles ballistic movements.

6.1.3 Rats have different unimodal capacities but very similar bimodal performance

Under the default lighting conditions, individual rats showed differing categorization capacities in the unimodal conditions; some were better in tactile-only trials, and some better in vision-only trials. Most rats however had superior performance in vision-only trials. This finding was surprising, since rats are often regarded as being "tactile animals" with poor vision. However, performance was always highest in the bimodal condition, indicating multisensory enhancement. The individual variability could arise from genetic and developmental differences among rats as well as different

strategies in solving the task: to a large extent rats were free to choose how to interact with the stimuli.

Multisensory enhancement increases the reliability of perceptual judgments and the perceptual signal-to-noise ratio especially when the stimuli are noisy, ambiguous or weak (Stein and Stanford, 2008). We observed the maximum enhancements in trials with the highest ambiguity (around category boundaries). This is an important aspect of the experiment as the stimulus object provides the opportunity to parametrize the sensory features (i.e. orientation) and allows for manipulating the ambiguity of the stimulus systematically. The ambiguity of the stimulus corresponds to the task difficulty and animal's performance in difficult trials can better reflect the effects of multisensory integration.

The current task design lends itself to rigorous psychophysical analysis. The psychometric function relates rats' performance to an independent variable (stimulus orientation) and describes animals' response thresholds and the rate within which performance improves as a function of orientation in each modality (Wichmann and Hill, 2001). The slope of this curve describes the change in performance of rats as a function of the change in orientation, hence it is a quantitative measure of the performance of rats at each orientation. Although rats received equal number of trials in every modality and in all orientations, the increase in maximum slope at the inflection point of the curve demonstrates performance improvement in bimodal condition.

Psychometric analysis allowed us to systematically measure (and manipulate) animals' psychophysical threshold (see section 2.1) and point of subjective equality (see section 4 and Fig. 2.1.5).

6.2 Is the multisensory enhancement optimal with respect to the best linear combination?

We used the measured thresholds, defined as the standard deviation, σ, of the fitted cumulative Gaussian psychometric curves in each unimodal condition to compute the predicted multisensory thresholds expected by opti-

mal integration in the framework of Bayesian cue combination. We found that most rats combine visual and tactile information better than predicted by the standard ideal-observer model (maximum likelihood prediction). For the sake of discussion we refer to this deviation from optimal prediction as "supra-optimality".

Two additional computational analyses confirmed these findings: probabilities of independent events and summation of mutual information for each sensory channel (see behavioral results in chapter 4).

Previous studies have reported supra-optimal behavior (Fetsch et al., 2012, 2009; Kiani et al., 2013; Raposo et al., 2012). Raposo et al. (2012) argued that one cause of supra-optimality might be the fact that performance on unimodal trials provides an imperfect estimate of that modality's reliability which could lead to an underestimate of reliability under unimodal conditions. They attributed the underestimate to motivational reasons: rats are sensitive to overall reward rate, and unimodal trials yield lower average reward rates compared with multisensory ones. Therefore animals might have decreased motivation on those trials especially when the trials with different modalities are interleaved. In a bounded evidence accumulation framework, subjects could adjust their expected evidence accumulation according to the more salient bimodal trials and would therefore under-perform in unimodal trials by truncating the processing of the unimodal stimuli prematurely (Kiani et al., 2013, 2008). In other words, uncertain of the benefit to be gained on such trials, the animal may give priority to speed over accuracy (Drugowitsch et al., 2015, 2014).

We sought to investigate this possibility by testing a group of trained rats on a block design where unimodal and bimodal trials were *not* interleaved. We collected data from blocks of seven subsequent sessions of unimodal trials followed by seven sessions of bimodal trials separately (i.e. 3 blocks of 7 session length for each of the conditions). Our hypothesis was that this protocol could minimize the motivational effects by forcing the rats to their unimodal or bimodal perceptual limits in each block. Then the psychophysical thresholds were computed as before and compared to the prediction of models. Although the unimodal and multimodal performance

slightly improved (compared to the data collected from these rats before the block experiment–data not shown), the supra-optimality was still observed, just as in the interleaved condition.

A basic assumption of the cue-combination framework described here is independence of the sensory channels. A possible explanation for the deviations from predictions of optimality is that vision and touch signals might not be completely independent in bimodal trials. In other words, one signal might affect how the other is *acquired*, *represented* or *processed* to a decision in the brain. This would in turn decrease (or increase) the variance (hence increase (decrease) the reliability) of the unimodal signals in the the bimodal condition accounting for a performance that is better (worse) than optimal prediction (Fig. 6.2.1, dashed lines). In terms of information theory, two sensory systems that do not encode information independently can be either synergistic, meaning that they convey more information in their joint responses than the sum of their individual information, or redundant, meaning that they jointly convey less. Therefore by measuring synergy, a measure of information independence, we could study the independence of sensory channels (Schneidman et al., 2003).

It is possible that rats acquire tactile and/or visual signals more efficiently when they are presented simultaneously. For instance rats might feel the gratings with their whiskers differently in the presence of visual stimulus, rendering visually guided touching more informative about stimulus angle than the tactile condition alone. Ongoing video recordings and accelerometer measurements could help us examine this possibility (Illustrated as blue dashed lines in Fig. 6.2.1-b–c).

Another intriguing possibility is that stimulus information in one early sensory area is augmented in the presence of other sensory modalities. The question of the contribution of primary sensory areas in multisensory integration has been debated over the past decade and remains open. There have been attempts to elucidate the contribution of these areas in the integration of sensory input; for example Iurilli et al. (2012) measured inhibitory responses to sensory stimuli from multiple modalities in primary sensory cortices of mice. In another study, Lemus et al. (2010) tried to

find out whether primary and secondary somatosensory cortices (S1, S2) encode auditory stimuli and/or primary auditory cortex (A1) encodes vibration to fingertip in monkeys. They presented monkeys with flutters of auditory clicks and vibrations on the fingertip in a match to sample task. In A1 and S1 they could not find encoding of the stimuli from a non-specific modality, but neurons in S2 showed activation when acoustic stimuli were present and also in the decision period. Their result suggests that the encoding of auditory rate does not happen as early as S1; however, these effects start to become apparent in S2. This and similar results do not rule out a potential contribution of primary sensory areas in multimodal integration altogether, since these effects might happen by alteration of attentional selection and/or excitability of local networks (Lakatos et al., 2009). Inhibition across cortical regions could allow one modality to suppress the non-specific noise in the other modality's cortical representation, leading to improved coding in the paired modality (Iurilli et al., 2012). Moreover, by reducing the trial-to-trial variability of responses, multisensory integration can increase the reliability and information carrying capacity of sensory representations in early sensory cortices (Kayser et al., 2010).

Nevertheless, it has been shown that there are higher numbers of multisensory neurons in association areas compared to primary sensory areas (Ghazanfar et al., 2005; Kayser et al., 2010, 2005, 2008; Schroeder and Foxe, 2002). The parcellation of neocortex allows for processing of information in various primary areas and into their bordering areas that bear a bigger number of multisensory neurons (Wallace et al., 2004). For example, Lippert et al. (2013) and colleagues found supra/sub-linear interactions between visual and somatosensory stimulation in the parietal association area of rats, which is located between the V1 and S1, as S2 lies between the S1 and A1, where Lemus et al. (2010) found neuronal response to the auditory flutter stimuli. Furthermore, visual stimulus-induced reset of ongoing neuronal oscillations and power modulation of the activity in S1 critically depend on the communication between primary sensory cortices (Sieben et al., 2013).

The study of multisensory neural processing in early sensory areas is po-

tentially interesting in our task and could provide insight into the supra-optimal behavior. Both direct connections between sensory specific areas and modulatory feedback from multisensory regions are likely to contribute to the behavior of rats (Iurilli et al., 2012; Olcese et al., 2013). Top-down modulatory influences might be important for spatially specific cross-modal links. These processes include cognitive factors such as decision making that are expected to engage control systems in frontal and parietal cortices. Direct connections between the early visual and tactile areas might be responsible for faster, but less specific cross-modal effects in sensory-specific areas (Macaluso, 2006).

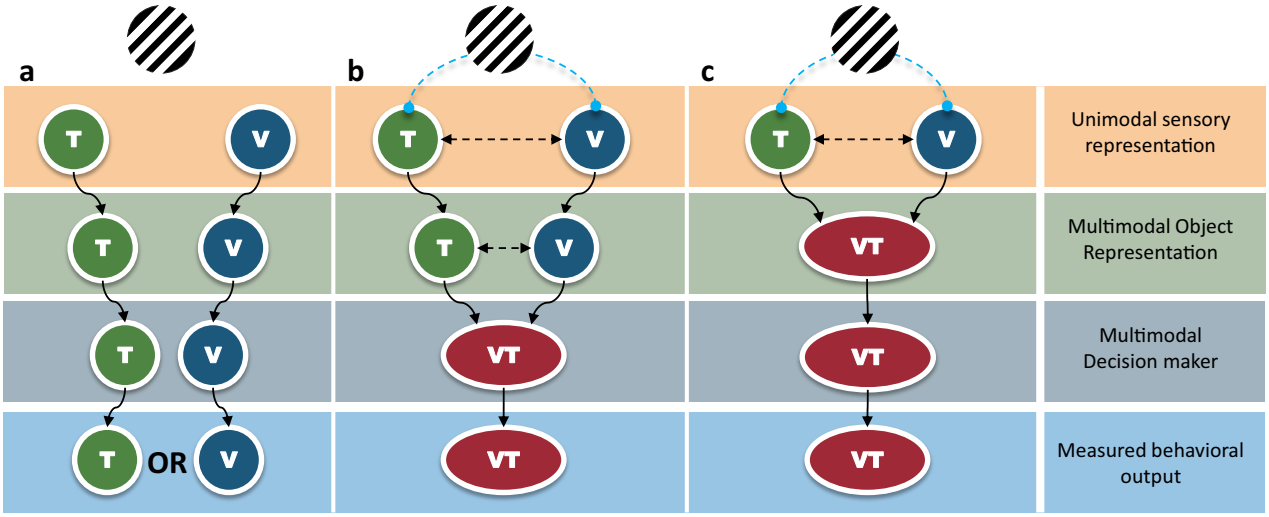

Figure 6.2.1: Results of our experiments would shed light on the possible schemes for the multisensory integration in this task: (a) Sensory cues are not integrated across modalities and therefore lead to independent behavioral outputs. In this case multisensory enhancement would not be expected and behavioral output will be "captured" by a preferred modality on any given trial. (b) Sensory cues are not integrated to form a multimodal representation but nonetheless lead to similar decisions and behavioral output regardless of the type of input due to convergence on a multimodal decision maker (c) Sensory cues are integrated in multisensory areas and form a supra-modal percept; they then would naturally lead to a similar behavioral output. The distinction between (b) and (c) could be made by neurophysiological evidence. Black dashed lines indicate possible cross-modal interactions in the brain. Blue dashed lines indicate sensory-motor interactions affecting the acquisition of sensory stimulus. Arrows indicate flow of information.

6.3 Posterior parietal cortex is involved in the task and encodes modality shared representations

6.3.1 PPC encodes animals' decisions

The neuronal substrates of multisensory integration were first addressed in the classical studies of Stein et al. in the 1980s with the discovery of neurons with receptive fields that encompass two or more modalities. Previous work has shown that rats require neocortical processing to accomplish the tactile and visual components of our task (Guic-Robles et al., 1992; Petruno et al., 2013; Von Heimendahl et al., 2007). Many cortical areas have been suggested to be involved in the multisensory integration and decision making. Indeed such interactions were observed in association areas such as primate MSTd[7] (Gu et al., 2008), rats' postero-lateral neocortex (Wallace et al., 2004), lateral and posterior parietal areas (Andersen, 1997; Lippert et al., 2013; Raposo et al., 2014) and prefrontal areas (Fuster et al., 2000; Graziano et al., 1994) as well as primary sensory areas (Iurilli et al., 2012).

[7] Dorsal medial superior temporal area.

As discussed in section 1.6, the rat posterior parietal cortex (PPC)[8], receives input from cortical areas representing all main sensory modalities and communicates back to these domains as well (Cavada and Goldman-Rakic, 1989; Leichnetz, 2001; Miller and Vogt, 1984). It is strongly and reciprocally connected to almost all of the other multimodal association cortices, such as prefrontal, frontal, temporal, and limbic association cortex as well as motor and premotor areas of the cortex (Akers and Killackey, 1978; Reep et al., 1994).

[8] In this thesis the definition of PPC is primarily based on and restricted to stereotaxic coordinates.

PPC is well positioned to embody essential neural mechanisms for decision making in rodents. Its strong connections to the primary sensory areas makes it a suitable candidate site for multisensory integration (Kolb and Walkey, 1987; Reep et al., 1994). It has also been shown to be involved in navigation and locomotion (Nitz, 2012; Whitlock et al., 2008). It has been shown that neurons in the PPC ramp up their activity during accumulation of sensory evidence (Hanks et al., 2015).

Based on the anatomical, functional and connectivity evidence we sought to first investigate the neuronal responses of PPC. We recorded PPC neurons while rats performed the orientation categorization task. We found that neurons in PPC exhibit two general categories of response patterns. A class of neurons (51.2%) carried a significant signal about decisions of rats in their discharge rate in a categorical manner. The activity of such neurons did not seem to be modulated by a specific stimulus angle but by the category to which the stimulus belonged. Another class of neurons (40.7%) showed a coding of the stimulus in a graded manner. The activity of these neurons was monotonically modulated by the stimulus angle and was either negatively or positively correlated with increasing stimulus angle (0–90 degrees). Because stimulus angle is correlated with perceptual ambiguity, it could be the strength of the category signal that is represented in a graded manner. In this sense, these neuronal response profiles are similar to those found in monkey PPC during visual motion discrimination tasks (Kiani and Shadlen, 2009; Roitman and Shadlen, 2002; Shadlen and Newsome, 2001), suggesting that PPC in rats and monkeys may share similar roles in decision formation. Since the population of PPC neurons expresses activity ranging from strongly stimulus-related (e.g. graded in relation to stimulus orientation) to strongly choice-related (e.g. modulated by stimulus category but not by orientation within a category) we suggest that this region in rat brain is involved in the percept-to-choice transformation (Fig. 6.2.1-c).

Using a simple ROC decoder we constructed neurometric functions for neurons. The resulting functions describe the probability that an ideal observer could accurately categorize the orientation of the stimulus by exercising a precise decision rule and operating that rule using neuronal responses. Comparing the maximum slopes of neurometric curves in different modalities revealed similar relationships between the sensitivity of "categorical" neurons and the psychophysical sensitivity (behavioral acuity) of rats—higher performance in a modality was correlated with the higher slope of the neurometric function.

6.3.2 PPC responses are supra-modal

Using ROC analysis, information theory and linear regression we sought to examine the effect of the animal's choice and stimulus modality on the neuronal responses during the task (Neuronal results, section 5.2). All of these analyses suggest that PPC responses are highly selective for the choices of the animals but only slightly for stimulus modality (throughout the task). This result differs from a previous report by Raposo et al. (2014) that rat PPC is strongly modulated by stimulus modality. One possibility is that PPC is only encoding the correlates of decisions irrespective of sensory modality that led to the decision formed. Another possibility for the observed modality independence could be the nature of the stimuli in our task. As discussed at the beginning of this chapter, the statistics of the stimuli that are processed by touch and vision are similar. Similar representation of the grating stimuli in both modalities could arise from a modality-shared feature of the stimulus shape, the orientation of gratings. The invariance of neuronal activity to modality could indicate abstraction of stimuli from sensory domains–an essential feature of conceptual knowledge.

7 Appendix

7.1 Appendix 1: The relationship between the psychophysical threshold and variance of the psychometric function

The discrimination threshold is defined as the difference between the PSE (abscissa of 50% point) and the value of the stimulus when it is judged ~84% of the time as one category. The 84% point roughly corresponds to $\sqrt{2}$ times the standard deviation of the underlying estimator (which we assumed is Gaussian: $N \sim (\mu, \sigma)$). The bigger the value of σ, the smaller is the slope and the bigger the threshold, because:

$$reliability = \frac{1}{\sigma^2} \tag{7.1}$$

In more mathematical terms, we can assume that F is an error function that describes the performance of the underlying psychological mechanism of

interest. Now, while slope is F' (1st derivative) of the Gaussian CDF at each performance point (like F'_{50}), the threshold is the inverse of F at some particular performance level (like F^{-1}_{50}) (Wichmann and Hill, 2001). Now, the inverse of the cumulative distribution function (The quantile function or the probit function) for a normal random variable with mean μ and variance σ^2 is:

$$F^{-1}(p) = \mu + \sigma\sqrt{2}erf^{-1}(2p-1), p \in (0,1). \tag{7.2}$$

For $p = 0.84$ it turns out that $F^{-1}_{84} = \sigma$ which roughly corresponds to the stimulus value at 84% performance. Why 84? Because it corresponds to $1\sigma(50 + 34.1)$ point in the CDF. Which makes sense if we do the calculation:

$$F^{-1}_{84} = \mu + \sigma\sqrt{2}erf^{-1}(2 \times 0.841 - 1) = \mu + \sigma \tag{7.3}$$

Since:

$$\sqrt{2}erf^{-1}(2 \times 0.841 - 1) = 0.999 \cong 1 \tag{7.4}$$

Therefore, σ is taken as the threshold—the difference between the PSE and the orientation of the stimulus when it is judged vertical with probability ~0.84.

7.2 Appendix 2: Micro-Lesioning With TDT Arrays

We empirically determined guidelines for microlesioning techniques to localize individual electrode sites via histology. The following equation normalizes for site area, current, and time to yield an optimal charge density for microlesions[1]:

$$\frac{\mu A \cdot sec}{\mu m^2} = 0.056 \mu C/\mu m^2 \tag{7.5}$$

[1] Based on: http://neuronexus.com/images/TechNotes/niPOD_Microlesioning.pdf

For the TDT probes these values could be calculated like the following: for 33 μm arrays with angle of cut 45 deg:
Aprroximate diameter of the cut surface:

$$D_{tip} = \frac{33 \mu m}{cos(45)} \simeq 46.6 \mu m \tag{7.6}$$

Assuming the cross section is an ellipse:

$$Area_{tip} = \frac{46.6 \times 33 \times \pi}{4} \simeq 1207 \mu m^2 \tag{7.7}$$

according to equation 7.5

$$1207 \mu m^2 \times .056 \mu C/\mu m^2 = \mu A \cdot sec \tag{7.8}$$

So in this example one could lesion with ~9.5 μA current for ~7 sec. We kept the stimulation time under 15 seconds.

Using a NanoZ microstimulator (Neuralynx) we performed DC electroplattion, with plating current and duration according to the calculations explained above or using the table 7.2.1.

Wire Diameter	Angle of cut	Duration	Current
$33\mu m$	0 (blunt)	7 s	$6.8\mu A$
$33\mu m$	30 deg	7 s	$7.9\mu A$
$33\mu m$	45 deg	7 s	$9.5\mu A$
$33\mu m$	60 deg	7 s	$13.5\mu A$
$50\mu m$	0 (blunt)	7 s	$15.7\mu A$
$50\mu m$	30 deg	7 s	$18\mu A$
$50\mu m$	45 deg	10 s	$15.5\mu A$
$50\mu m$	60 deg	10 s	$21\mu A$

Table 7.2.1: Example values for lesioning, using different TDT arrays.

7.3 Appendix 3: Performance of rats in control condition

During each session as control catch trials (comprising 4 percent of trials) rats could not see nor touch the stimulus—the transparent panel was put in front of the stimulus and lights were off. The expected performance on these trials is one that is at chance (50% performance). The main purpose of catch trials was to determine whether rats are using sensory cues irrelevant to the conditions in the task. Most importantly we had to make sure that the tactile-only condition involved complete darkness. Black curve in figure 7.3.1 shows the average performance of rats in control conditions which is at chance. However, these control trials led to the discovery that Long-Evans rats are capable of discriminating a high-contrast black and white visual stimulus under narrow-band (almost monochromatic) red LEDs. This finding contradicts to the common belief that laboratory rats cannot see under red light (Blue curve in Fig. 7.3.1).

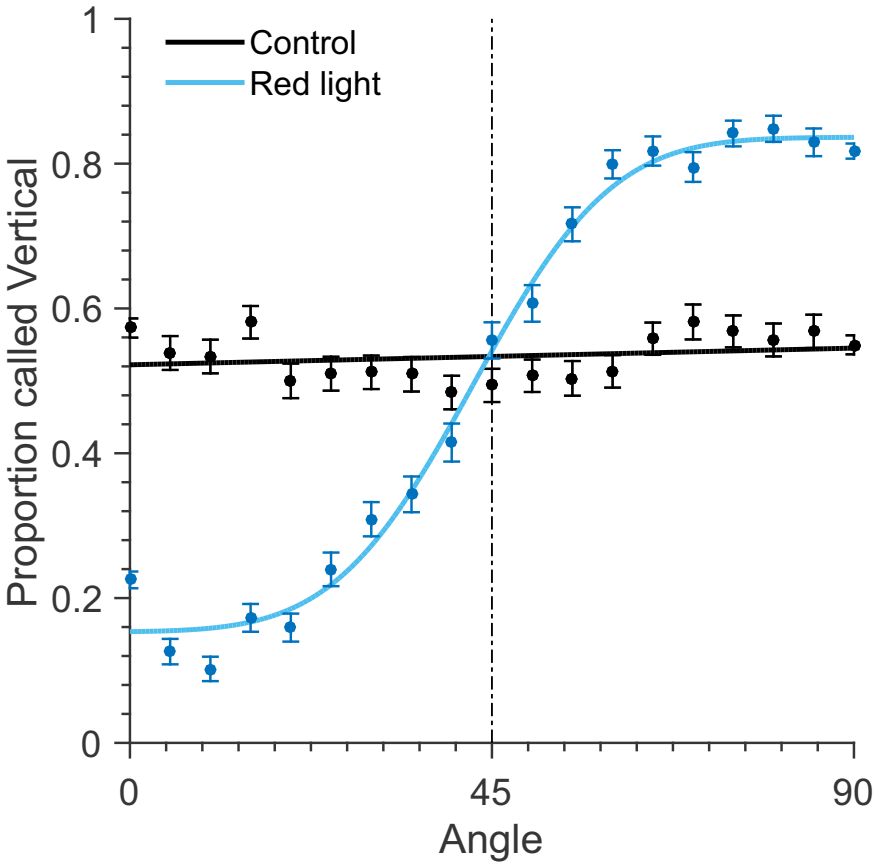

Figure 7.3.1: Performance of rats on catch trials (black) compared to the one under narrow-band (almost monochromatic) red LEDs (blue).

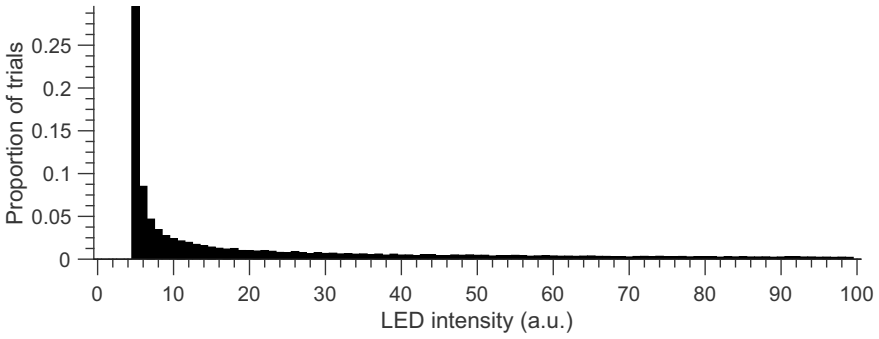

Figure 7.4.1: Distribution of visual stimulus brightness intensity taken randomly from a gamma distribution.

7.4 Appendix 4: Equating visual and tactile performance

Quantifying rats performance in all modalities, we found that rats had good orientation acuity using their whiskers and snout (T condition); however under our default conditions, typically performance was superior by vision (V condition). Using pulse-width modulation (Behavioral methods 2), illumination of the stimulus could be adjusted to render V and T performance (hence, reliability) equivalent. On each trial we sampled the intensity values of LED brightness in visual and bimodal conditions randomly from a gamma distribution (Fig. 7.4.1). Then a Matlab algorithm was used to search for the intensity threshold of visual trials that would render the performance of each rat equal to tactile trials[2]. Independently of whether V and T performance was made equivalent, performance was found to be always highest in the VT condition, indicating multisensory enhancement (Fig. 7.4.2).

[2] Only rats with superior visual performance were used in these experiments.

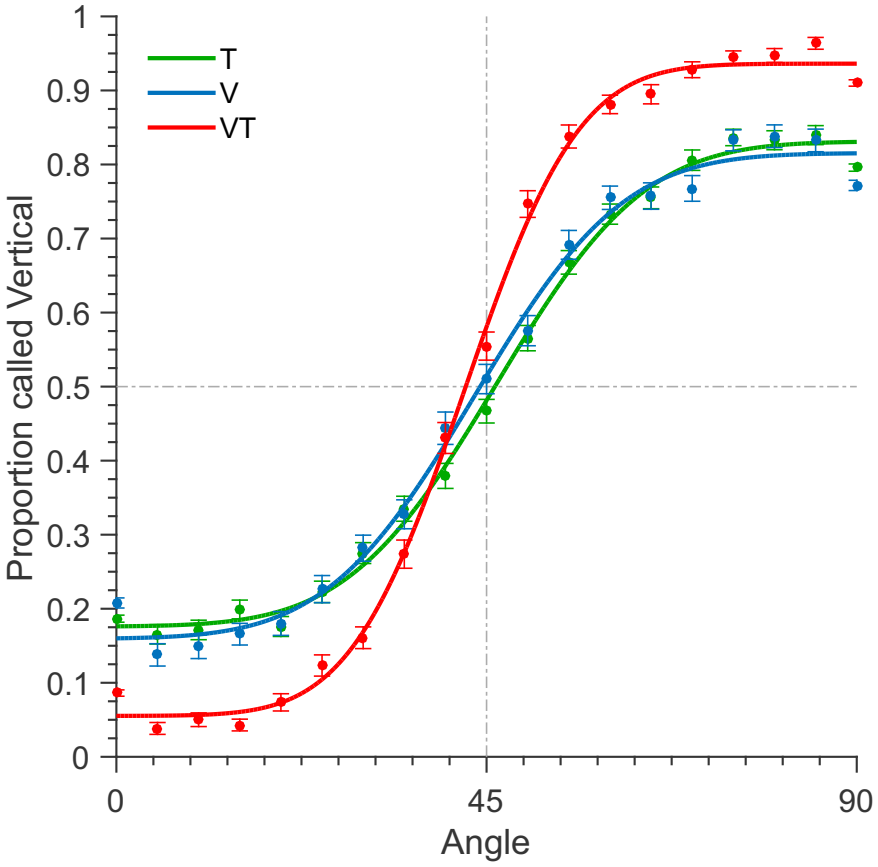

Figure 7.4.2: Equalized psychometric performance on visual and tactile trials by pulse-width modulation of visual stimulus illumination. Data averaged across 4 rats.

References

Abbott, A. (2010). Neuroscience: The rat pack. *Nature News*, 465(7296):282–283.

Adrian, E. (1928). *The Basis of Sensation: The Action of the Sense Organs*. O-P books. Christophers.

Akers, R. M. and Killackey, H. P. (1978). Organization of corticocortical connections in the parietal cortex of the rat. *journal of Comparative Neurology*, 181(3):513–537.

Alais, D. and Burr, D. (2004). The ventriloquist effect results from near-optimal bimodal integration. *Current biology*, 14(3):257–262.

Allman, J. M. (2000). *Evolving brains*. Scientific American Library New York.

Andersen, R. A. (1997). Multimodal integration for the representation of space in the posterior parietal cortex. *Philosophical Transactions of the Royal Society B: Biological Sciences*, 352(1360):1421–1428.

Andersen, R. A. and Cui, H. (2009). Intention, action planning, and decision making in parietal-frontal circuits. *Neuron*, 63(5):568–583.

Angelaki, D. E., Gu, Y., and DeAngelis, G. C. (2009). Multisensory integration: psychophysics, neurophysiology, and computation. *Current opinion in neurobiology*, 19(4):452–458.

Angelaki, D. E., Shaikh, A. G., Green, A. M., and Dickman, J. D. (2004). Neurons compute internal models of the physical laws of motion. *Nature*, 430(6999):560–564.

Astur, R. S., Klein, R. L., Mumby, D. G., Protz, D. K., Sutherland, R. J., and Martin, G. M. (2002). A role for olfaction in object recognition by normal and hippocampal-damaged rats. *Neurobiology of learning and memory*, 78(1):186–191.

Barnett, S. A. (2007). *The rat: A study in behavior*. Transaction Publishers.

Battaglia, P. W., Jacobs, R. A., and Aslin, R. N. (2003). Bayesian integration of visual and auditory signals for spatial localization. *JOSA A*, 20(7):1391–1397.

Birch, D. and Jacobs, G. H. (1979). Spatial contrast sensitivity in albino and pigmented rats. *Vision research*, 19(8):933–937.

Birdwell, J. A., Solomon, J. H., Thajchayapong, M., Taylor, M. A., Cheely, M., Towal, R. B., Conradt, J., and Hartmann, M. J. (2007). Biomechanical models for radial distance determination by the rat vibrissal system. *Journal of Neurophysiology*, 98(4):2439–2455.

Bisley, J. W. and Goldberg, M. E. (2010). Attention, intention, and priority in the parietal lobe. *Annual review of neuroscience*, 33:1.

Bizley, J. K., Nodal, F. R., Bajo, V. M., Nelken, I., and King, A. J. (2007). Physiological and anatomical evidence for multisensory interactions in auditory cortex. *Cerebral cortex*, 17(9):2172–2189.

Bonin, V., Histed, M. H., Yurgenson, S., and Reid, R. C. (2011). Local diversity and fine-scale organization of receptive fields in mouse visual cortex. *The Journal of neuroscience*, 31(50):18506–18521.

Brecht, M., Preilowski, B., and Merzenich, M. M. (1997). Functional architecture of the mystacial vibrissae. *Behavioural brain research*, 84(1):81–97.

Britten, K. H., Shadlen, M. N., Newsome, W. T., and Movshon, J. A. (1992). The analysis of visual motion: a comparison of neuronal and psychophysical performance. *The Journal of Neuroscience*, 12(12):4745–4765.

Brunton, B. W., Botvinick, M. M., and Brody, C. D. (2013). Rats and humans can optimally accumulate evidence for decision-making. *Science*, 340(6128):95–98.

Burn, C. C. (2008). What is it like to be a rat? rat sensory perception and its implications for experimental design and rat welfare. *Applied Animal Behaviour Science*, 112(1):1–32.

Campbell, F. and Gubisch, R. (1966). Optical quality of the human eye. *The Journal of Physiology*, 186(3):558.

Carandini, M. and Churchland, A. K. (2013). Probing perceptual decisions in rodents. *Nature neuroscience*, 16(7):824–831.

Cavada, C. and Goldman-Rakic, P. S. (1989). Posterior parietal cortex in rhesus monkey: Ii. evidence for segregated corticocortical networks linking sensory and limbic areas with the frontal lobe. *Journal of Comparative Neurology*, 287(4):422–445.

Chen, G., King, J. A., Burgess, N., and O'Keefe, J. (2013). How vision and movement combine in the hippocampal place code. *Proceedings of the National Academy of Sciences*, 110(1):378–383.

Clarke, W. and Bowsher, D. (1962). Terminal distribution of primary afferent trigeminal fibers in the rat. *Experimental neurology*, 6(5):372–383.

Cover, T. M. and Thomas, J. A. (2012). *Elements of information theory*. John Wiley & Sons.

Cowles, J. and Pennington, L. (1943). An improved conditioning technique for determining auditory acuity of the rat. *The Journal of Psychology*, 15(1):41–47.

Daan, S., Spoelstra, K., Albrecht, U., Schmutz, I., Daan, M., Daan, B., Rienks, F., Poletaeva, I., Dell'Omo, G., Vyssotski, A., et al. (2011). Lab mice in the field: unorthodox daily activity and effects of a dysfunctional circadian clock allele. *Journal of Biological Rhythms*, 26(2):118–129.

Dawkins, R. (2010). *The ancestor's tale: A pilgrimage to the dawn of life*. Weidenfeld & Nicolson.

Dean, P. (1981). Grating detection and visual acuity after lesions of striate cortex in hooded rats. *Experimental brain research*, 43(2):145–153.

Deschênes, M., Timofeeva, E., Lavallée, P., and Dufresne, C. (2005). The vibrissal system as a model of thalamic operations. *Progress in brain research*, 149:31–40.

Diamond, M. E. (2010). Texture sensation through the fingertips and the whiskers. *Current opinion in neurobiology*, 20(3):319–327.

Diamond, M. E. and Arabzadeh, E. (2013). Whisker sensory system–from receptor to decision. *Progress in neurobiology*, 103:28–40.

Diamond, M. E., von Heimendahl, M., and Arabzadeh, E. (2008a). Whisker-mediated texture discrimination. *PLoS Biol*, 6(8):e220.

Diamond, M. E., von Heimendahl, M., Knutsen, P. M., Kleinfeld, D., and Ahissar, E. (2008b). 'where'and'what'in the whisker sensorimotor system. *Nature Reviews Neuroscience*, 9(8):601–612.

Dörfl, J. (1985). The innervation of the mystacial region of the white mouse: A topographical study. *Journal of anatomy*, 142:173.

Drugowitsch, J., DeAngelis, G. C., Angelaki, D. E., and Pouget, A. (2015). Tuning the speed-accuracy trade-off to maximize reward rate in multisensory decision-making. *eLife*, 4:e06678.

Drugowitsch, J., DeAngelis, G. C., Klier, E. M., Angelaki, D. E., and Pouget, A. (2014). Optimal multisensory decision-making in a reaction-time task. *eLife*, 3:e03005.

Ebara, S., Kumamoto, K., Matsuura, T., Mazurkiewicz, J. E., and Rice, F. L. (2002). Similarities and differences in the innervation of mystacial vibrissal follicle-sinus complexes in the rat and cat: a confocal microscopic study. *The Journal of comparative neurology*, 449(2):103–19.

Ernst, M. O. and Banks, M. S. (2002). Humans integrate visual and haptic information in a statistically optimal fashion. *Nature*, 415(6870):429–433.

Faisal, A. A., Selen, L. P., and Wolpert, D. M. (2008). Noise in the nervous system. *Nature Reviews Neuroscience*, 9(4):292–303.

Fassihi, A., Akrami, A., Esmaeili, V., and Diamond, M. E. (2014). Tactile perception and working memory in rats and humans. *Proceedings of the National Academy of Sciences*, 111(6):2331–2336.

Feierstein, C. E., Quirk, M. C., Uchida, N., Sosulski, D. L., and Mainen, Z. F. (2006). Representation of spatial goals in rat orbitofrontal cortex. *Neuron*, 51(4):495–507.

Fetsch, C. R., DeAngelis, G. C., and Angelaki, D. E. (2013). Bridging the gap between theories of sensory cue integration and the physiology of multisensory neurons. *Nature Reviews Neuroscience*, 14(6):429–442.

Fetsch, C. R., Pouget, A., DeAngelis, G. C., and Angelaki, D. E. (2012). Neural correlates of reliability-based cue weighting during multisensory integration. *Nature neuroscience*, 15(1):146–154.

Fetsch, C. R., Turner, A. H., DeAngelis, G. C., and Angelaki, D. E. (2009). Dynamic reweighting of visual and vestibular cues during self-motion perception. *The Journal of neuroscience*, 29(49):15601–15612.

Frens, M. A., Van Opstal, A. J., and Van der Willigen, R. F. (1995). Spatial and temporal factors determine auditory-visual interactions in human saccadic eye movements. *Perception & Psychophysics*, 57(6):802–816.

Fuster, J. M., Bodner, M., and Kroger, J. K. (2000). Cross-modal and cross-temporal association in neurons of frontal cortex. *Nature*, 405(6784):347–351.

Gaffan, E., Healey, A., and Eacott, M. (2004). Objects and positions in visual scenes: effects of perirhinal and postrhinal cortex lesions in the rat. *Behavioral neuroscience*, 118(5):992.

Gepshtein, S. (2010). Two psychologies of perception and the prospect of their synthesis. *Philosophical Psychology*, 23(2):217–281.

Ghazanfar, A. A., Maier, J. X., Hoffman, K. L., and Logothetis, N. K. (2005). Multisensory integration of dynamic faces and voices in rhesus monkey auditory cortex. *The Journal of Neuroscience*, 25(20):5004–5012.

Ghazanfar, A. A. and Schroeder, C. E. (2006). Is neocortex essentially multisensory? *Trends in cognitive sciences*, 10(6):278–285.

Girman, S. V., Sauvé, Y., and Lund, R. D. (1999). Receptive field properties of single neurons in rat primary visual cortex. *Journal of Neurophysiology*, 82(1):301–311.

Gold, J. I. and Shadlen, M. N. (2007). The neural basis of decision making. *Annu. Rev. Neurosci.*, 30:535–574.

Gourevitch, G. (1965). Auditory masking in the rat. *The Journal of the Acoustical Society of America*, 37(3):439–443.

Gourevitch, G. and Hack, M. H. (1966). Audibility in the rat. *Journal of Comparative and Physiological Psychology*, 62(2):289.

Graziano, M. S., Yap, G. S., and Gross, C. G. (1994). Coding of visual space by premotor neurons. *SCIENCE-NEW YORK THEN WASHINGTON-*, pages 1054–1054.

Green, D. and Swets, J. (1966). *Signal Detection Theory and Psycophysics*. John Wiley & Sons.

Gu, Y., Angelaki, D. E., and DeAngelis, G. C. (2008). Neural correlates of multisensory cue integration in macaque mstd. *Nature neuroscience*, 11(10):1201–1210.

Guic-Robles, E., Jenkins, W. M., and Bravo, H. (1992). Vibrissal roughness discrimination is barrelcortex-dependent. *Behavioural brain research*, 48(2):145–152.

Hanks, T. D., Kopec, C. D., Brunton, B. W., Duan, C. A., Erlich, J. C., and Brody, C. D. (2015). Distinct relationships of parietal and prefrontal cortices to evidence accumulation. *Nature*, 520(7546):220–223.

Harris, J. A., Petersen, R. S., and Diamond, M. E. (1999). Distribution of tactile learning and its neural basis. *Proceedings of the National Academy of Sciences*, 96(13):7587–7591.

Harvey, C. D., Coen, P., and Tank, D. W. (2012). Choice-specific sequences in parietal cortex during a virtual-navigation decision task. *Nature*, 484(7392):62–68.

Harvey, M., Roberto, B., and Zeigler, H. P. (2001). Discriminative whisking in the head-fixed rat: optoelectronic monitoring during tactile detection and discrimination tasks. *Somatosensory & motor research*, 18(3):211–222.

Heffner, H. E., Heffner, R. S., Contos, C., and Ott, T. (1994). Audiogram of the hooded norway rat. *Hearing research*, 73(2):244–247.

Hut, R. A., Pilorz, V., Boerema, A. S., Strijkstra, A. M., and Daan, S. (2011). Working for food shifts nocturnal mouse activity into the day. *PLoS One*, 6(3):e17527.

Iurilli, G., Ghezzi, D., Olcese, U., Lassi, G., Nazzaro, C., Tonini, R., Tucci, V., Benfenati, F., and Medini, P. (2012). Sound-driven synaptic inhibition in primary visual cortex. *Neuron*, 73(4):814–828.

Jacobs, R. A. (1999). Optimal integration of texture and motion cues to depth. *Vision research*, 39(21):3621–3629.

Jamison, J. H. (1951). Measurement of auditory intensity thresholds in the rat by conditioning of an autonomic response. *Journal of comparative and physiological psychology*, 44(2):118.

Jenks, R. A., Vaziri, A., Boloori, A.-R., and Stanley, G. B. (2010). Self-motion and the shaping of sensory signals. *Journal of neurophysiology*, 103(4):2195–2207.

Jerison, H. (2012). *Evolution of the Brain and Intelligence*. Elsevier.

Jezek, K., Henriksen, E. J., Treves, A., Moser, E. I., and Moser, M.-B. (2011). Theta-paced flickering between place-cell maps in the hippocampus. *Nature*, 478(7368):246–249.

Jung, R. (1984). *Sensory research in historical perspective: Some philosophical foundations of perception*. Wiley Online Library.

Kaas, J. (2010). The evolution of neocortex from early mammals to humans. *International Journal of Developmental Neuroscience*, 28(8):648.

Kayser, C., Logothetis, N. K., and Panzeri, S. (2010). Visual enhancement of the information representation in auditory cortex. *Current Biology*, 20(1):19–24.

Kayser, C., Petkov, C. I., Augath, M., and Logothetis, N. K. (2005). Integration of touch and sound in auditory cortex. *Neuron*, 48(2):373–384.

Kayser, C., Petkov, C. I., and Logothetis, N. K. (2008). Visual modulation of neurons in auditory cortex. *Cerebral Cortex*, 18(7):1560–1574.

Keller, J., Strasburger, H., Cerutti, D. T., and Sabel, B. A. (2000). Assessing spatial vision—automated measurement of the contrast-sensitivity function in the hooded rat. *Journal of neuroscience methods*, 97(2):103–110.

Kelly, J. B. and Masterton, B. (1977). Auditory sensitivity of the albino rat. *Journal of comparative and physiological psychology*, 91(4):930.

Kepecs, A., Uchida, N., Zariwala, H. A., and Mainen, Z. F. (2008). Neural correlates, computation and behavioural impact of decision confidence. *Nature*, 455(7210):227–231.

Kiani, R., Churchland, A. K., and Shadlen, M. N. (2013). Integration of direction cues is invariant to the temporal gap between them. *The Journal of Neuroscience*, 33(42):16483–16489.

Kiani, R., Hanks, T. D., and Shadlen, M. N. (2008). Bounded integration in parietal cortex underlies decisions even when viewing duration is dictated by the environment. *The Journal of Neuroscience*, 28(12):3017–3029.

Kiani, R. and Shadlen, M. N. (2009). Representation of confidence associated with a decision by neurons in the parietal cortex. *science*, 324(5928):759–764.

Knill, D. C. and Pouget, A. (2004). The bayesian brain: the role of uncertainty in neural coding and computation. *TRENDS in Neurosciences*, 27(12):712–719.

Knill, D. C. and Saunders, J. A. (2003). Do humans optimally integrate stereo and texture information for judgments of surface slant? *Vision research*, 43(24):2539–2558.

Kolb, B. and Walkey, J. (1987). Behavioural and anatomical studies of the posterior parietal cortex in the rat. *Behavioural brain research*, 23(2):127–145.

Körding, K. P., Beierholm, U., Ma, W. J., Quartz, S., Tenenbaum, J. B., and Shams, L. (2007). Causal inference in multisensory perception.

Körding, K. P. and Wolpert, D. M. (2006). Bayesian decision theory in sensorimotor control. *Trends in cognitive sciences*, 10(7):319–326.

Krieg, W. J. (1946). Connections of the cerebral cortex. i. the albino rat. *Journal of Comparative Neurology (and Psychology)*.

Krubitzer, L. (1995). The organization of neocortex in mammals: are species differences really so different? *Trends in neurosciences*, 18(9):408–417.

Krubitzer, L. (2007). The magnificent compromise: cortical field evolution in mammals. *Neuron*, 56(2):201–208.

Lak, A., Costa, G. M., Romberg, E., Koulakov, A. A., Mainen, Z. F., and Kepecs, A. (2014). Orbitofrontal cortex is required for optimal waiting based on decision confidence. *Neuron*, 84(1):190–201.

Lakatos, P., Chen, C.-M., O'Connell, M. N., Mills, A., and Schroeder, C. E. (2007). Neuronal oscillations and multisensory interaction in primary auditory cortex. *Neuron*, 53(2):279–292.

Lakatos, P., O'Connell, M. N., Barczak, A., Mills, A., Javitt, D. C., and Schroeder, C. E. (2009). The leading sense: supramodal control of neurophysiological context by attention. *Neuron*, 64(3):419–430.

Landy, M. S., Banks, M. S., and Knill, D. C. (2011). Ideal-observer models of cue integration. *Sensory cue integration*, pages 5–29.

Leichnetz, G. R. (2001). Connections of the medial posterior parietal cortex (area 7m) in the monkey. *The Anatomical Record*, 263(2):215–236.

Lemus, L., Hernández, A., Luna, R., Zainos, A., and Romo, R. (2010). Do sensory cortices process more than one sensory modality during perceptual judgments? *Neuron*, 67(2):335–348.

Lippert, M. T., Takagaki, K., Kayser, C., and Ohl, F. W. (2013). Asymmetric multisensory interactions of visual and somatosensory responses in a region of the rat parietal cortex.

Macaluso, E. (2006). Multisensory processing in sensory-specific cortical areas. *The neuroscientist*, 12(4):327–338.

Magri, C., Whittingstall, K., Singh, V., Logothetis, N. K., and Panzeri, S. (2009). A toolbox for the fast information analysis of multiple-site lfp, eeg and spike train recordings. *BMC neuroscience*, 10(1):81.

Masterton, B. and Diamond, I. T. (1973). Hearing: Central neural mechanisms. *Handbook of perception: biology of perceptual systems*, 3:407–482.

Masterton, R. and Diamond, I. (1964). Effects of auditory cortex ablation on discrimination of small binaural time differences. *Journal of neurophysiology*.

Meaney, M. J. and Stewart, J. (1981). A descriptive study of social development in the rat (rattus norvegicus). *Animal Behaviour*, 29(1):34–45.

Mei, N., Martin, G., and Gallego, A. (2012). *Progress in Sensory Physiology*. Number v. 4 in Progress in Sensory Physiology. Springer Berlin Heidelberg.

Meredith, M. A., Nemitz, J. W., and Stein, B. E. (1987). Determinants of multisensory integration in superior colliculus neurons. i. temporal factors. *The Journal of neuroscience*, 7(10):3215–3229.

Meredith, M. A. and Stein, B. E. (1986). Visual, auditory, and somatosensory convergence on cells in superior colliculus results in multisensory integration. *Journal of neurophysiology*, 56(3):640–662.

Meredith, M. A. and Stein, B. E. (1996). Spatial determinants of multisensory integration in cat superior colliculus neurons. *Journal of Neurophysiology*, 75(5):1843–1857.

Merigan, W. H. and Katz, L. M. (1990). Spatial resolution across the macaque retina. *Vision research*, 30(7):985–991.

Meyniel, F., Sigman, M., and Mainen, Z. F. (2015). Confidence as bayesian probability: From neural origins to behavior. *Neuron*, 88(1):78–92.

Miller, M. W. and Vogt, B. A. (1984). Direct connections of rat visual cortex with sensory, motor, and association cortices. *Journal of Comparative Neurology*, 226(2):184–202.

Montemurro, M. A., Panzeri, S., Maravall, M., Alenda, A., Bale, M. R., Brambilla, M., and Petersen, R. S. (2007). Role of precise spike timing in coding of dynamic vibrissa stimuli in somatosensory thalamus. *Journal of neurophysiology*, 98(4):1871–1882.

Morris, R. G. (1981). Spatial localization does not require the presence of local cues. *Learning and motivation*, 12(2):239–260.

Muller, R. U. and Kubie, J. L. (1987). The effects of changes in the environment on the spatial firing of hippocampal complex-spike cells. *J Neurosci*, 7(7):1951–1968.

Murphy, R. A., Mondragón, E., and Murphy, V. A. (2008). Rule learning by rats. *Science*, 319(5871):1849–1851.

Nakamura, K. (1999). Auditory spatial discriminatory and mnemonic neurons in rat posterior parietal cortex. *Journal of Neurophysiology*, 82(5):2503–2517.

Naumer, M. J. and Kaiser, J. (2010). *Multisensory object perception in the primate brain*. Springer.

Nelson, M. E. and MacIver, M. A. (2006). Sensory acquisition in active sensing systems. *Journal of Comparative Physiology A*, 192(6):573–586.

Nicholls, J. G., Martin, A. R., Wallace, B. G., Fuchs, P. A., Diamond, M. E., and Weisblat, D. A. (2012). *From Neuron to Brain*. 5th Ed. Sinauer Associates Sunderland, MA.

Nitz, D. A. (2012). Spaces within spaces: rat parietal cortex neurons register position across three reference frames. *Nature neuroscience*, 15(10):1365–1367.

Northcutt, R. G. and Kaas, J. H. (1995). The emergence and evolution of mammalian neocortex. *Trends in neurosciences*, 18(9):373–379.

O'Keefe, J. and Speakman, A. (1987). Single unit activity in the rat hippocampus during a spatial memory task. *Experimental Brain Research*, 68(1):1–27.

Olcese, U., Iurilli, G., and Medini, P. (2013). Cellular and synaptic architecture of multisensory integration in the mouse neocortex. *Neuron*, 79(3):579–593.

O'Leary, M. A., Bloch, J. I., Flynn, J. J., Gaudin, T. J., Giallombardo, A., Giannini, N. P., Goldberg, S. L., Kraatz, B. P., Luo, Z.-X., Meng, J., et al. (2013). The placental mammal ancestor and the post–k-pg radiation of placentals. *Science*, 339(6120):662–667.

Ölveczky, B. P. (2011). Motoring ahead with rodents. *Current opinion in neurobiology*, 21(4):571–578.

Pack, C. C. and Bensmaia, S. J. (2015). Seeing and feeling motion: Canonical computations in vision and touch. *PLoS Biol*, 13(9):e1002271.

Paxinos, G. and Watson, C. (2007). *The Rat Brain in Stereotaxic Coordinates: Hard Cover Edition*. Elsevier Science.

Petruno, S. K., Clark, R. E., and Reinagel, P. (2013). Evidence that primary visual cortex is required for image, orientation, and motion discrimination by rats. *PloS one*, 8(2):e56543.

Polley, D. B., Rickert, J. L., and Frostig, R. D. (2005). Whisker-based discrimination of object orientation determined with a rapid training paradigm. *Neurobiology of learning and memory*, 83(2):134–142.

Powers, M. K. and Green, D. G. (1978). Single retinal ganglion cell responses in the dark-reared rat: grating acuity, contrast sensitivity, and defocusing. *Vision research*, 18(11):1533–1539.

Prescott, T. J., Diamond, M. E., and Wing, A. M. (2011a). Active touch sensing. *Philosophical Transactions of the Royal Society of London B: Biological Sciences*, 366(1581):2989–2995.

Prescott, T. J., Mitchinson, B., and Grant, R. A. (2011b). Vibrissal behavior and function. *Scholarpedia*, 6(10):6642.

Prusky, G. T., Harker, K. T., Douglas, R. M., and Whishaw, I. Q. (2002). Variation in visual acuity within pigmented, and between pigmented and albino rat strains. *Behavioural brain research*, 136(2):339–348.

Prusky, G. T., West, P. W., and Douglas, R. M. (2000). Behavioral assessment of visual acuity in mice and rats. *Vision research*, 40(16):2201–2209.

Quiroga, R. Q., Nadasdy, Z., and Ben-Shaul, Y. (2004). Unsupervised spike detection and sorting with wavelets and superparamagnetic clustering. *Neural computation*, 16(8):1661–1687.

Raposo, D., Kaufman, M. T., and Churchland, A. K. (2014). A category-free neural population supports evolving demands during decision-making. *Nature neuroscience*.

Raposo, D., Sheppard, J. P., Schrater, P. R., and Churchland, A. K. (2012). Multisensory decision-making in rats and humans. *The Journal of neuroscience*, 32(11):3726–3735.

Reep, R., Chandler, H., King, V., and Corwin, J. (1994). Rat posterior parietal cortex: topography of corticocortical and thalamic connections. *Experimental Brain Research*, 100(1):67–84.

Roitman, J. D. and Shadlen, M. N. (2002). Response of neurons in the lateral intraparietal area during a combined visual discrimination reaction time task. *The Journal of neuroscience*, 22(21):9475–9489.

Romo, R. and de Lafuente, V. (2013). Conversion of sensory signals into perceptual decisions. *Progress in neurobiology*, 103:41–75.

Sarko, D. K., Ghose, D., and Wallace, M. T. (2013). Convergent approaches toward the study of multisensory perception. *Frontiers in systems neuroscience*, 7.

Schneidman, E., Bialek, W., and Berry, M. J. (2003). Synergy, redundancy, and independence in population codes. *the Journal of Neuroscience*, 23(37):11539–11553.

Schroeder, C. E. and Foxe, J. J. (2002). The timing and laminar profile of converging inputs to multisensory areas of the macaque neocortex. *Cognitive Brain Research*, 14(1):187–198.

Seilheimer, R. L., Rosenberg, A., and Angelaki, D. E. (2014). Models and processes of multisensory cue combination. *Current opinion in neurobiology*, 25:38–46.

Shadlen, M. N. and Newsome, W. T. (2001). Neural basis of a perceptual decision in the parietal cortex (area lip) of the rhesus monkey. *Journal of neurophysiology*, 86(4):1916–1936.

Shannon, C. E. (1948). A mathematical theory of communication. *Bell System Technical Journal*, 22:379–423,623–656.

Shaw, C., Yinon, U., and Auerbach, E. (1975). Receptive fields and response properties of neurons in the rat visual cortex. *Vision research*, 15(2):203–208.

Sieben, K., Röder, B., and Hanganu-Opatz, I. L. (2013). Oscillatory entrainment of primary somatosensory cortex encodes visual control of tactile processing. *The Journal of Neuroscience*, 33(13):5736–5749.

Simon, S. A., de Araujo, I. E., Gutierrez, R., and Nicolelis, M. A. (2006). The neural mechanisms of gustation: a distributed processing code. *Nature Reviews Neuroscience*, 7(11):890–901.

Stanford, T. R., Quessy, S., and Stein, B. E. (2005). Evaluating the operations underlying multisensory integration in the cat superior colliculus. *The Journal of Neuroscience*, 25(28):6499–6508.

Stein, B. E., Huneycutt, W. S., and Meredith, M. A. (1988). Neurons and behavior: the same rules of multisensory integration apply. *Brain research*, 448(2):355–358.

Stein, B. E., London, N., Wilkinson, L. K., and Price, D. D. (1996). Enhancement of perceived visual intensity by auditory stimuli: a psychophysical analysis. *Cognitive Neuroscience, Journal of*, 8(6):497–506.

Stein, B. E. and Meredith, M. A. (1993). *The merging of the senses.* The MIT Press.

Stein, B. E. and Stanford, T. R. (2008). Multisensory integration: current issues from the perspective of the single neuron. *Nature Reviews Neuroscience*, 9(4):255–266.

Suzuki, S., Augerinos, G., and Black, A. H. (1980). Stimulus control of spatial behavior on the eight-arm maze in rats. *Learning and motivation*, 11(1):1–18.

Tafazoli, S., Di Filippo, A., and Zoccolan, D. (2012). Transformation-tolerant object recognition in rats revealed by visual priming. *The Journal of Neuroscience*, 32(1):21–34.

Torvik, A. (1956). Afferent connections to the sensory trigeminal nuclei, the nucleus of the solitary tract and adjacent structures. an experimental study in the rat. *Journal of Comparative Neurology*, 106(1):51–141.

Uchida, N. and Mainen, Z. F. (2003). Speed and accuracy of olfactory discrimination in the rat. *Nature neuroscience*, 6(11):1224–1229.

van Hemmen, J. L., van der Smagt, P., and Stein, B. E. (2012). Foreword for the special issue on multimodal and sensorimotor bionics. *Biological cybernetics*, 106(11-12):615.

Van Hooser, S. D., Heimel, J. A. F., Chung, S., Nelson, S. B., and Toth, L. J. (2005). Orientation selectivity without orientation maps in visual cortex of a highly visual mammal. *The Journal of neuroscience*, 25(1):19–28.

Vincent, S. B. (1912). *The functions of the vibrissae in the behavior of the white rat...*, volume 1. University of Chicago.

Von Heimendahl, M., Itskov, P. M., Arabzadeh, E., and Diamond, M. E. (2007). Neuronal activity in rat barrel cortex underlying texture discrimination. *PLoS Biol*, 5(11):e305.

Wallace, D. J., Greenberg, D. S., Sawinski, J., Rulla, S., Notaro, G., and Kerr, J. N. (2013). Rats maintain an overhead binocular field at the expense of constant fusion. *Nature*, 498(7452):65–69.

Wallace, M. T., Ramachandran, R., and Stein, B. E. (2004). A revised view of sensory cortical parcellation. *Proceedings of the National Academy of Sciences of the United States of America*, 101(7):2167–2172.

Weijnen, J. A. (1998). Licking behavior in the rat: measurement and situational control of licking frequency. *Neuroscience & Biobehavioral Reviews*, 22(6):751–760.

Whitfield, I. (1979). The object of the sensory cortex. *Brain, behavior and evolution*, 16(2):129–154.

Whitlock, J. R., Sutherland, R. J., Witter, M. P., Moser, M.-B., and Moser, E. I. (2008). Navigating from hippocampus to parietal cortex. *Proceedings of the National Academy of Sciences*, 105(39):14755–14762.

Wichmann, F. A. and Hill, N. J. (2001). The psychometric function: I. fitting, sampling, and goodness of fit. *Perception & psychophysics*, 63(8):1293–1313.

Wilber, A. A., Clark, B. J., Demecha, A. J., Mesina, L., Vos, J. M., and McNaughton, B. L. (2014). Cortical connectivity maps reveal anatomically distinct areas in the parietal cortex of the rat. *Frontiers in neural circuits*, 8.

Woolsey, T. A., Welker, C., and Schwartz, R. H. (1975). Comparative anatomical studies of the sml face cortex with special reference to the occurrence of "barrels" in layer iv. *Journal of Comparative Neurology*, 164(1):79–94.

Wurtz, R. H. and Albano, J. E. (1980). Visual-motor function of the primate superior colliculus. *Annual review of neuroscience*, 3(1):189–226.

Zampini, M. and Spence, C. (2004). The role of auditory cues in modulating the perceived crispness and staleness of potato chips. *Journal of sensory studies*, 19(5):347–363.

Zoccolan, D. (2015). Invariant visual object recognition and shape processing in rats. *Behavioural brain research*, 285:10–33.

Zoccolan, D., Oertelt, N., DiCarlo, J. J., and Cox, D. D. (2009). A rodent model for the study of invariant visual object recognition. *Proceedings of the National Academy of Sciences*, 106(21):8748–8753.

Zuo, Y., Perkon, I., and Diamond, M. E. (2011). Whisking and whisker kinematics during a texture classification task. *Philosophical Transactions of the Royal Society of London B: Biological Sciences*, 366(1581):3058–3069.

Colophon

This thesis was typeset using LaTeX, originally developed by Leslie Lamport and based on Donald Knuth's TeXand modified by the author (Nader Nikbakht). The sidenotes are inspired by the design of Tufte-LaTeX. The body text is set in 11 point Arno Pro, designed by Robert Slimbach in the style of book types from the Aldine Press in Venice, and issued by Adobe in 2007. A template, which can be used to format a PhD thesis with this look and feel, has been released under the permissive MIT (X11) license, and can be found online at github.com/suchow/ or from the author at suchow@post.harvard.edu.